

MASTER

A comparative performance assessment of infrared heating panels and conventional heating solutions in Dutch residential buildings

Corsten, A.J.H. (Guus)

Award date:
2021

[Link to publication](#)

Disclaimer

This document contains a student thesis (bachelor's or master's), as authored by a student at Eindhoven University of Technology. Student theses are made available in the TU/e repository upon obtaining the required degree. The grade received is not published on the document as presented in the repository. The required complexity or quality of research of student theses may vary by program, and the required minimum study period may vary in duration.

General rights

Copyright and moral rights for the publications made accessible in the public portal are retained by the authors and/or other copyright owners and it is a condition of accessing publications that users recognise and abide by the legal requirements associated with these rights.

- Users may download and print one copy of any publication from the public portal for the purpose of private study or research.
- You may not further distribute the material or use it for any profit-making activity or commercial gain

*Eindhoven University of Technology
Department of the Built Environment
Unit Building Physics and Services
Building Performance*

Master's thesis on

**A comparative performance assessment of infrared heating panels
and conventional heating solutions in Dutch residential buildings**

**A.J.H. Corsten
1004155**

Supervised by
prof. dr. ir. J. Hensen
dr. ir. P. Hoes
S. Wang, MSc.

Eindhoven, 2021

Highlights

Infrared panels, thermal comfort, occupancy, space heating

Nomenclature

HERSCHEL - Harnessing Effective Radiation Solutions with Comfortable Heated Energy Levels

RVO – Dutch Enterprise Agency

WoON – Woon Onderzoek Nederland

BENG – Bijna Energieneutrale Gebouwen (Nearly Zero Energy Buildings)

EU – European Union

KPI – key performance indicator

TCO – Total Cost of Ownership

R_c -value – thermal resistance over a construction element (m^2K/W)

T_{sp} – setpoint temperature ($^{\circ}C$)

T_{op} – operative temperature ($^{\circ}C$)

T_{pr} – plane radiant temperature ($^{\circ}C$)

ACH – air changes per hour

NMBE – normalized mean bias error

$Cv(RMSE)$ – coefficient of variation of the root mean square error

Abstract

The ongoing climate change has pressured countries to take action against global warming, which is done by several climate agreements. As the building sector also has a major role global warming, new regulations were created in the Netherlands to ensure that the built environment is becoming more sustainable. In most cases, this is done by means of renovations, in which both passive and active measures are taken. Passive measures include the improvement of the building envelope by adding insulation and increasing the airtightness. Active measures include improvements in technical systems, such as heating systems. In the Netherlands, old heating systems are often replaced with high efficiency gas boilers or air source heat pumps. However, this raises the question if there are any other viable alternatives to these heating systems. A proposed alternative is the use of infrared heating panels, which can be applied in the ceiling and include a heat source and heating terminal unit all in one. Therefore, the research question this study aims to answer is: *“How does the overall performance (energy and thermal comfort) of infrared panels compare with conventional heating solutions for Dutch residential buildings?”*. To answer this question, an assessment is done by means of building simulations in which the performances of the different systems are compared in various scenarios. These scenarios are created by changing several parameters, based on what can realistically be expected in Dutch dwellings. These parameters include occupancy, envelope quality and heating control strategy. For the envelope, two qualities are investigated: one that represents the current buildings stock, which is considered low insulation in this study, and one that represents the current building standards, which corresponds to high insulation. As for occupancy, a single senior profile and nuclear family profile are used to compare the performances of the heating systems. The simulations are carried out for a mid-terraced house and a freestanding house. The performance of the heating systems is evaluated by considering thermal comfort, peak energy demand, the total cost of ownership (TCO) and operational carbon emissions.

The simulations show that the performance of the infrared panels is highly dependent on the scenario in which it is used. It is able to maintain setpoint temperatures and the indoor operative temperatures remain within the 80% acceptability range most of the time in all cases. However, the heat pump combined with floor heating is able to maintain the most constant indoor temperature. With respect to radiant temperature asymmetry, floor heating is more comfortable compared to infrared panels, which is caused mainly by the fact that occupants are generally more sensitive to overhead heating compared to floor heating. However, in high insulated dwellings the radiant temperature asymmetry caused by infrared panels is significantly lower compared to low insulation dwellings. Furthermore, it is observed that lower setpoint temperatures can lead less radiant temperature asymmetry when using infrared panels. As for the peak electricity loads, the simulations showed that the peaks are substantially higher for infrared panels compared to the heat pump. Similarly, the operational costs and carbon emissions are higher for infrared panels in all considered cases. However, the TCO of infrared panels is lower than the TCO of heat pumps in the case of high insulated terraced houses. For low insulated houses, the TCO of infrared panels is always higher compared to a heat pump or gas boiler. As for occupancy, the TCO and radiant temperature asymmetry are lower in the case of a nuclear family compared to a single senior.

Based on the results of the simulations, it is recommended to use infrared panels for domestic space heating only in buildings that meet the current building standards, as the performance in high insulation buildings is significantly better overall compared to low insulation buildings. More specifically, mid-terraced houses are more suitable for the application of infrared panels than freestanding houses, due to the higher perceived thermal comfort and lower TCO. The simulation results also show that the use of lower thermostat setpoint temperatures is recommended for the use of infrared panels, as it results in a lower TCO and the radiant temperature asymmetry is less compared to higher thermostat setpoints.

Samenvatting

De huidige klimaatverandering heeft ertoe geleid dat landen door middel van klimaatakkoorden actie hebben ondernomen tegen de opwarming van de aarde. Aangezien de bouwsector hierin ook een grote rol speelt, is de regelgeving in Nederland aangepast om te zorgen voor een duurzamere gebouwde omgeving. In veel gevallen gebeurt dit door renovaties, waarbij zowel actieve als passieve maatregelen worden getroffen. Onder passieve maatregelen valt het verbeteren van de gebouwschil door het toevoegen van isolatie en het verbeteren van de luchtdichtheid. Onder actieve maatregelen valt het verbeteren van technische systemen, zoals de warmtesystemen. In Nederland worden oude warmtesystemen vaak vervangen door Hr-ketels en lucht-water warmtepompen. Echter leidt dit tot de vraag of er ook andere geschikte alternatieven zijn voor deze warmtesystemen. Een voorstel is het gebruik van infrarode panelen, welke in het plafond ingebouwd worden en zowel de warmtebron als het afgiftesysteem van de warmte bevatten. Daarom is de onderzoeksvraag van deze studie als volgt: *“Hoe verhouden de prestaties van infrarode panelen (energie en thermisch comfort) zich tot conventionele verwarmingssystemen in Nederlandse woningen?”*. Om die vraag te beantwoorden is een beoordeling gemaakt aan de hand van gebouwsimulaties waarin de prestaties van de diverse systemen onder variërende scenario's worden vergeleken. Deze scenario's worden gecreëerd door een aantal parameters te veranderen op basis van wat verwacht kan worden in Nederlandse woningen. Deze parameters bevatten het gebruikersprofiel, de kwaliteit van de gebouwschil en de controlestrategie van de verwarming. Voor de gebouwschil worden twee typen vergeleken: een die de huidige woningvoorraad vertegenwoordigt, wat in deze studie overeenkomt met laag geïsoleerd, en een die voldoet aan het nieuwe bouwbesluit, wat overeenkomt met hoog geïsoleerd. Bij de gebruikersprofielen wordt een alleenstaande oudere vergeleken met een gezin. De simulaties worden gedaan voor een tussenwoning en een vrijstaande woning. De prestaties van de warmtesystemen worden beoordeeld op basis van thermisch comfort, de piekvraag, de totale eigendomskosten (TCO) en de operationele koolstofemissies.

De simulaties laten zien dat de prestaties van infrarode panelen zeer afhankelijk zijn van de omstandigheden. Ze zijn meestal in staat de operationele binnentemperatuur binnen de grenzen van 80% aanvaardbaarheid te houden. Echter is de warmtepomp met vloerverwarming in staat om een constantere binnentemperatuur te leveren. Met betrekking tot stralingsasymmetrie is vloerverwarming comfortabeler dan infrarode panelen, wat met name komt doordat bewoners over het algemeen gevoeliger zijn voor verwarming boven het hoofd dan vloerverwarming. De stralingsasymmetrie van infrarode panelen is echter minder in hoog geïsoleerde woningen vergeleken met laag geïsoleerde woningen. Daarnaast is de stralingsasymmetrie lager bij een lagere thermostaattemperatuur in het geval van infrarode panelen. De piekvraag van infrarode is substantieel hoger dan die van een warmtepomp. Ook zijn de operationele kosten en koolstofemissies van infrarode panelen hoger dan die van een warmtepomp. Echter is de TCO van infrarode panelen lager in hoog geïsoleerde woningen vergeleken met een warmtepomp. In laag geïsoleerde woningen is de TCO van infrarode panelen altijd hoger dan die van een warmtepomp of Hr-ketel. De TCO en stralingsasymmetrie zijn lager in het geval van een gezin dan een alleenstaande oudere.

Gebaseerd op de resultaten wordt het aangeraden om infrarode panelen alleen te gebruiken voor ruimteverwarming in woningen die voldoen aan het nieuwe bouwbesluit, aangezien de prestaties daar aanzienlijk beter zijn dan in laag geïsoleerde woningen. Specifiek gezien is een tussenwoning geschikter voor de toepassing van infrarode panelen dan een vrijstaande woning, door het hogere waargenomen thermisch comfort en de lagere TCO. De simulaties laten ook zien dat een lagere thermostaattemperatuur aangeraden wordt vanwege de lagere TCO en stralingsasymmetrie vergeleken met hogere thermostaattemperaturen.

Acknowledgements

During the entire process of this study I have received extensive support and feedback from the members of my graduation committee: prof. dr. ir. Jan Hensen, dr. ir. Pieter-Jan Hoes and Shuwei Wang, MSc. I would like to express my gratitude for their guidance and suggestions throughout the project.

I would also like to thank the members of the building performance group, who have attended my monthly presentations during the progress meetings. By asking detailed questions and providing suggestions they have contributed to the improvement of my project.

Finally, I would like to thank dr. ir. Twan van Hooff for carrying out the measurements of the infrared panels in the laboratory. His measurements have allowed me to make a validated model of the infrared panel, which was essential for the simulations.

Table of Contents

Highlights	3
Nomenclature	3
Abstract	4
Samenvatting	5
Acknowledgements	6
1. Introduction	9
2. Literature review	11
2.1. Heating systems	11
2.2. Case buildings	13
2.2.1. Building typologies	13
2.2.2. Envelope quality	14
2.2.3. Occupancy scenarios	16
2.3. Evaluation criteria / Key performance indicators	18
2.3.1. Operative temperature.....	18
2.3.2. Radiant temperature asymmetry.....	19
3. Methodology	21
3.1. Heating system peak loads	21
3.2. Total cost of ownership	22
3.3. Environmental impact	22
3.4. Simulation experiment	23
3.5. Software	23
3.6. Infrared panel model validation	24
3.6.1. Boundary conditions.....	24
3.6.2. Infrared heating panel model	25
3.6.3. Model calibration	25
4. Results.....	29
4.1. Thermal comfort	29
4.1.1. Indoor operative temperature.....	29
4.1.2. Radiant temperature asymmetry.....	33
4.2. Heating system peak loads	36
4.3. Operational costs and TCO	37
4.4. Environmental impact.....	39
5. Discussion.....	40
6. Conclusion.....	43
References	44

Appendix I: Case buildings details	48
Appendix II: envelope details	49
Low insulation terraced house details	51
Low insulation freestanding house details	53
High insulation details	55
Appendix III: Occupancy schedules	57
Single senior	57
Nuclear family	58
Appendix IV: Heating systems.....	60
Infrared panels	60
Heat pump	62
Gas boiler	63
Appendix V: Radiant temperature asymmetry analysis	64
Terraced house position 1	64
Terraced house position 2	66
Freestanding house position 1	68
Freestanding house position 2	70
Appendix VI: Indoor operative temperature	72
Single senior	72
Nuclear family	74
Appendix VII: Radiant temperature asymmetry	76
Single senior	76
Nuclear family	78
Appendix VIII: Infrared panel load duration curves	80
Single senior	80
Nuclear family	81
Appendix IX: Total cost of ownership.....	82

1. Introduction

As a result of increased greenhouse gas emissions due to human activity, the Earth's climate has been changing over the course of the last century. This change manifests itself in the form of global warming, as glaciers are shrinking fast and trees are flowering earlier nowadays (NASA, 2020). The built environment also contributes to increased emissions in the form of electricity consumption, material impacts and site allocation (Younger, M., Morrow-Almeida, Vindigni, & Dannenberg, 2008). The Paris Agreement and the Dutch Climate Agreement from 2019 aim to reduce the environmental impact of the building sector by achieving a fully energy neutral built environment by 2050. Renovations and upgrades of the current Dutch housing stock is essential for this purpose (Visscher, 2019).

This study is part of the HERSCHEL project. The main objective of this project is to realize a predictive comfort and energy model to indicate under which conditions infrared heating panels can be a sustainable and viable alternative to air source heat pumps for residential heating (O-Nexus, Beligreen, Eindhoven University of Technology & Jheronimus Academy of Data Science, 2019). An earlier study within the HERSCHEL project already analyzed the performance of infrared heating panels in similar conditions to the measured conditions in a real case building (Biliotti, 2020). This study aims to build upon that knowledge by analyzing the performance of both infrared heating panels and heat pumps in different situations to investigate which system has the best overall performance regarding energy and thermal comfort. The importance of investigating alternative heating solutions is made clear by the fact that the majority of renovations in the Netherlands are focused on heating systems (Filippidou, Nieboer, & Visscher, 2016).

A major difference between infrared heaters and heat pumps is the way in which heat is produced and provided to the occupants. Infrared heaters heat up surfaces directly by means of radiation in the form of infrared waves, meaning that the air itself is not heated directly. Occupants receive the radiant heat directly to their skin and from reflections of the other surfaces within the space, such as walls (Barker, 2002). The use of infrared heating systems is still fairly limited within the built environment sector, with a major application being industrial workplaces, as the individual stations are often placed at a relatively large distance from each other and therefore need local heating solutions to prevent excessive energy consumption for heating and provide sufficient thermal comfort (Dudkiewicz & Jeżowiecki, 2009). Another common application of infrared heaters is in the food industry for thermal processing, which includes peeling, baking, pasteurization, sterilization and drying. Some of the advantages of infrared heating in the food industry are the reduced processing time, improved energy efficiency and high heat delivery rate (Pan, Atungulu, & Li, 2014). A study into electric overhead radiant heating in churches concluded from irradiation at floor level that the temperature in the church increased and the relative humidity decreased. However, it also demonstrated a major weakness of radiant heating systems, namely that the heating effect on surfaces that are not directly irradiated by the system is very small. Therefore this system is mostly useful for personalized heating in places where people come together, at least when considering large spaces with characteristics similar to those in churches (Samek, L., et al., 2007). Advantages of electric radiant heating panels in residential applications include the ease of installation and the possibility to save space in the house, as no additional boiler or heat pump is required to generate heat. As for the energy efficiency, a study found that the efficiency of these panels is close to one in steady state conditions. In transient conditions the electric panels were found to be much more reactive compared to conventional hydronic systems, but the study also warns that primary energy should be taken into account for a fair comparison (Ferrarini, et al., 2018). However, previous studies do not compare the performance of infrared panels for different building typologies, envelope qualities, occupancy scenarios and control schemes.

The aim of this study is to investigate the feasibility of infrared panels for space heating in Dutch dwellings, by comparing their performance to conventional methods of heating in different scenarios. This study uses computational building performance assessment as the main research method. The main research question of this study is therefore as follows:

How does the overall performance (energy and thermal comfort) of infrared panels compare with conventional heating solutions for Dutch residential buildings?

In order to answer this question, several sub-questions have been formulated to investigate specific aspects of the overall performance of each system. These questions are:

- 1. *What are the conventional heating solutions in Dutch residential buildings?***
- 2. *What building typologies and building characteristics represent Dutch residential buildings?***
- 3. *What are the relevant KPIs for comparing the performance?***
 - a. How does each system perform with respect to the indoor operative temperature, taking into account different building aspects and occupancy profiles?*
 - b. How does each system perform with regard to the radiant temperature asymmetry, taking into account different building aspects, occupancy profiles and positions within a room?*
 - c. What are the peak energy loads of each heating system?*
 - d. How do the heating systems compare regarding the total cost of ownership?*
 - e. How do the heating systems compare in terms of their environmental impact?*
- 4. *How to model the performance of the heating solutions?***
 - a. What modeling approach should be used?***
 - b. What operational strategies should be included?***
 - i. What is the difference in performance when comparing on/off-controls and modulating controls for the infrared panels?*
- 5. *How to compare the performance of the heating solutions?***

2. Literature review

2.1. Heating systems

In this study three different heating systems are considered: an air source heat pump, a gas boiler and infrared panels, as these are the most conventional systems for renovations (Van der Knijff, 2018) (Majcen, Itard, & Visscher, 2016). Details for each of these systems can be found in appendix IV. The heat pump and gas boiler are both connected to an underfloor heating system based on water heating. Both heating systems are operated with modulating controls. For the infrared panels, two different control strategies are used: a simple on/off control and a modulating control strategy. The on/off control switches between off and on, meaning that the power output is either at 0 W when switched off or at 240 W when switched on. The control scheme is shown in more detail in Table 1. For the modulating controls, the power output varies, depending on the difference between the indoor operative temperature and the setpoint temperature. The control scheme for the modulating controls of the infrared panels is shown in Table 2.

Table 1: Control scheme of the on/off-controls for the infrared panels

Mode	Condition
On	$T_{op} < T_{sp} - 0.5 \text{ }^\circ\text{C}$
Off	$T_{op} \geq T_{sp} + 0.5 \text{ }^\circ\text{C}$

Table 2: Control scheme of the modulating controls for the infrared panels

Mode	Condition
100% capacity	$T_{op} \leq T_{sp} - 0.5 \text{ }^\circ\text{C}$
95% capacity	$T_{sp} - 1.0 \text{ }^\circ\text{C} < T_{op} \leq T_{sp} - 0.75 \text{ }^\circ\text{C}$
80% capacity	$T_{sp} - 0.75 \text{ }^\circ\text{C} < T_{op} \leq T_{sp} - 0.5 \text{ }^\circ\text{C}$
50% capacity	$T_{sp} - 0.5 \text{ }^\circ\text{C} < T_{op} \leq T_{sp} - 0.25 \text{ }^\circ\text{C}$
20% capacity	$T_{sp} - 0.25 \text{ }^\circ\text{C} < T_{op} < T_{sp}$

The advantage of modulating controls compared to on/off controls is that modulating controls are capable of keeping the operative temperature more constant, as the power output becomes smaller when the difference between the operative temperature and setpoint temperature becomes smaller. Simple on/off controls cause much more fluctuations in operative temperature due to the constant switching in power output between 0 W and 240 W. The difference in indoor temperature between these two control strategies is visualized in Figure 1, where the modulating control overshoots the setpoint temperature initially, but then modulates the power to keep the temperature constant.

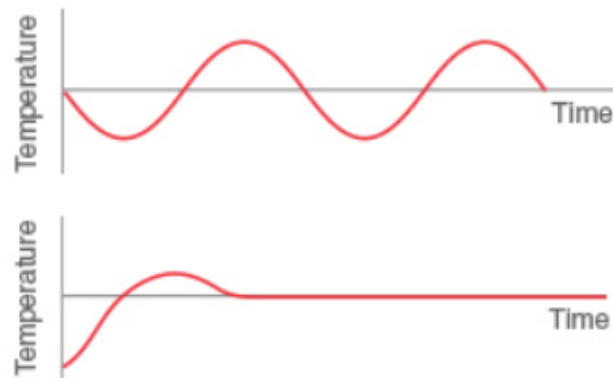


Figure 1: Difference in indoor temperature over time between a simple on/off control (upper graph) and a modulating control (lower graph) (Spirax Sarco, 2004).

2.2. Case buildings

For this study, the heating systems are not analyzed for existing dwellings, but instead the reference dwellings of RVO are used. The RVO has published a document that describes the characteristics of these reference dwellings, which are based on the general characteristics of existing dwellings. The aim of the document is to provide a theoretical basis in the form of different building typologies for projects where details regarding the building design are yet to be defined (Agentschap NL, 2013). The document contains detailed information for various building typologies, such as freestanding, apartment or terraced houses. Furthermore, subtypes for each typology are also distinguished in the document, for instance an apartment at the top floor of a building or an apartment situated between other apartments.

2.2.1. Building typologies

Two building typologies are selected for this study: a freestanding house and a mid-terraced house. The reason for this choice is that these are the two most common typologies in the Dutch housing stock. As can be seen in Figure 2, there are significant differences in the composition of the housing stock between different provinces. For instance, the urban provinces such as Zuid-Holland and Noord-Holland consist primarily of terraced houses and apartments, whereas in rural provinces such as Drenthe, Friesland and Groningen freestanding houses are the most common building typology. However, when considering the country as a whole, terraced houses are by far the most common housing type, accounting for 42.5% of the Dutch housing stock, followed by the freestanding housing type, which accounts for 23%. Of particular interest for this project is difference in heat loss between both building typologies, considering that freestanding houses have a significantly larger envelope area and therefore higher heat loss compared to terraced houses. Especially when considering a mid-terraced house, the heat loss is lower due to the fact that there are dwellings on both sides and it is assumed in this study that the temperature in the adjacent dwellings is equal to the investigated dwelling, so no heat loss occurs through the wall that separates the dwellings. Details regarding the case buildings can be found in appendix I. Floorplans and dimensions of the dwellings are taken from a document released by the Dutch government that describes these aspects for different types of dwellings in the Netherlands (Agentschap NL, 2013).

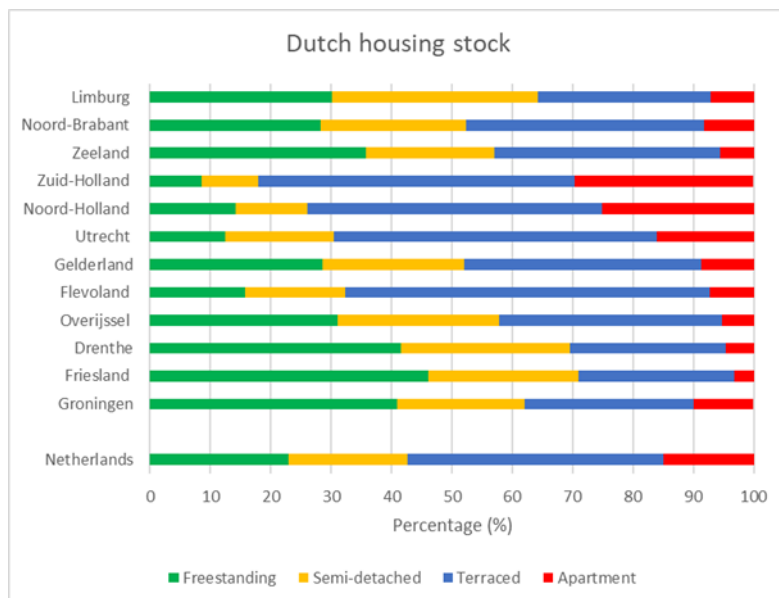


Figure 2: Composition of the housing stock in the Netherlands by province and for the country as a whole (Statistics Netherlands, 2016)

2.2.2. Envelope quality

The envelope quality has an crucial impact on the performance of a space heating system and should be addressed. In this study, two envelope qualities are used for each building. Envelope quality here refers to the infiltration rates, the types of windows and amount of insulation that is used in the exterior walls, roof and ground floor. The first envelope quality is one that represents the current building stock, which is defined by using data from the WoON-database. The WoON-database is created from the WoON-research that has been carried out nationwide since 2006. The WoON-research focusses on obtaining statistical information regarding the living situation and desires of the Dutch population. For instance, it contains data on household composition, number of occupants, age and the dwelling itself (Statistics Netherlands, 2012).

2.2.2.1. Walls

Two envelope qualities are defined for this research: a quality that is currently common in the Dutch building stock (according to WoON database) and a quality that meets the BENG requirements for newly built dwellings. The quality that represents the current building stock is referred to in this study as the 'low insulation' case, while the quality that represents the BENG requirements is referred to as the 'high insulation' case. This is done to clarify the difference between the two cases. BENG is a set of requirements to make buildings more energy efficient that must be met for all new building permits starting from January 1st 2021 (Netherlands Enterprise Agency, 2021). In order to meet the BENG requirements, measures should be taken in buildings to minimize the energy consumption, for instance by increasing the insulation in the building envelope with the aim of reducing the heat losses. A reduced heat loss corresponds to a lower heating demand and therefore less energy is needed for space heating. The introduction of BENG came with a change in the Dutch building codes and a new assessment method called NTA-8800. The minimum R_c -values for construction elements have been updated accordingly. For walls, the minimum R_c -value is 4.7 m²K/W (NEN, 2020). In this study, the required insulation thickness to meet these R_c -values is calculated based on standard constructions, for instance a typical Dutch brick cavity wall. Sections of each construction element in the DesignBuilder model can be found in appendix II, while Table 3 contains the R_c -values of each construction.

2.2.2.2. Windows

Regarding the windows, two window types are selected in a similar way to the walls, meaning that one type is representative for the window type that is often found in buildings of the current building stock in the Netherlands, whilst the other type is required in order to meet the BENG criteria. Regarding the window types of the current dwellings, the type is once again selected based on data from the WoON-database. As can be seen in Figure 39 in appendix II, standard double glazing is still the most common type of glazing in both terraced and freestanding houses. For the fulfillment of the BENG requirements minimum requirement is that the windows are the HR++ type.

2.2.2.3. Infiltration

For freestanding houses an infiltration air flow rate of 0.980 dm³/s per m² is assumed and for terraced houses an infiltration air flow rate of 0.7 dm³/s per m² is assumed (Isover Saint-Gobain, 2013). The Dutch building codes specify three classes of infiltration that are considered acceptable: ‘basic’, ‘good’ and ‘excellent’. The ‘excellent’ class corresponds to buildings that are constructed according to the BENG-requirements. It is assumed that the higher insulated buildings meet the BENG-standards and therefore the airtightness is increased, resulting in an infiltration of 0.14 dm³/s per m² floor area. According to the Dutch building codes, the infiltration rate should be less than 0.15 dm³/s per m² floor area in order to meet the BENG-requirements (IsoBouw, 2016).

Table 3: Overview of the characteristics of the envelopes per building type

Insulation level	Terraced		Freestanding	
	Low	High	Low	High
External wall R _c -value (m ² K/W)	1.74	4.74	1.99	4.74
Roof R _c -value (m ² K/W)	1.99	6.49	2.74	6.49
Floor R _c -value (m ² K/W)	1.40	3.75	1.40	3.75
Window type	Standard double glazing	HR++	Standard double glazing	HR++
Infiltration rate (dm ³ /s per m ² floor area)	0.7	0.14	0.98	0.14

2.2.3. Occupancy scenarios

One of the variables that is investigated in this study is the influence of occupancy on the performance of each heating system. Two occupancy profiles are selected: a single senior profile and a nuclear family profile. The nuclear family consists of two adults and two children. Each of the profiles consists of schedules regarding presence, heating setpoints, ventilation and thermostat setpoints. The definition of these schedules is based on results of studies that analyzed occupancy profiles of different Dutch household types. One of these studies made use of the WoON-database to extract profiles from the dataset based on statistical analysis (Guerra-Santin & Silvester, 2017). This is also the study which is used as the basis to define most of the occupancy schedules. The presence schedule of the nuclear family is based on another study that investigated occupancy profiles in the Netherlands by means of a simplified Knowledge Discovery in Database (KDD) based on a selection of 150 Dutch dwellings (Muroni, Gaetani, Hoes, & Hensen, 2019). The details on the schedules and internal gains can be found in appendix III. The simulations are performed for the heating season only, which here is assumed start October 1st and end May 1st.

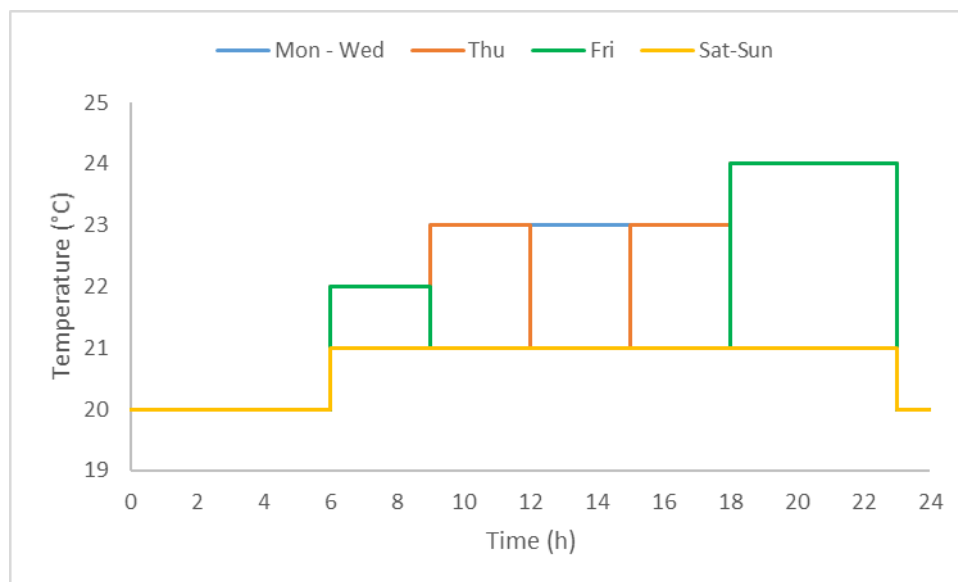


Figure 3: Heating setpoint schedule of the living room for the single senior household profile. The setback temperatures for unoccupied hours are 20 °C at night and 21 °C during the day.

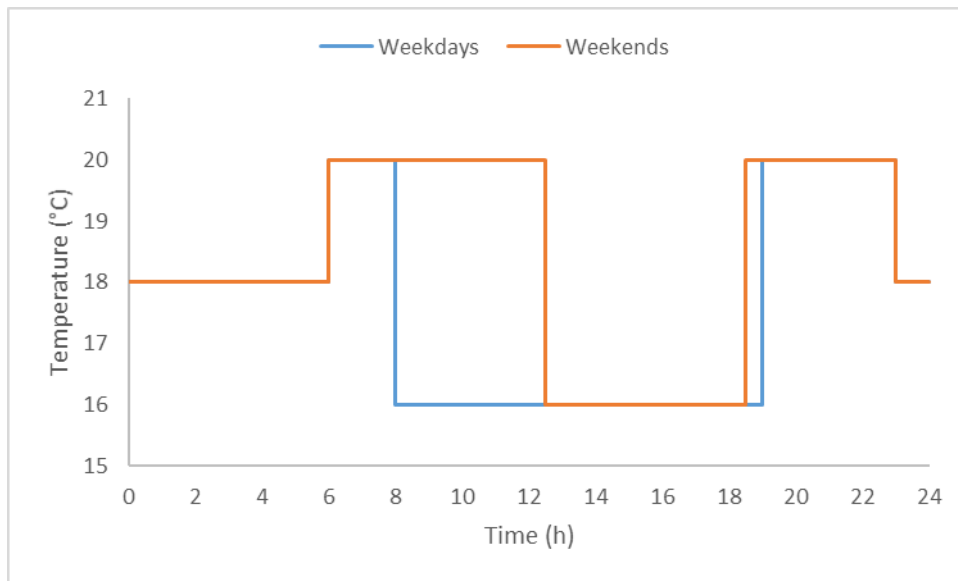


Figure 4: Heating setpoint schedule of the living room for the nuclear family household profile. The setback temperatures for unoccupied hours are 18 °C at night and 16 °C during the day.

Ventilation profiles are assumed to be similar for both household types, as according to the WoON-database more than 50% of people ventilate their homes while heating (Guerra-Santin & Silvester, 2017). Furthermore, it is assumed that natural ventilation is used during daytime between 6 in the morning and 18 in the evening, but only when the occupants are at home. As most dwellings have natural ventilation (Majcen, Itard, & Visscher, 2016), this is also assumed for this case, except for the kitchen and bathroom, where mechanical extraction of air makes more sense due to higher levels of contamination of the room air originating from food in the kitchen and the occupant's body in the bathroom (Van Ginkel & Hasselaar, 2006). Establishing the ventilation rates associated with natural ventilation is difficult, as the rates are dependent on local weather conditions such as wind velocity and direction. Furthermore, the degree to which a window is opened also significantly influences the ventilation rates. However, in this study it is assumed that windows are only slightly opened as only the heating season is taken into consideration. The ventilation rate for the windows is assumed to be 0.8 air changes per hour (ACH), in accordance with the minimum expected ventilation rate for slightly opened windows (Nash, 2013). The ventilation rates for mechanical ventilation in the kitchen and bathroom are also assumed to be 0.8 ACH.

2.3. Evaluation criteria / Key performance indicators

The performance of the heating systems is evaluated for each case based on several key performance indicators. The first indicator is the operative temperature in the living room, as this room is the central room in a house and the room where most activities tend to take place throughout the day. The objective is to assess whether the operative temperature is within the range of comfort for occupants. The second indicator is radiant temperature asymmetry, as heating systems might cause a difference in temperature between the upper and lower bodies of occupants, which may be perceived as uncomfortable if this difference is too large. The third indicator is the peak loads of the heating systems in each of the cases. The energy cost is the fourth indicator and is calculated for all cases based on the results of the simulations and literature in order to determine if and when infrared panels are cheaper to operate than a heat pump or a gas boiler. Related to this is the fifth and last key performance indicator: the environmental impact in terms of CO₂-emissions during the lifespan of each system. This section explains each of these key performance indicators in more detail.

2.3.1. Operative temperature

The operative temperature in the living room is the first key performance indicator that is assessed. Regarding the indoor operative temperature, comfort limits have been defined for different scenarios. The limits defined in ASHRAE 55 are general limits, but for the specific rooms such as the living room separate comfort limits have been defined in a study, which specifically considered thermal comfort in houses. As this study focuses on thermal comfort in the living room, the comfort limits defined in the aforementioned study are used and explained here. A neutral temperature, which specifies the temperature in which the Predicted Percentage of Dissatisfied (PPD) is equal to 0%, is calculated as follows (Peeters, De Daer, Hensen, & D'Haeseleer, 2009):

$$T_n = 20.4 + 0.06 \cdot T_{e,ref} \text{ for } T_{e,ref} < 12.5 \text{ } ^\circ\text{C} \quad [1]$$

$$T_n = 16.63 + 0.36 \cdot T_{e,ref} \text{ for } T_{e,ref} \geq 12.5 \text{ } ^\circ\text{C} \quad [2]$$

Where T_n is the neutral temperature ($^\circ\text{C}$) and $T_{e,ref}$ is the reference external temperature ($^\circ\text{C}$). $T_{e,ref}$ not only represents the external temperature on day x , but also on the three days prior to day x . In mathematical form, the equation to determine $T_{e,ref}$ for any given day is as follows (Peeters, De Daer, Hensen, & D'Haeseleer, 2009):

$$T_{e,ref} = (T_{\text{today}} + 0.8 \cdot T_{\text{today-1}} + 0.4 \cdot T_{\text{today-2}} + 0.2 \cdot T_{\text{today-3}}) / 2.4 \quad [3]$$

In this study it is stated that people are generally more sensible to cold conditions and therefore the lower comfort limit is closer to the neutral temperature than the upper limit. The limits are defined using the following equations (Peeters, De Daer, Hensen, & D'Haeseleer, 2009):

$$T_{\text{upper}} = T_n + \omega \cdot \alpha \quad [4]$$

$$T_{\text{lower}} = T_n - \omega \cdot (1-\alpha) \quad [5]$$

Where T_{upper} is the upper comfort limit ($^\circ\text{C}$), T_{lower} is the lower comfort limit ($^\circ\text{C}$), ω the width of the comfort range ($^\circ\text{C}$) and α is a constant smaller than or equal to 1.

For these comfort limits, which are based on the Predicted Percentage of Dissatisfied (PPD), the parameters are taken from Table 4Table 4.

Table 4: Parameters for comfort limits regarding the operative temperature in the living room (Peeters, De Daer, Hensen, & D'Haeseleer, 2009)

10% PPD	20% PPD
$\omega = 5 \text{ }^\circ\text{C}$	$\omega = 7 \text{ }^\circ\text{C}$
$\alpha = 0.7$	$\alpha = 0.7$

2.3.2. Radiant temperature asymmetry

For the determination of the radiant temperature asymmetry, the method developed by Fanger is used, similar to what is described in the ASHRAE Fundamentals Handbook and the ISO 7730 standard, both of which describe limits regarding radiant temperature asymmetry (Fanger, et al., 1985) (ASHRAE, 2001) (Olesen & Parsons, 2002). The determination of the radiant temperature asymmetry at an arbitrary position in the room is defined as the plane radiant temperature difference (ΔT_{pr}), which is the difference in plane radiant temperature (T_{pr}) of the opposite sides of a small plane element, which represents the occupant. The plane radiant temperature is defined as the uniform surface temperature of an enclosure, where the incident flux on one of the sides of the aforementioned small plane element is the same as in the actual environment (ASHRAE, 2001). The orientation of the element is of importance when assessing radiant temperature asymmetry, as it could be either vertical or horizontal. However, in this study only vertical radiant temperature asymmetry is relevant, considering that the heat is supplied in a vertical direction in all cases, similar to another study that investigated radiant temperature asymmetry with radiant ceilings and floors (Wang, et al., 2009).

The following types of asymmetric radiation have been classified: cool wall, warm wall, cool ceiling and warm ceiling. Research has found that people feel most uncomfortable when the radiant asymmetry is caused by a warm ceiling or a cool wall (Fanger, et al., 1985). This can be seen in Figure 5, as the curve of the 'warm ceiling' case starts rising much earlier than the other curves. Therefore, the limit for the radiant asymmetry is much lower for cases with a warm ceiling compared to cases with a cool ceiling. The limit for warm ceiling cases is a PPD of 5%, whereas the limit for cool ceiling cases is a PPD of 14% (Wang, et al., 2009). However, a recent study argues that the limit of a PPD of 5% from ASHRAE 55 can be raised to 10%, as the majority of participants in that research still felt a 'neutral' thermal sensation for the majority of their body parts (Safizadeh, Schweiker, & Wagner, 2018). Therefore, in this study a PPD of 5% and 10% are taken as limits to compare how the system performs regarding these two limits.

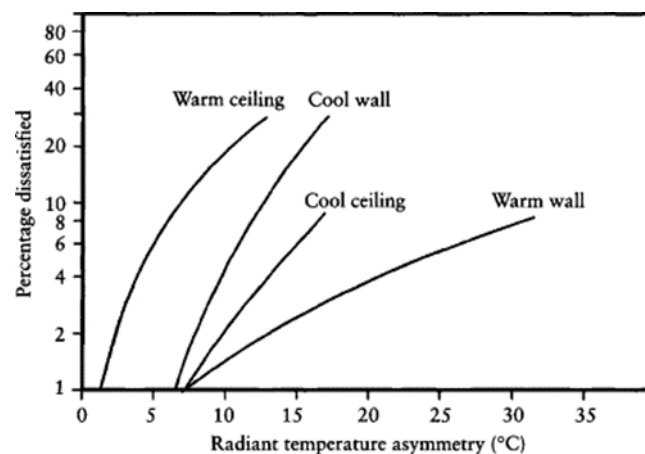


Figure 5: Types of radiant temperature asymmetry and corresponding curves of the PPD (Olesen, et al., 2001)

In order to calculate the T_{pr} , the angle factors of each surface element within the room needs to be determined first, to account for the shape and size of a surface element and its distance to the occupant in a given position within the room (Kehayova, 2014). In this study, two positions are assumed for the occupant: one in the center of the living room and one in the corner, at 0.5 m from both walls. Furthermore, it is assumed that the occupant is in a seated position, which corresponds to a height of 0.6 m for the small plane element that represents the occupant. The angle factors can be calculated in multiple ways, depending on how the occupant is represented. One method for determining the angle factors is by means of ray-tracing, where vectors are distributed throughout the room from a point source in a spherical pattern and the intersections between these vectors and the surfaces within the room can be used to determine the angle factors. A major advantage of this method is that it can be used for rooms with any given geometry. However, a disadvantage associated with this model is that it is computationally intensive (Mackey, Baranova, Petermann, & Menchaca-Brandan, 2017). A second method for determining angle factors is by means of integrating, which can be either area-integration or contour-integration. The latter is significantly more accurate than area-integration (Bopche & Sridharan, 2009).

The last method is the one proposed by Fanger, which is also described in the ASHRAE Fundamentals Handbook (ASHRAE, 2001). It is a relatively simple method, where only parameters need to be known per surface element to determine its angle factor: the height and width of the surface element and the distance between the surface element and the small plane element, which as mentioned represents the occupant. Once the parameters are known, the angle factors can be determined by using the formulae shown in Figure 6. This method is used for this study, as it is less computationally demanding compared to the other methods.

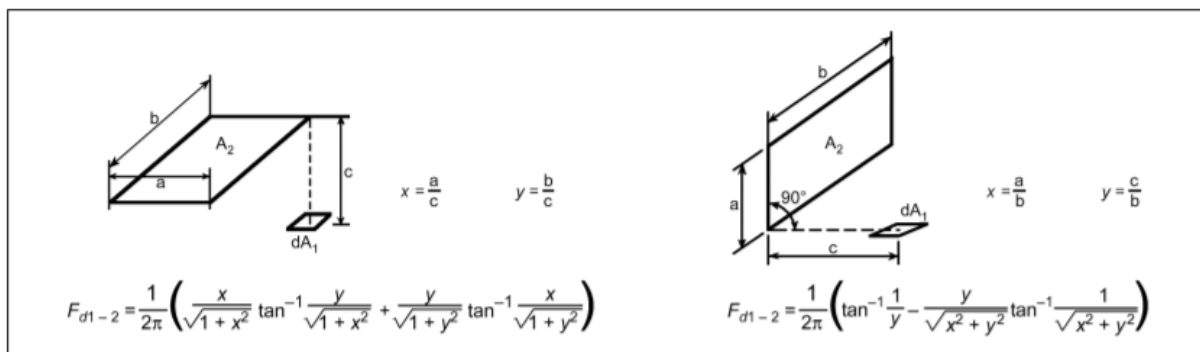


Figure 6: Method for determining angle factors based on their size and position relative to the small plane element dA_1 (ASHRAE, 2001)

With the angle factors known, T_{pr} can be calculated by multiplying the surface temperature of each surface element by its corresponding angle factor relative to the small plane element at the assumed position within the room. This calculation method is described in the ISO 7726 standard (Kehayova, 2014). The following equation is used to determine T_{pr} :

$$T_{pr}^4 = T_1^4 \cdot F_{p-1} + T_2^4 \cdot F_{p-2} + \dots + T_n^4 \cdot F_{p-n}$$

Where T_{pr} is the plane radiant temperature, T_n is the temperature of surface n in Kelvins and F_{p-n} the angle factor between surface n and the small plane element at the assumed position. This calculation process is the same as for the mean radiant temperature (MRT), but in that case T_{pr} has to be calculated for six directions to account for all the surfaces in a room. The positions that are analyzed are shown in appendix V for each of the buildings.

3. Methodology

The methodology of this study and the steps in each phase are shown in Figure 7. In the first part, the literature review is conducted to define the input parameters and key performance indicators. Once these parameters have been defined, a validation study is carried out in order to validate the model for the infrared panel in EnergyPlus. This must be done, as EnergyPlus currently does not contain a validated model for infrared panels. After the model of the infrared panel is validated, the buildings and heating systems are modelled using DesignBuilder software. The models are then exported to EnergyPlus, where occupancy schedules are defined and the simulations are carried out. EnergyPlus also contains the weather file and in this study the weather file for Amsterdam is used.

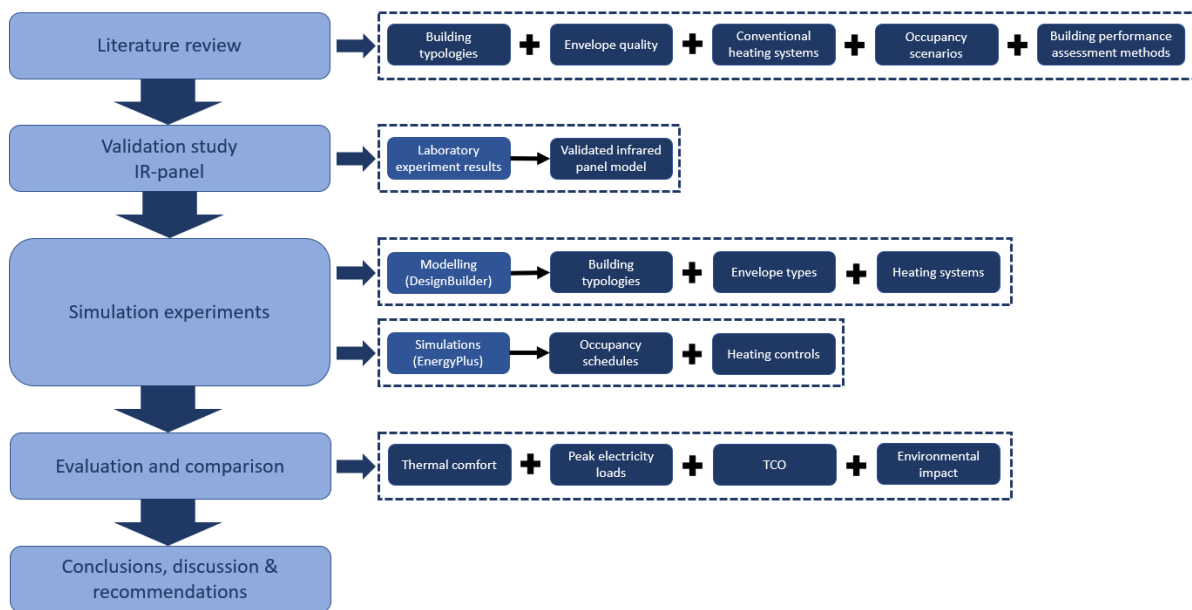


Figure 7: overview of the methodology used to approach this study. The light blue boxes on the left represent the main phases of the study, while the dashed boxes on the right represent the individual steps taken in each phase. Within these dashed boxes, the light blue boxes refer to the 'tools' that are used to model or create the dark blue boxes to which the arrows point.

3.1. Heating system peak loads

The peak loads regarding the energy demand is a key performance indicator that is also considered in this study. The peak loads of each system are compared for each scenario in order to investigate which systems have the lowest peak loads in each scenario. The energy demand is assessed with intervals of 10 minutes and therefore the peak load represents the 10 minute period during which the highest energy demand occurs during the heating season. In this study, the peak load only represents the peak energy demand of the heating system itself, meaning that other electrical equipment such as lighting and appliances are not taken into account for the peak loads.

3.2. Total cost of ownership

The total cost of ownership (TCO) is the fourth key performance indicator that is investigated, as it is important for suppliers and customers to gain insight in the financial performance of each system under different circumstances. For this, the total energy consumption for space heating during the heating season is used to calculate the associated costs for electricity and gas for each heating system. In the Netherlands, the pricing of electricity is based on the energy consumption in kWh and the pricing of gas is based on the energy consumption in m³ gas. In the Netherlands, the energy prices of 2021 are on average € 0.22 per kWh of electricity and € 0.79 per m³ gas (Milieu Centraal, 2021). In this study, it is assumed that the electricity and gas prices remain constant over the lifespan of the systems. However, in real life these prices are likely to increase or decrease relative to the current price. While the lifespan of each system is still mostly unknown, it is estimated that a lifespan of 15 years is achievable for all systems (Meijer & Loonen, 2020) and therefore that is also assumed for this study. For the calculation of the TCO, the investment costs also need to be known. These costs are described in appendix IX.

3.3. Environmental impact

The environmental impact of each system in terms of CO₂-emissions during operation are also calculated as an alternative to energy costs. The reason for this is that energy costs are more likely to vary over time compared to the environmental impact of different fuel sources. The environmental impact may change due to improved fuel extraction methods, but improving those methods may take many years, while energy costs can vary from year to year. The CO₂-emissions can be calculated from the energy consumption by applying emission factors. These factors depend on the type of fuel that is used for heating. For instance, the infrared panels and heat pump use electricity, whilst the gas boiler uses natural gas. The used CO₂-emission factors in this study are shown in Table 5. As with the energy costs, the CO₂-emission factors are assumed to remain constant in this study.

Table 5: CO₂-emission factors for electricity and natural gas (CO₂ Emissiefactoren, 2020)

Fuel type	Unit	CO ₂ -emission factor (kg/unit)
Electricity	kWh	0.556
Natural gas	Nm ³	1.884

3.4. Simulation experiment

An overview of the simulation experiments is provided in Figure 8 below, which describes each of the variables that are investigated for this study.

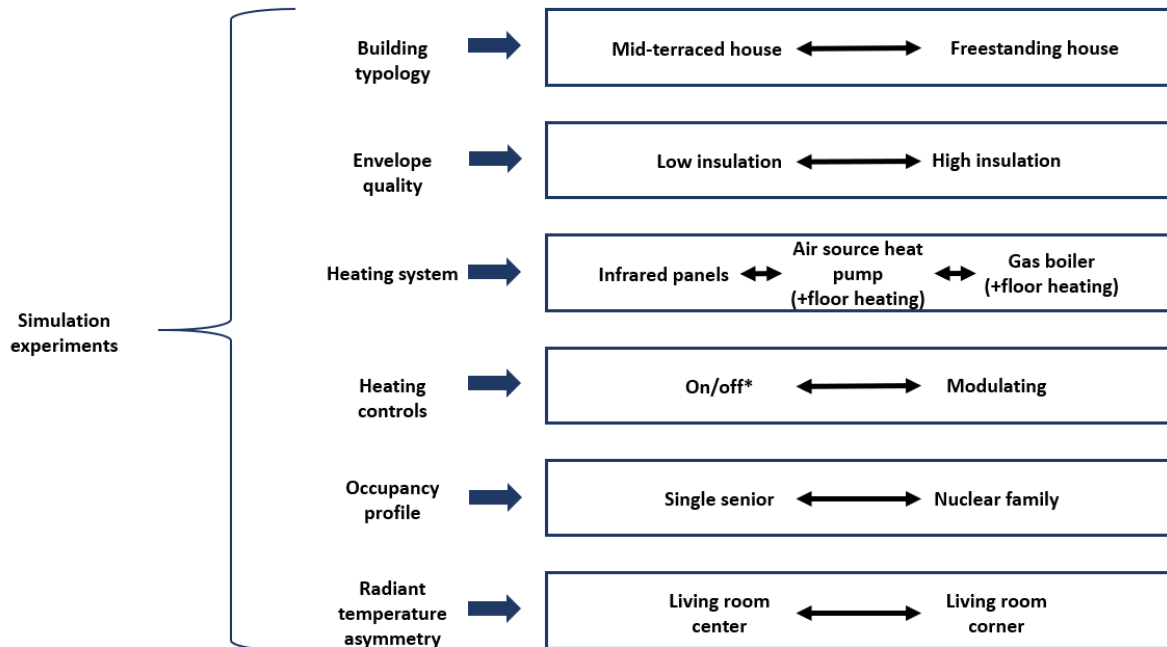


Figure 8: overview of each parameter that is investigated in the simulation experiment. *The on/off control is only used for the infrared panels, as the heat pump and gas boiler are assumed to have modulating controls

3.5. Software

In this study, DesignBuilder software is used to make the models of the houses and define the constructions of the building elements. Furthermore, the models of the infrared panels and the HVAC templates for the heat pump and gas boiler are also defined in DesignBuilder. Energyplus is then used to define the remaining input variables, such as occupancy schedules and the weather file.

3.6. Infrared panel model validation

As stated, the model of the infrared panels in EnergyPlus needs to be validated before the application study, considering there is not yet a standardized model for infrared heating panels available yet. This section describes the steps taken in the validation study.

3.6.1. Boundary conditions

The validation of the infrared heating panel is based on measurements carried out in a laboratory at Eindhoven University of Technology. These measurements were not part of this study and were carried out by researchers involved in the HERSCHEL project. However, the results of these measurements are used for this study with the aim of validating the simulation model of the infrared panel by comparing its performance to the real infrared panel from the measurements. During the measurements, the panel was switched on between approximately 8:30 and 9:20 and then again between 10:30 and 11:15. The controls of the panel consisted of two modes: on and off. This means that the panel operates at its full capacity of 240 W when switched on. The room in which the measurements were performed had the following dimensions: 5.4 x 3.6 x 2.7 m (L x W x H) and is located within one of the buildings of Eindhoven University of Technology. A DesignBuilder model of the laboratory is shown in Figure 9. The walls of the laboratory are assumed to be made of 100 mm EPS insulation with 12 mm of gypsum on either side of the insulation and a lightweight concrete floor is assumed. An ventilation rate of 1 ac/h is assumed and the measurements yielded an indoor temperature of approximately 21°C.

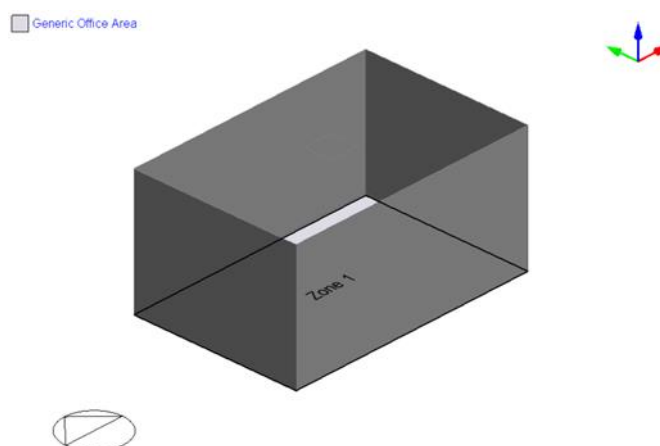


Figure 9: model of the laboratory room in DesignBuilder

3.6.2. Infrared heating panel model

The model of the infrared panel in DesignBuilder is based on earlier research (Biliotti, 2020). The panel is modeled by creating a subsurface in the ceiling and is constructed as shown in Table 6. A visual overview of the panel model with the internal source is shown in Figure 10.

Table 6: layers of the infrared panel. Note that the internal heat source is located between the insulation and ceramic material.

Layer	Thickness (mm)
Air gap	5
Insulation	20
Ceramic material	6

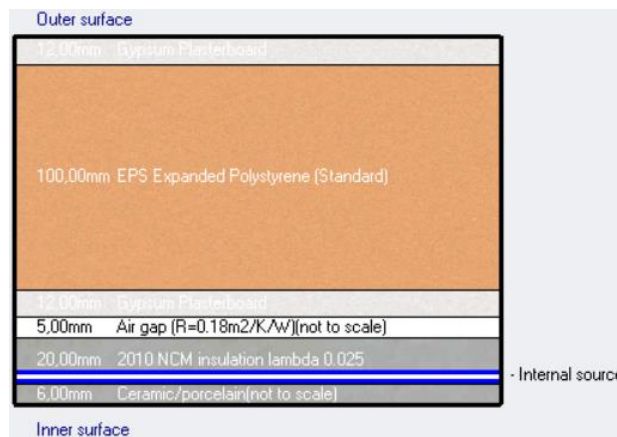


Figure 10: visual overview of the infrared panel model with the ceiling of the laboratory room in DesignBuilder. The 3 upper layers represent the construction of the laboratory room (gypsum – EPS insulation – gypsum), while the 3 lower layers represent the model of the infrared panel (outside to inside: ceramic layer – heat source – insulation).

The other technical details of the infrared panel, such as setpoints and schedules, are specified using EnergyPlus IDF-Editor. A “ZoneHVAC: LowTemperatureRadiant:Electric” unit is selected and applied to the subsurface. The heating setpoint is set at 50 °C to ensure that the panel reaches full capacity once switched on.

3.6.3. Model calibration

In order to achieve a calibrated model that accurately represents the measurement data, multiple variables are considered for adjustment: ceramic layer density, ceramic layer thermal absorptance and the convective heat transfer coefficient near the infrared panel. One calibrated model is created, in which it is assumed that mixed conditions occur with both natural and forced convection. The values of the adjusted variables are shown in Table 7. The reason for not selecting purely forced convection is that the correlations for the heat transfer coefficients for forced convection assume high ventilation rates and jet ventilation, which is not assumed for the laboratory (Peeters, Beausoleil-Morrison & Novoselac, 2011). It is assumed that the air is stably stratified near the ceiling, meaning that the air temperature is lower than the surface temperature of the infrared panel. For natural convection, the stable ceiling equation from Alamdari and Hammond is used and for mixed convection, the stable ceiling equation from Beausoleil-Morrison is used. These equations were compared to other equations that appeared suitable as well, but the curves of the other equations differed too much from the desired curves of the selected equations. The other equations are the ASHRAE equation for

a downward facing heated plate, the Awbi and Hatton equation for partially heated ceilings and lastly the equation for heated ceilings by Min et al (Peeters, Beausoleil-Morrison & Novoselac, 2011). The comparison is based on the temperature difference between the infrared panel surface and the mean air temperature in the room and the results can be seen in Figure 11.

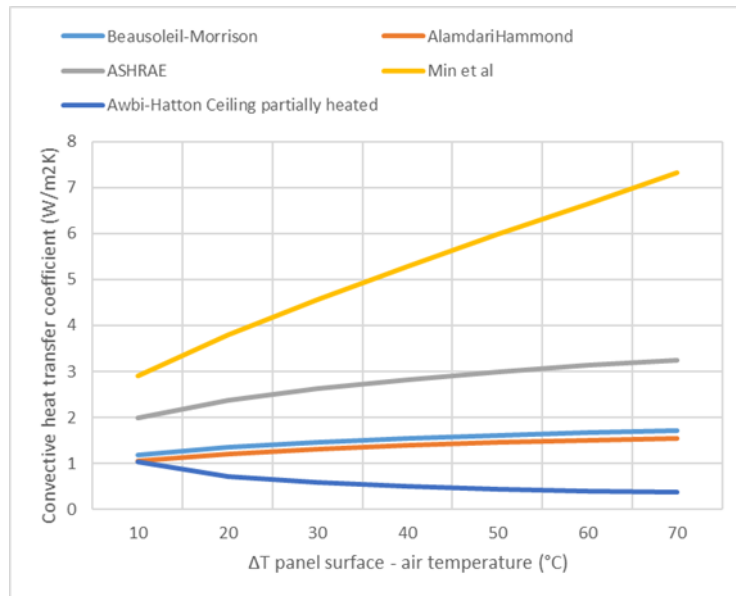


Figure 11: comparison of various correlations for heat transfer coefficients for heated ceilings

Two equations are compared to each other in Figure 12 and it can be seen that both equations show similar results, even if they are meant for different conditions. This can be explained by the fact that the Beausoleil-Morrison equation is partly based on the equation by Alamdari and Hammond (Peeters, Beausoleil-Morrison & Novoselac, 2011). However, in this case the Beausoleil-Morrison equation is used, as it is assumed that both natural and forced convection will play a role.

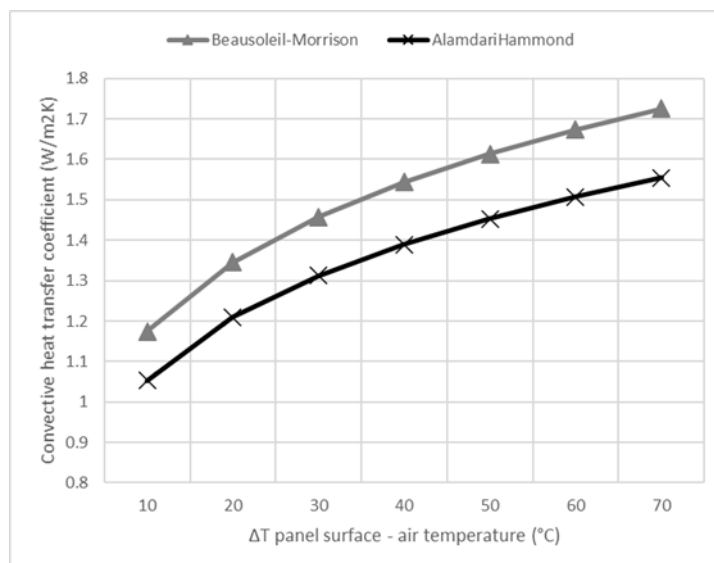


Figure 12: comparison of the Alamdari & Hammond equation with the Beausoleil-Morrison equation.

Lastly, the density, thermal conductivity and specific heat capacity of the ceramic layer of the infrared panel were adjusted in order to match the curves of the measurements as close as possible.

Table 7: overview of relevant variables of the calibrated model

Convection type	Convection correlation	Ceramic layer density (kg/m ³)	Ceramic layer thermal conductivity (W/mK)	Ceramic layer specific heat capacity (J/kg·K)
Mixed	Beausoleil-Morrison	2000	1.7	800

As can be seen in Figure 13, the calibrated model shows a good match with the measurements in terms of the infrared panel surface temperature. This is further proven by the results shown in Table 8, as both the NMBE and Cv(RMSE) are very low and well within the limits set in ASHRAE guideline 14 that states a limit of 10% for the NMBE and 30% for the Cv(RMSE) (ASHRAE, 2014). As the results are well within the limits regarding the NMBE and Cv(RMSE) according to ASHRAE guideline 14, the calibrated model is sufficiently representative of the real infrared panel and can therefore be used for further research in this study.

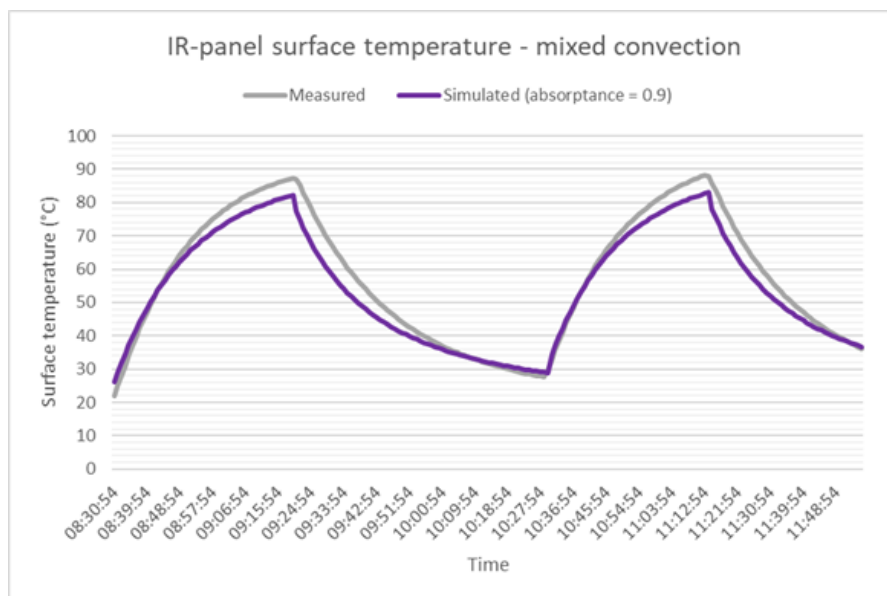


Figure 13: graphs of the measured and simulated panel surface temperature

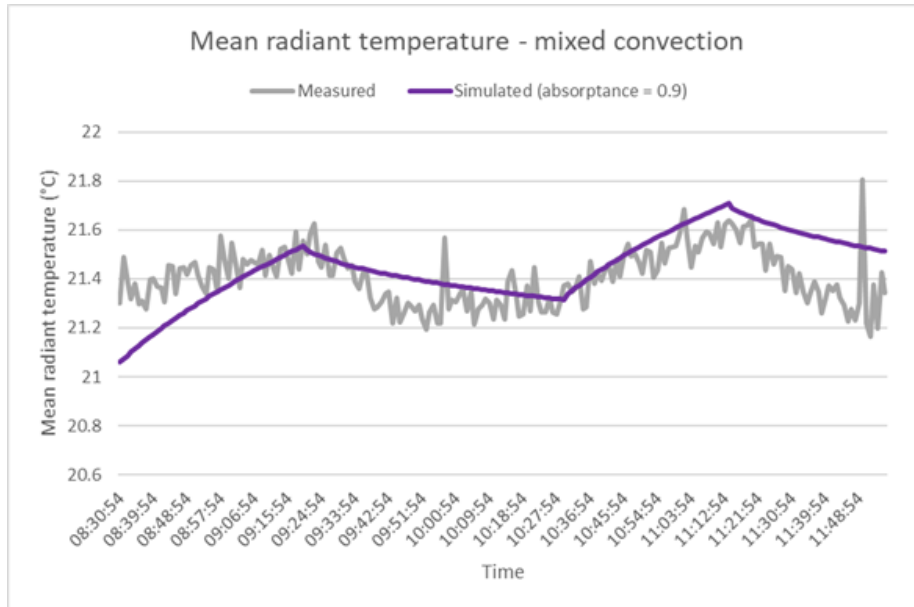


Figure 14: graphs of the measured and simulated mean radiant temperature

Table 8: Normalized Mean Bias Error (NMBE) and Coefficient of Variation of the Root Mean Square Error (Cv(RMSE)) regarding the panel surface temperature and mean radiant temperature

	Panel surface temperature	Mean radiant temperature
NMBE	5.17%	-0.18%
Cv(RMSE)	7.65%	0.64%

4. Results

This section discusses the results from the simulations for the key performance indicators defined in the previous section. The results related to thermal comfort are discussed first, as that is the main focus of this study. The energy aspects are discussed next, with the peak energy loads being the first key performance indicator related to energy. The TCO is also discussed in the form of annual costs and finally the environmental impact of each system is discussed.

4.1. Thermal comfort

The results of the key performance indicators regarding thermal comfort are discussed in this section. First, the operative temperatures in the living room throughout the heating season are compared for each heating system in all cases during the occupied hours. The radiant temperature asymmetry is then discussed by considering the exceedance of the PPD-limits throughout the heating season.

4.1.1. Indoor operative temperature

As stated, the indoor operative temperature is analyzed during the heating season for the occupied hours only. The results regarding the indoor operative temperatures are summarized in the figures below, where in Figure 15 the exceedance of the 10% acceptability limit is shown for all cases and in Figure 16 the same is done for the 20% limit. Overall, the exceedance of the 20% limit is relatively small, as in all cases the exceedance is below 4% of the occupied hours. As for the 10% limit, the exceedance occurs less than 14% of all occupied hours for all cases. Both Figure 15 and Figure 16 show that the exceedance of the comfort limits occurs mainly in the nuclear family scenario. Furthermore, the infrared panels with on/off controls fall outside of the comfort limits longer than the other heating systems. The heat pump with floor heating on the other hand is the system that can keep the indoor operative temperature more within the comfort limits than the other systems.

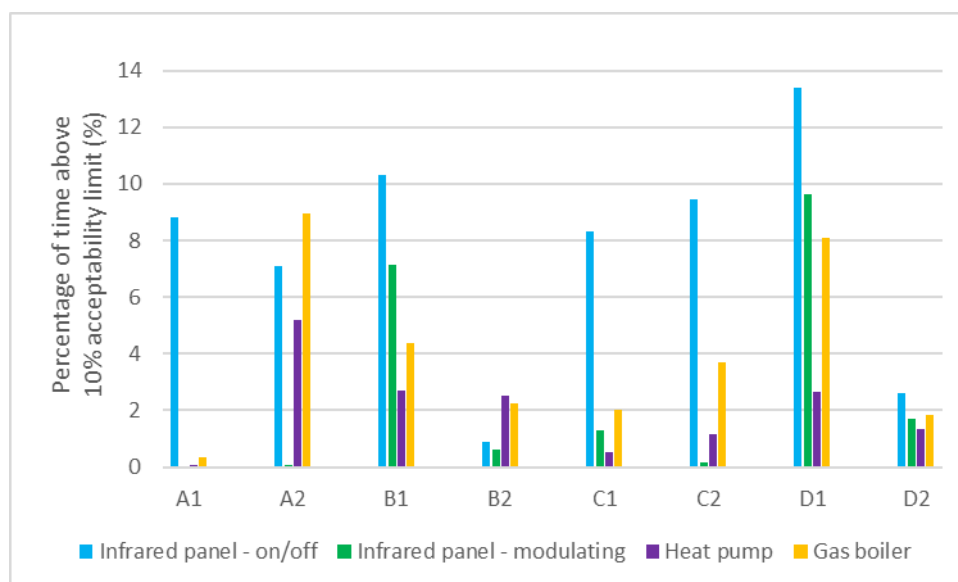


Figure 15: percentage of occupied hours when the indoor operative temperature is outside the 10% acceptability limits for each of the heating systems in all scenarios. The classification is as follows: 'A' is the terraced house with single senior profile, 'B' is the terraced house with nuclear family profile, 'C' is the freestanding house with single senior profile and 'D' is the freestanding house with the nuclear family profile. A '1' indicates a low insulation house and a '2' indicates a high insulation house

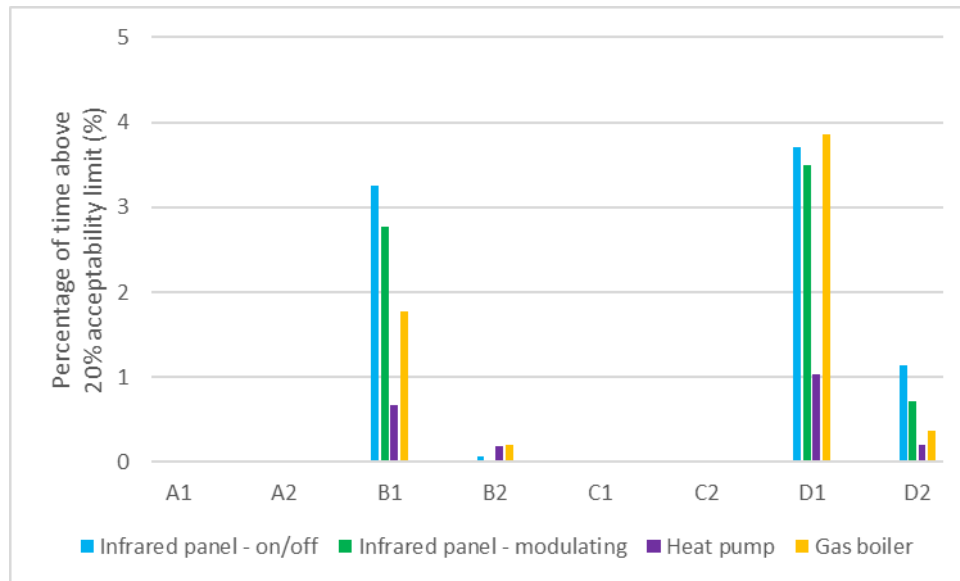


Figure 16: percentage of occupied hours when the indoor operative temperature is outside the 20% acceptability limits for each of the heating systems in all scenarios. The classification is as follows: 'A' is the terraced house with single senior profile, 'B' is the terraced house with nuclear family profile, 'C' is the freestanding house with single senior profile and 'D' is the freestanding house with the nuclear family profile. A '1' indicates a low insulation house and a '2' indicates a high insulation house

Figure 17 shows the indoor temperature in a more detailed way for the single senior profile in the low insulation terraced house, with the indoor temperature shown for corresponding reference outdoor air temperature and the thermal comfort limits. Similarly, Figure 18 and Figure 19 show these results for the nuclear family in the terraced house, but Figure 19 contains the results of the high insulation case, as there is some difference compared to the low insulation case shown in Figure 18. Similar graphs are made for all other cases, which can be found in appendix VI. As can be seen, the indoor operative temperatures of the single senior household are within a larger range compared to the nuclear family household. This is consistent with the setpoint temperatures, as the nuclear family has a constant setpoint temperature of 20 °C during the occupied hours, while in the case of the single senior household the setpoint varies from 22 to 24 degrees during the occupied hours. Furthermore, in Figure 17 the results show that the heat pump is capable of maintaining a more consistent operative temperature than the other heating systems. In Figure 18, at a reference outdoor temperature of approximately 14 °C, the infrared panels maintain 20 °C operative temperature in the low insulation case, whilst the other heating systems cause higher operative temperatures. However, in the case of high insulation, all heating systems cause higher operative temperatures, as can be seen in Figure 19.

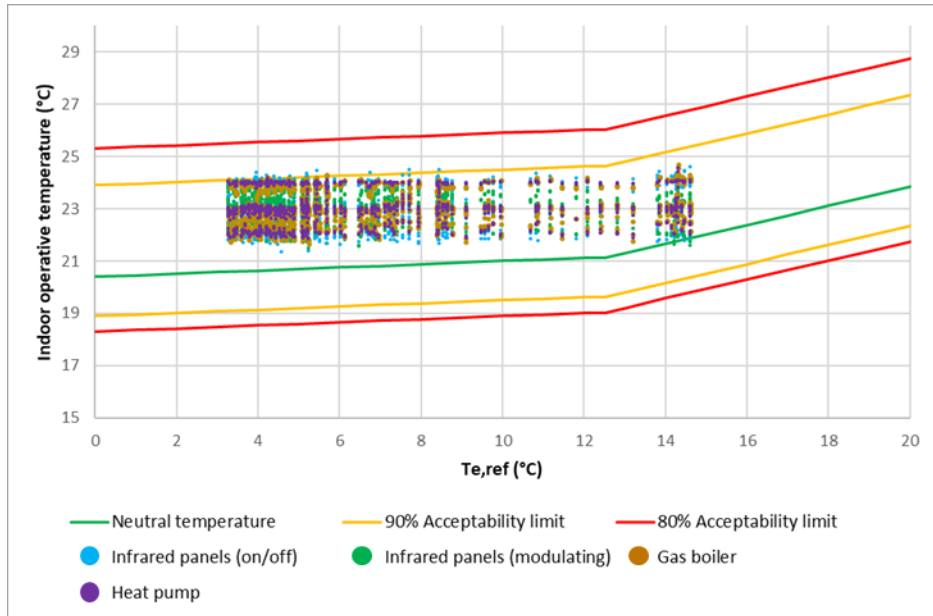


Figure 17: Operative temperatures in the living room throughout the heating season during the occupied hours for all heating systems in the low insulation terraced house for single senior

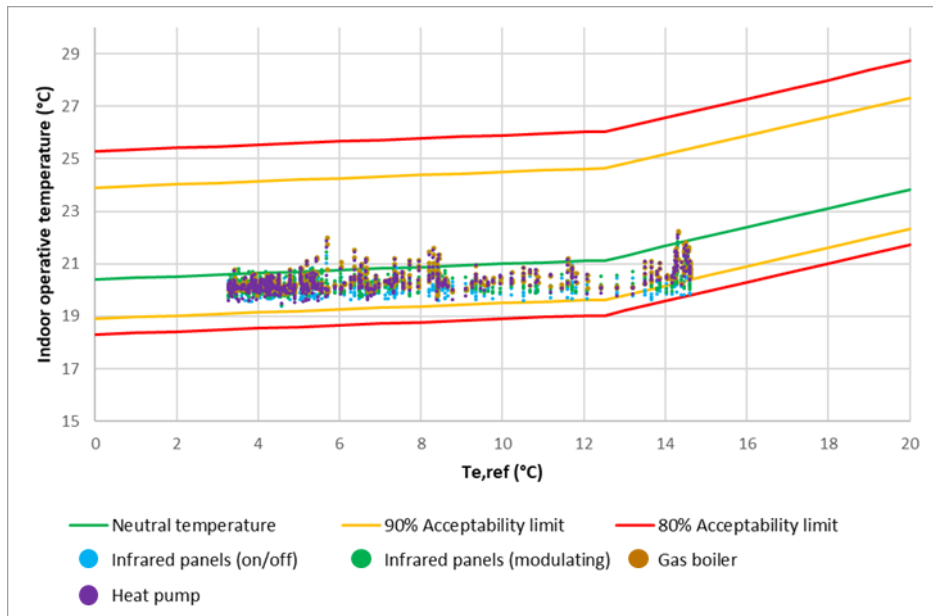


Figure 18: Operative temperatures in the living room throughout the heating season during the occupied hours for all heating systems in the low insulation terraced house

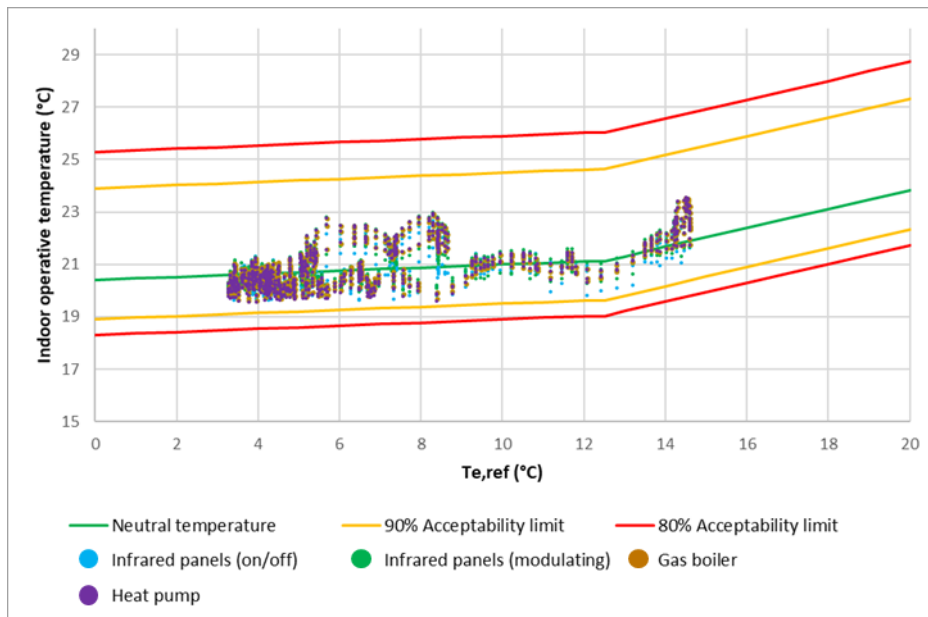


Figure 19: Operative temperatures in the living room throughout the heating season during the occupied hours for all heating systems in the high insulation terraced house

4.1.2. Radiant temperature asymmetry

This section contains the results regarding radiant temperature asymmetry, by focusing on the percentage of time that the PPD-limits of 5% and 10% are exceeded during the heating season. Boxplots showing the amount of exceedance above the limits in terms of temperature are shown in appendix VII. The heat pump and gas boiler with floor heating never exceeded the comfort limit of 14% and are therefore not included here. The radiant temperature asymmetry in low insulation houses is higher compared to high insulation houses. This can be explained by the fact that low insulation houses have higher heat losses, causing the floor surface to cool down faster compared to high insulation houses. This in turn leads to a greater difference between the ceiling and floor temperature than the high insulation houses, causing higher radiant temperature asymmetry. In position 2 the PPD as a consequence of radiant temperature asymmetry is always lower compared to position 1, but in general the difference in PPD between the two positions is smaller in the high insulation buildings than in the low insulation buildings. As for the comparison between the two control strategies, the infrared panels with on/off controls result in a lower PPD in all low insulation cases compared to infrared panels with modulating controls, while the opposite happens in the high insulation cases.

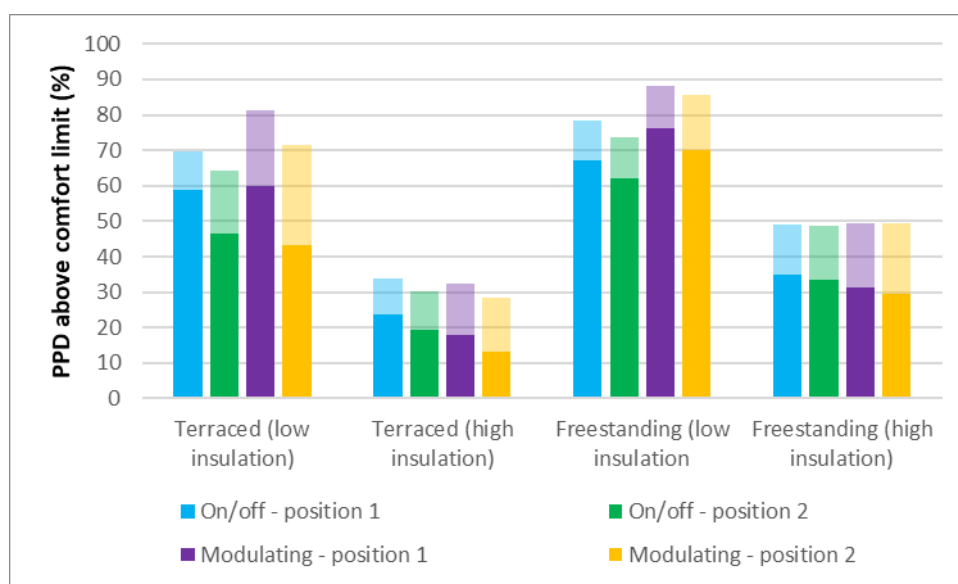


Figure 20: Exceedance of the PPD-limits regarding radiant temperature asymmetry during occupied hours for the single senior household. The transparent parts at the top represent the exceedance above the 5% limit and the opaque part represents the exceedance above the 10% limit

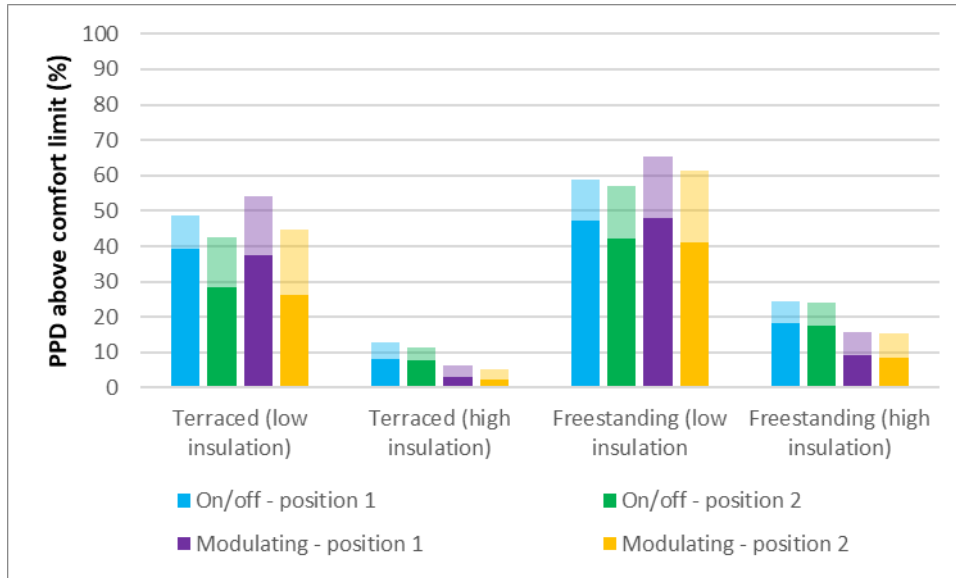


Figure 21: Exceedance of the PPD-limits regarding radiant temperature asymmetry during occupied hours for the nuclear family household. The transparent parts at the top represent the exceedance above the 5% limit and the opaque part represents the exceedance above the 10% limit

Figure 23 and Figure 24 show the distribution of ΔT_{pr} throughout the heating season for the terraced house in the case for both profiles, with Figure 22 showing the results of the single senior scenario and Figure 23 and Figure 24 for the nuclear family. The results of Figure 22 and Figure 23 show that ΔT_{pr} is well above the 5% and 10% comfort limits during many occupied hours in the case of a low insulated terraced house. The exceedance of the comfort limits is significantly higher in the case of the single senior scenario compared to the nuclear family scenario, which is due to the higher thermostat setpoints of the single senior. However, Figure 24 shows that for a high insulated terraced house, the ΔT_{pr} is well below both comfort limits for the majority of the occupied hours.

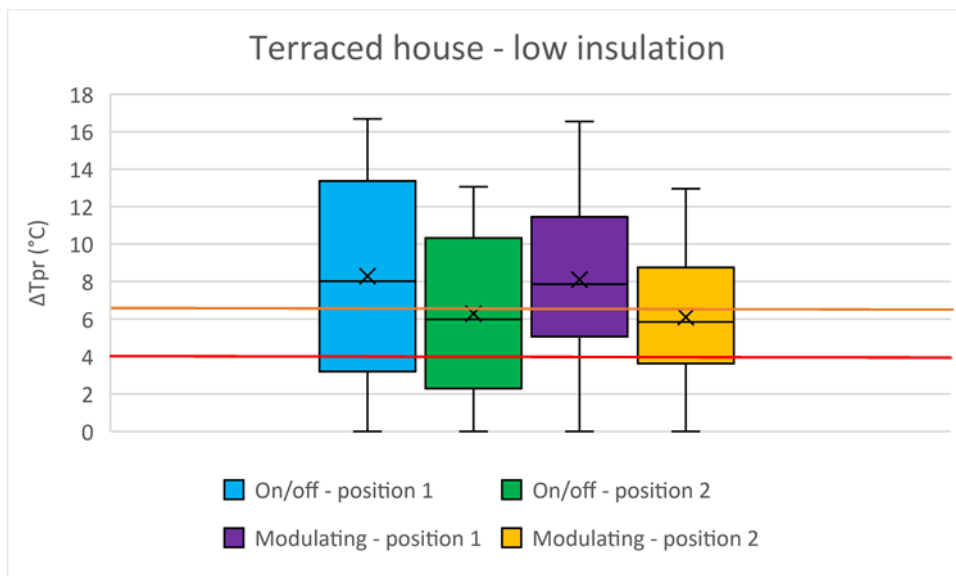


Figure 22: Difference in plane radiant temperature between the ceiling and the floor throughout the heating season for the infrared panels at different positions in the single senior scenario, taking into account both control types. The dark orange line represents a PPD of 10% and the red line a PPD of 5%

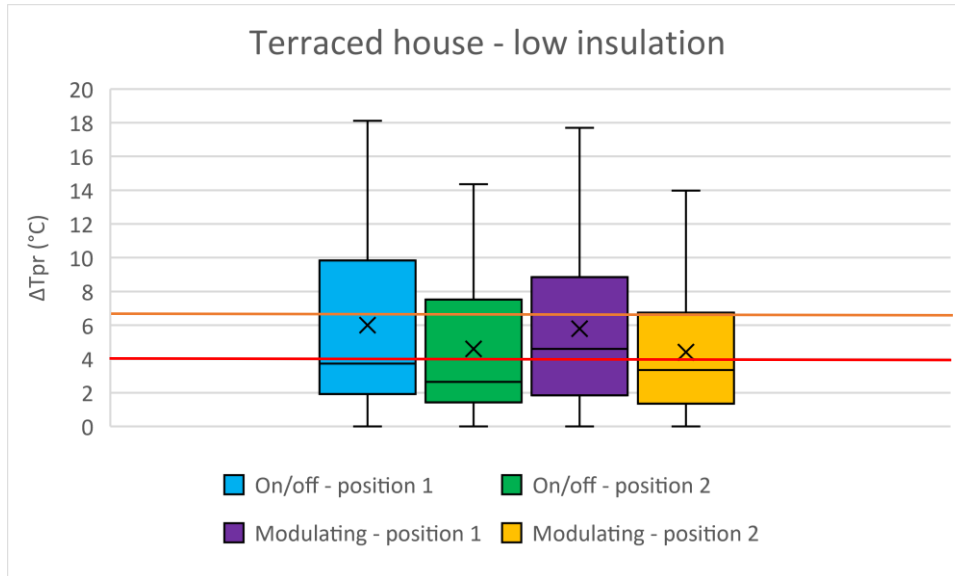


Figure 23: Difference in plane radiant temperature between the ceiling and the floor throughout the heating season for the infrared panels at different positions in the nuclear family scenario, taking into account both control types. The dark orange line represents a PPD of 10% and the red line a PPD of 5

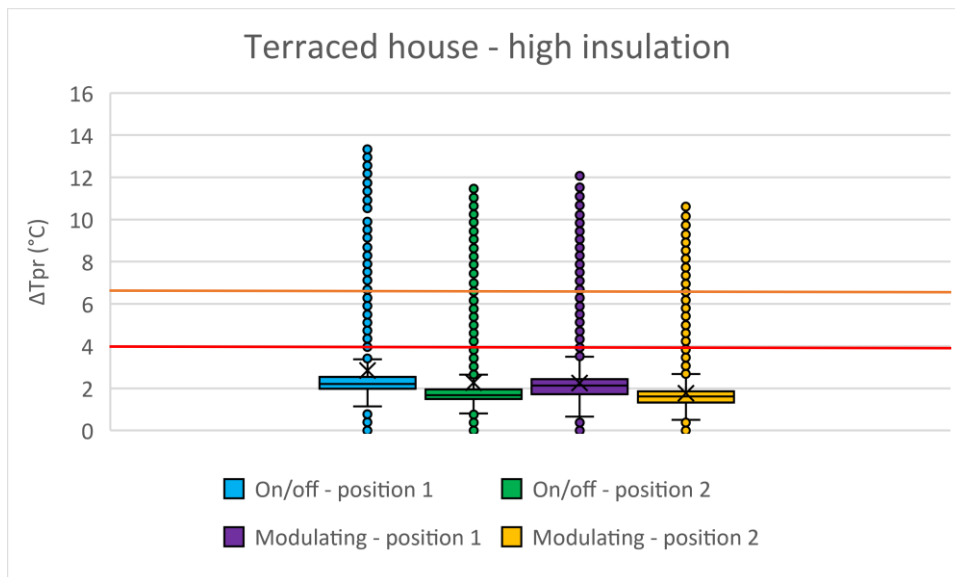


Figure 24: Difference in plane radiant temperature between the ceiling and the floor throughout the heating season for the infrared panels at different positions in the nuclear family scenario, taking into account both control types. The dark orange line represents a PPD of 10% and the red line a PPD of 5

4.2. Heating system peak loads

This section covers the results of the peak loads for each heating system. The results are shown in the two figures below, with Figure 25 containing the results for the single senior household and Figure 26 for the nuclear family. The load duration curves of the infrared panels are shown in appendix VIII for further details between the two control types. The results show very high peaks for the gas boiler compared to the other heating systems. However, when comparing the heat pump with the infrared panels, both consuming electricity, the results are quite similar as the heat pump always has lower peak loads compared to the infrared panels.

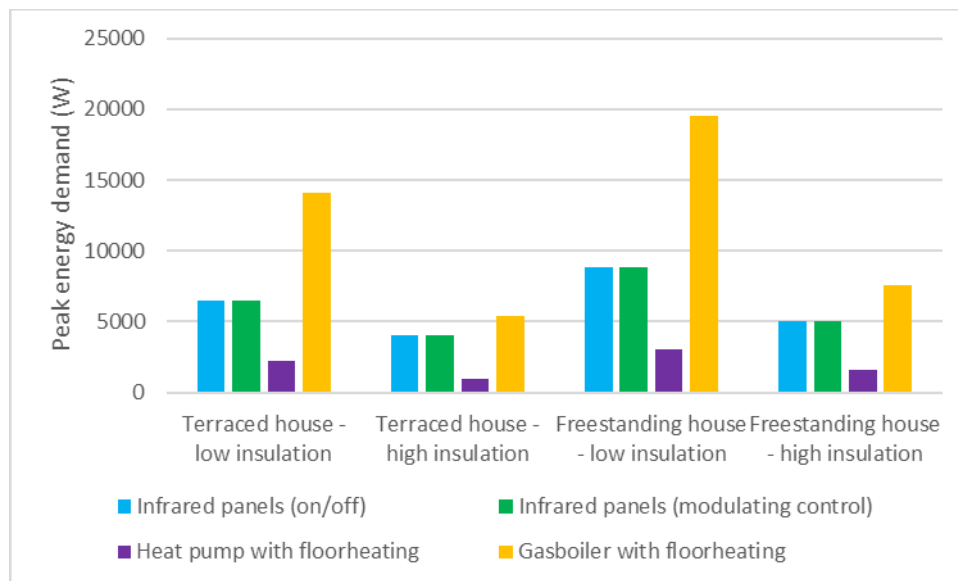


Figure 25: Heating system peak loads for all systems in the case of a single senior household

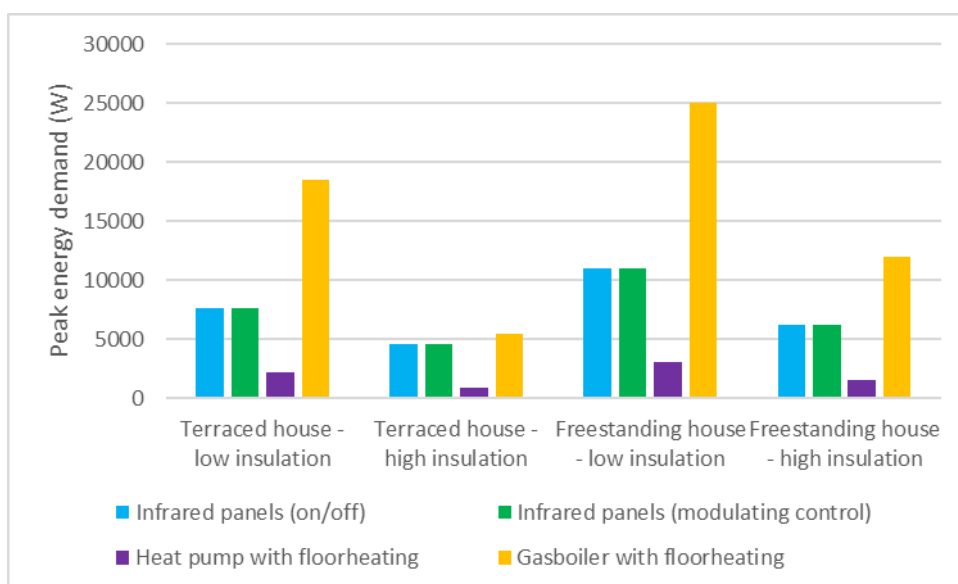


Figure 26: Heating system peak loads for all systems in the case of a nuclear family household

4.3. Operational costs and TCO

The energy costs associated with the energy consumption during the heating system are covered in this section. Figure 27 shows the results of the terraced house and Figure 28 shows the results of the freestanding house. The infrared panels have the highest operational costs in all scenarios, while the heat pump has the lowest operational costs overall. In high insulation dwellings the cost is lower compared to low insulation dwellings. Furthermore, the nuclear family has lower energy costs than the single senior. The operational energy costs are also lower in the terraced house overall. This is true for the assumed price, but as mentioned earlier this study does not investigate future pricing scenarios, which could lead to higher or lower energy prices.

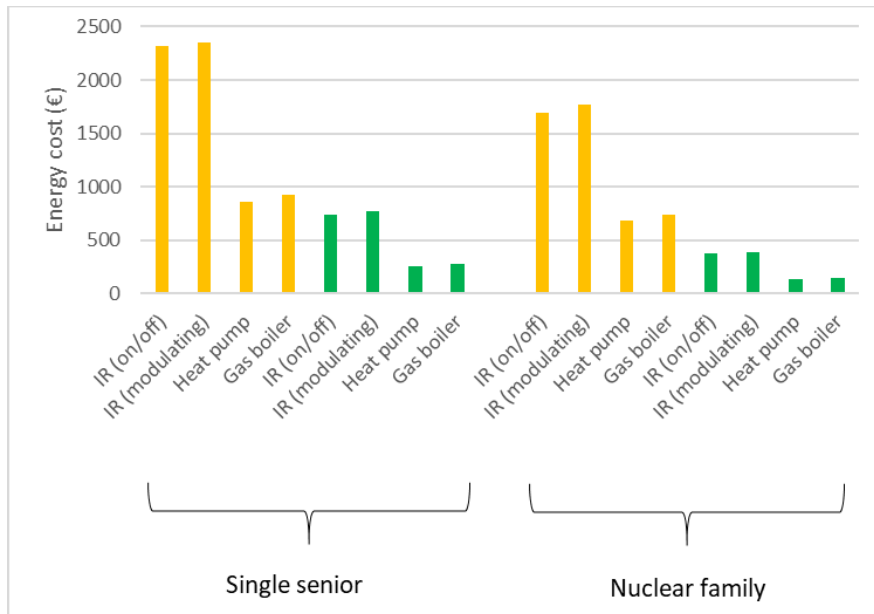


Figure 27: Annual energy costs for each heating system for a terraced house. The yellow bars represent the low insulation variants and the green bars the high insulation variants

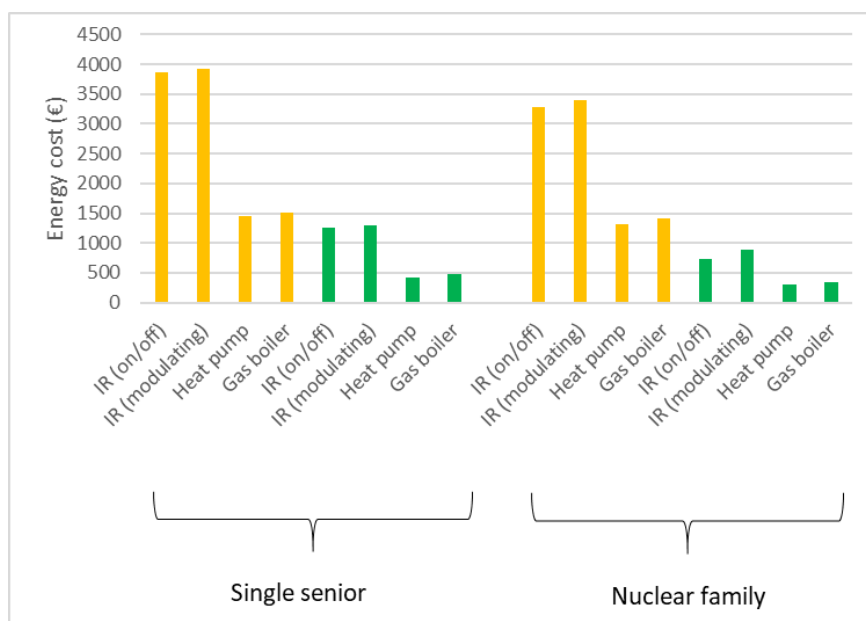


Figure 28: Annual energy costs for each heating system for a freestanding house. The yellow bars represent the low insulation variants and the green bars the high insulation variants

When considering the TCO, the performances are more dependent on the scenario, as shown in Figure 29 and Figure 30. For instance, in all low insulated dwellings, the infrared panels have the highest TCO, whilst the high efficiency gas boiler has the lowest TCO. When considering the high insulation terraced houses, the infrared panels have a lower TCO compared to the heat pump. Furthermore, in the case of a nuclear family in the high insulated terraced house, the infrared panels have the lowest TCO of all evaluated heating systems. With regard to the freestanding house, the infrared panels have the highest TCO in almost all scenarios as can be seen in Figure 30, except for a high insulation variant with a nuclear family, in which case the heat pump has a slightly higher TCO compared to the on/off controlled infrared panels.

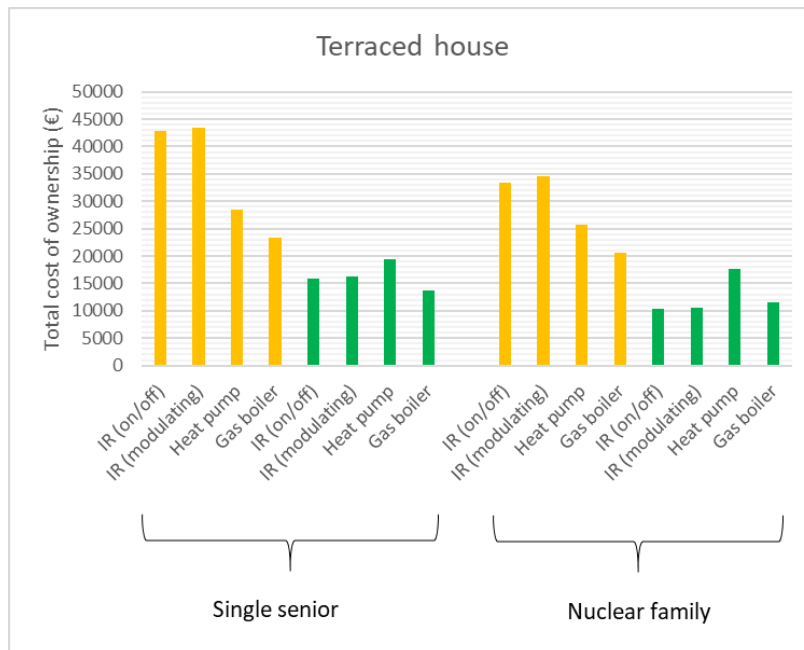


Figure 29: TCO for each heating system for a terraced house over a 15 year lifespan. The yellow bars represent the low insulation variants and the green bars the high insulation variants

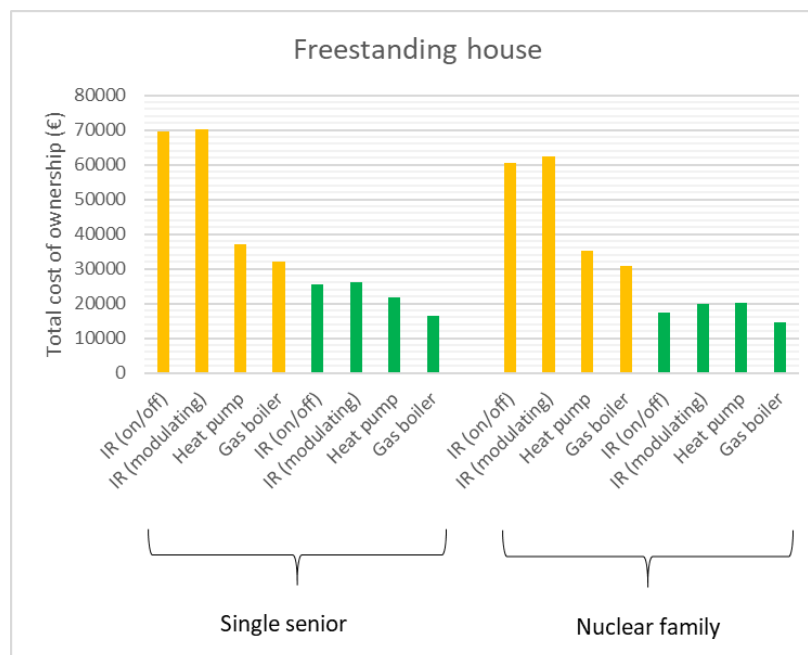


Figure 30: TCO for each heating system for a terraced house over a 15 year lifespan. The yellow bars represent the low insulation variants and the green bars the high insulation variants

4.4. Environmental impact

This CO₂-emissions for the entire heating season for each of the heating systems are shown in this section. Figure 31 shows the results for the terraced house and Figure 32 shows the results of the freestanding house. The infrared panels have the highest operational carbon emissions in all scenarios, whilst the heat pump has the lowest operational carbon emissions. As with the energy costs, the environmental impact is lower in high insulation dwellings and also lower in scenarios with the nuclear family profile. Moreover, the carbon emissions are significantly higher in the freestanding house. It should be noted that this is true only if the emissions from the electricity imported from the grid and gas remain at the assumed values.

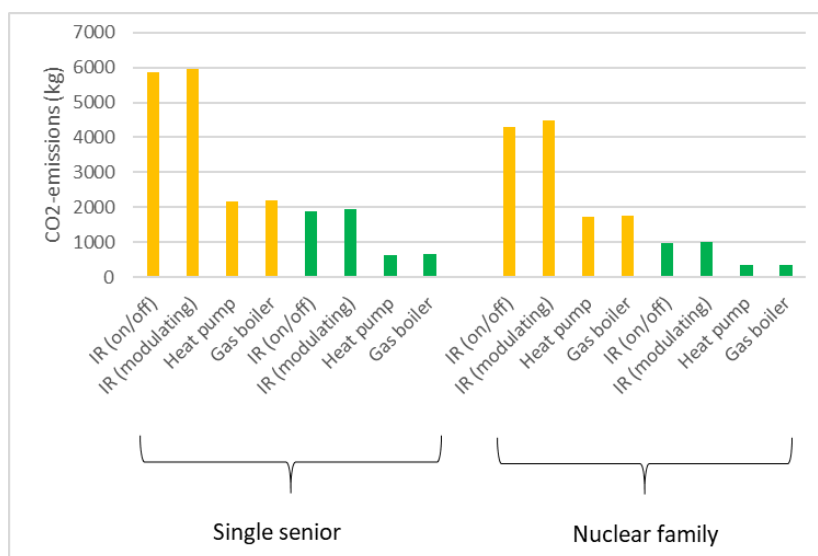


Figure 31: CO₂-emissions for each heating system for a terraced house. The yellow bars represent the low insulation variants and the green bars the high insulation variants

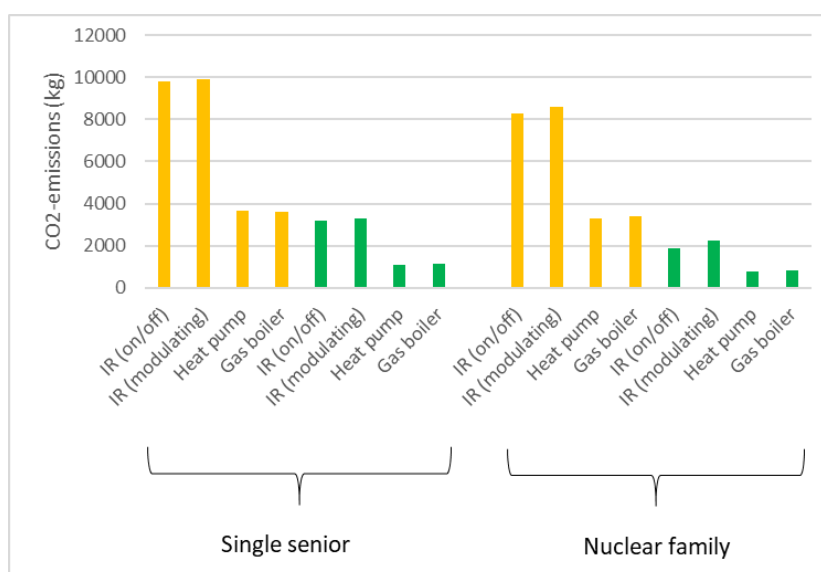


Figure 32: CO₂-emissions for each heating system for a freestanding house. The yellow bars represent the low insulation variants and the green bars the high insulation variants

5. Discussion

The results of the indoor operative temperature show that the infrared panels in the nuclear family scenario at a reference outdoor temperature of approximately 14 °C maintain an indoor operative temperature of 20 °C, whilst the other heating systems cause higher operative temperatures. A possible explanation is that underfloor heating also creates heat transfer in the form of convection.

Regarding radiant temperature asymmetry, a limitation in this study is the way the human body is represented. A small plane surface is used to represent the human body, which is in accordance with the method developed by Fanger to determine the angle factors, as mentioned in the ASHRAE 55 standard (ASHRAE, 2001). However, it is obvious that the human body is far more complex than a simple plane element and therefore a recommendation for further research is to investigate different ways of representing the human body more accurately. This has been done in other studies, but it should be noted that it also takes significantly more time to make assessments with more accurate models (Su, Wang, Xu, & Liu, 2020). Another point of concern is the influence of windows on radiant temperature asymmetry in a room. In this study, only vertical radiant asymmetry is analyzed, because PPD calculations for the used method can only be done for plane radiant temperature differences in one direction, for instance the interaction between the ceiling and the floor or one wall and its opposite wall. However, future research should also include the effect of windows, as it may influence the perceived thermal comfort. It might be necessary to perform a real life test with occupants similar to what Fanger did in his original study into thermal comfort. That way, effects of different cases that are currently viewed separately, such as 'warm ceiling' or 'cool wall', can be combined.

The sensitivity of occupants to radiant temperature asymmetry also remains a point of discussion. The current standards ASHRAE 55 and ISO 7730 are quite strict with a limit of 5% regarding the PPD. However, standards regarding radiant temperature asymmetry appear to be mostly based on Fanger's studies from the 80s, while more recent studies indicate that less stringent limitation regarding the PPD are also suitable. For instance, one study concluded that a PPD between 5% and 40% can still be considered acceptable in case of non-uniform environments, since the thermal sensation of occupants is still neutral under those circumstances (Zhang & Zhao, 2007). It is noteworthy however, that this study was carried out in cooling conditions, while this study focuses on heating, which may influence the occupant's thermal sensation differently compared to cooling.

When considering thermal comfort, one should be careful to draw conclusions from the results. The standard methods for calculating PPD does not take into account differences in types of occupants. For instance, this study compares a nuclear family with an elderly person, while both occupant types have different thermostat setpoints. As the single senior has higher thermostat setpoints, it can be expected that the radiant asymmetry is also higher and lasts longer, because the infrared panels need to be switched on for longer and therefore the ceiling temperature remains high for a longer duration of time compared to the nuclear family profile. It could be that elderly people may not feel uncomfortable when the PPD of 5% is exceeded. One study argues that elderly people perceive thermal comfort differently from younger people due to differences in behavior and physical ageing and that the current PMV/PPD model is not entirely accurate for elderly people (Van Hoof & Hensen, 2006). Another study states that current standards often underpredict thermal comfort of elderly people and suggests a new model with a lower error rate (Hughes, Natarajan, Liu, Chung, & Herrera, 2019).

The energy consumption (and thus also the associated energy costs) of the infrared panels with modulating controls is higher those with on/off control in all cases. This appears to be counterintuitive, as modulating controls were expected to result in energy savings compared to on/off controls. However, the cause of this result is most likely in the control scheme of the on/off controls. In this study, the on/off control scheme allows the indoor operative temperature to vary between 0.5 °C below and 0.5 °C above the setpoint temperature. This range may be fairly large compared to the modulating controls, which is controlled in such a way that the indoor operative temperature is almost constantly at the setpoint temperature. As can be seen in Figure 33 and Figure 34, the mean radiant temperature and mean air temperature in the living room are on average almost equal between both systems, which implies that the control strategies are correct. The same behavior is seen in the other rooms as well, so that does not explain the difference in energy consumption. However, the on/off controls switch continuously between on and off as can be seen in both figures, which means that perhaps the lower energy consumption is caused by the periods when the infrared panels are switched off.

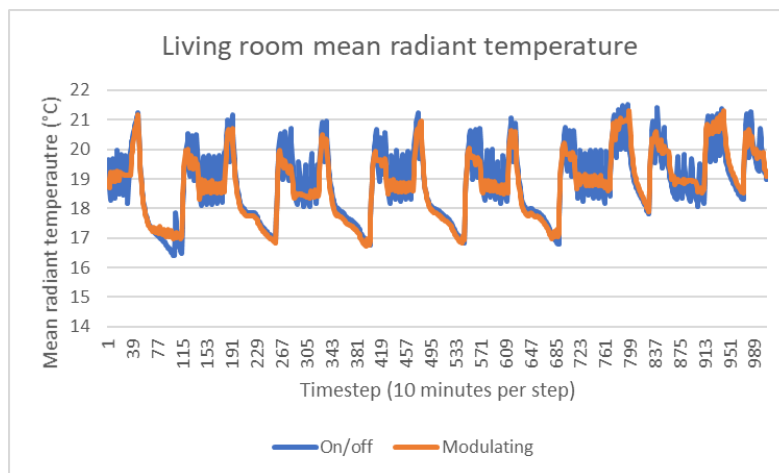


Figure 33: living room mean radiant temperature for both control types of the infrared panel between 8 and 14 January in the low insulation terraced house with a nuclear family

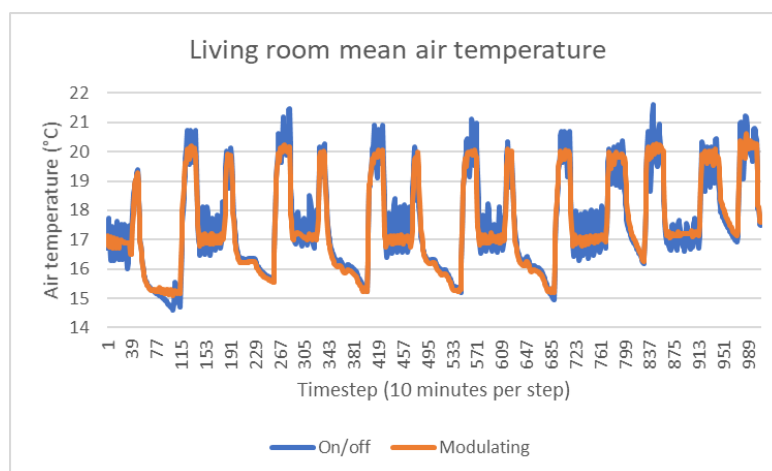


Figure 34: living room mean air temperature for both control types of the infrared panel between 8 and 14 January in the low insulation terraced house with a nuclear family

As for the TCO, the infrared panels always have higher operational costs compared to the heat pump and gas boiler. However, when comparing the investment costs, the infrared panels are cheaper than the conventional solutions. The investment costs of conventional solutions are higher due to the fact that a heat source, which can be the heat pump or gas boiler, is required and also a terminal unit, which in this case is the underfloor heating system. As the infrared panels operate fully on electricity, future research should investigate the benefits of using renewable energy sources such as PV-panels in order to assess if infrared panels would be a more viable alternative to conventional heating systems under those circumstances.

In preparation for this research, models were made in DesignBuilder for other building typologies: an apartment and a semi-detached house. Due to time constraints, these typologies were not investigated any further. However, future studies should also consider for instance an apartment, as it has the lowest heat loss of any building typology and may therefore be more suitable for infrared panels. The results of this study show that a terraced house is more suitable for infrared panels than a freestanding house, so based on these findings it is likely that an apartment is equally if not more suitable for infrared panels compared to a terraced house. Moreover, more occupancy profiles were initially selected for this study, but once again not selected due to time constraints. As with the typologies, it is recommended for future research to also include different occupancy profiles.

This study focused on heating by infrared panels and floor heating, but a suggestion for further research would be to investigate different ways of heating, such as radiators. This was initially done for this study, but time limitations made it difficult to include this as well. Moreover, the effects of having objects between the infrared panels and the occupant needs to be assessed. As it is a radiant system, infrared panels heat surfaces directly, but if there is an object between the panel and the occupant, the occupant might not feel the heat from the panel sufficiently. A manufacturer states that no object should be placed within 400 mm of the front of the panel as the system would not work sufficiently if done so (Herschel Infrared Ltd, 2014).

A final recommendation for future research is a more general one, namely to investigate thermal comfort in houses. Assessment methods for thermal comfort appear to be scarce and as mentioned earlier, thermal comfort models often do not account for different types of occupants. It is important to make a distinction between occupants, for instance in terms of age. Furthermore, some studies argue that the limits for radiant temperature asymmetry of overhead heating might be too strict (Safizadeh, Schweiker, & Wagner, 2018) and therefore future research should investigate if the limits could be more higher, which could make infrared panels more suitable as an alternative to underfloor heating.

6. Conclusion

This study presents a research into the feasibility of infrared panels for space heating in Dutch dwellings as an alternative to heat pumps and gas boilers with floor heating. The main focus is on thermal comfort in the indoor environment, by considering the indoor operative temperature and local thermal discomfort in the form of radiant temperature asymmetry. Besides thermal comfort, this study also takes into account peak energy loads, TCO and the environmental impact of these heating systems during the heating season.

Regarding the indoor operative temperatures, all systems are capable of maintaining the desired setpoint temperatures relatively well. Therefore, the indoor operative temperature stays within the 80% acceptability limits most of the time for both the single senior household and nuclear family household. The modulating controls appear to perform better than the on/off controls, as the on/off controls sometimes lead to either too high or too low operative temperatures. However, the heat pump provides the most consistent indoor operative temperatures off all investigated heating systems. As for radiant temperature asymmetry, floor heating results never exceeds the comfort limits, due to occupants being less sensitive to underfloor heating compared to overhead heating. Infrared panels exceed the comfort limits to various degrees, depending on the situation. In general, infrared panels perform significantly better in high insulation houses. Moreover, the radiant temperature asymmetry is lower when modulating controls are used in high insulation houses. In terraced houses the radiant temperature asymmetry is lower compared to freestanding houses. With respect to the difference between the two households, the nuclear family profile results in less radiant temperature asymmetry compared to the senior household. This implies that lower setpoint temperatures are recommended when using infrared panels in order to reduce local thermal discomfort.

As for the peak energy loads, the heat pump has the lowest peak loads, followed by the infrared panels and lastly the gas boiler. The results of the peak loads follow a similar pattern to those of the radiant temperature asymmetry, meaning that high insulation houses have lower peak loads and that overall terraced houses have the lowest peak loads. However, the nuclear family has higher peak loads than the single senior family due to the fact that more rooms are occupied in the nuclear family household. When considering the energy costs, infrared panels have higher operational costs than the heat pump and gas boiler. However, the TCO of infrared panels is lower in high insulated terraced houses compared to the heat pump with floor heating. The comparatively low investment costs of infrared panels can be a major advantage in high insulation dwellings as it causes a lower TCO for the infrared panels than the other heating systems. Similarly, the operational CO₂-emissions are higher for the infrared panels compared to the heat pump and gas boiler. Overall, the simulations show that heat pumps and high efficiency gas boilers outperform and infrared panels in the investigated scenarios. Heat pumps can provide a more consistent indoor operative temperature, whilst gas boilers have a lower TCO in all cases. The use of infrared panels is recommended only for high insulated terraced houses, as that yields the lowest TCO and the highest degree of thermal comfort. Regarding freestanding houses, it is advised to only use infrared panels in high insulated dwellings as well, although the benefit is smaller compared to terraced houses. Furthermore, the use of lower setpoints is recommended over higher setpoints in order to reduce the chance and degree of local thermal discomfort.

References

- Agentschap NL. (2013). *Referentiewoningen nieuwbouw 2013*. Sittard: Agentschap NL.
- ASHRAE. (2001). *ASHRAE HVAC 2001 Fundamentals Handbook*. Atlanta: American Society of Heating, Refrigerating and Air-Conditioning Engineers.
- ASHRAE. (2014). *Measurement of Energy, Demand, and Water Savings*. ASHRAE.
- Barker, M. (2002). Using infrared heating. *Plant Engineering*, 34-36.
- Big Ladder. (2018, April 16). *Group – Internal Gains (People, Lights, Other internal zone equipment)*. Retrieved from Big Ladder: <https://bigladdersoftware.com/epx/docs/8-9/input-output-reference/group-internal-gains-people-lights-other.html>
- Biliotti, F. (2020). *Performance assessment of heating solutions for Dutch residential houses: evaluation of IR-panels systems and comparison with heat pumps and low-temperature heating*. Eindhoven: Eindhoven University of Technology.
- Bopche, S., & Sridharan, A. (2009). Determination of view factors by contour integral technique. *Annals of Nuclear Energy*, 1681-1688.
- CO2 Emissiefactoren. (2020, August 9). *Lijst emissiefactoren*. Retrieved from CO2 Emissiefactoren: <https://www.co2emissiefactoren.nl/lijt-emissiefactoren/>
- Cvketel-Weetjes. (2015, March 13). *Kosten hr-ketel*. Retrieved from Cvketel-Weetjes: <https://www.cvketel-weetjes.nl/kosten-cv-ketel/hr-ketel-kosten/>
- Damaskou, M. (2016). *Impact of different heat gains due to improved appliance efficiency on a building which meets the Passivhaus Standards*. Glasgow: University of Strathclyde, department of mechanical and aerospace engineering.
- Dudkiewicz, E., & Jeżowiecki, J. (2009). Measured radiant thermal fields in industrial spaces served by high intensity infrared heater. *Energy and Buildings*, 27-35.
- Fanger, P., Ipson, B., Langkilde, G., Olesen, B., Christensen, N., & Tanabe, S. (1985). Comfort Limits for Asymmetric Thermal Radiation. *Energy and Buildings*, 225-236.
- Ferrarini, G., Fortuna, S., Bortolin, A., Cadelano, G., Bison, P., Person, F., & Romagnoni, P. (2018). Numerical model and experimental analysis of the thermal Behavior of electric radiant heating panels. *Applied Sciences*.
- Filippidou, F., Nieboer, N., & Visscher, H. (2016). Energy efficiency measures implemented in the Dutch non-profit housing sector. *Energy and Buildings*, 107-116.
- Guerra-Santin, O., & Silvester, S. (2017). Development of Dutch occupancy and heating profiles for building simulation. *Building Research & Information*, 396-413.
- Herschel Infrared Ltd. (2014, December 17). *How close to objects can an Infrared panel be placed?* Retrieved from Herschel infrared heaters: <https://www.herschel-infrared.co.uk/support/close-infrared-panel-objects-placed/>
- Hughes, C., Natarajan, S., Liu, C., Chung, W., & Herrera, M. (2019). Winter thermal comfort and health in the elderly. *Energy Policy*, 134: 110954.

- IsoBouw. (2016, November 16). *Luchtdicht bouwen*. Retrieved from IsoBouw: <https://www.isobouw.nl/nl/kennisbank/luchtdicht-bouwen/>
- Isover Saint-Gobain. (2013). *Het belang van luchtdicht bouwen*. Retrieved from Isover Saint-Gobain: <https://www.isover.nl/service/wet-en-regelgeving/het-belang-van-luchtdicht-bouwen>
- Kehayova, N. (2014). *Procedure for assessment of plane radiant temperature distribution in occupied spaces*. Sofia: Technical University Sofia.
- Mackey, C., Baranova, V., Petermann, L., & Menchaca-Brandan, A. (2017). *Glazing and Winter Comfort Part 2: An Advanced Tool for Complex Spatial and Temporal Conditions*. Payette Associates.
- Majcen, D., Itard, L., & Visscher, H. (2016). Actual heating energy savings in thermally renovated Dutch dwellings. *Energy Policy*, 82-92.
- Meijer, B., & Loonen, P. (2020). *Infraroodverwarming versus de warmtepomp: een analyse van twee all-electric verwarmingsopties*. Utrecht: TKI Urban Energy.
- Milieu Centraal. (2021, January 15). *Energierkening*. Retrieved from Milieu Centraal: <https://www.milieucentraal.nl/energie-besparen/inzicht-in-je-energierkening/energierkening/>
- Muroni, A., Gaetani, I., Hoes, P., & Hensen, J. (2019). Occupant behavior in identical residential buildings: A case study for occupancy profiles extraction and application to building performance simulation. *Building Simulation*, 1047-1061.
- NASA. (2020). *The effects of climate change*. Retrieved from NASA Global Climate Change: <https://climate.nasa.gov/effects/>
- Nash, S. (2013). *Impact of mechanical ventilation systems on the indoor-air quality in highly energy-efficient houses*. Groningen: University of Groningen.
- NEN. (2020). *NTA 8800+A1: Energy performance of buildings - Determination method*. Delft: NEN.
- Netherlands Enterprise Agency. (2021, April 4). *Energieprestatie indicatoren - BENG*. Retrieved from Netherlands Enterprise Agency: <https://www.rvo.nl/onderwerpen/duurzaam-ondernemen/gebouwen/wetten-en-regels/nieuwbouw/energieprestatie-beng>
- Olesen, B., & Parsons, K. (2002). Introduction to thermal comfort standards and to the proposed new version of EN ISO 7730. *Energy and Buildings*, 537-548.
- Olesen, B., Moreno-Beltrón, D., Grau-Rios, M., Tähti, E., Niemelä, R., Olander, L., & Hagström, K. (2001). Industrial Ventilation Design Guidebook. *Academic Press*, 355-413.
- O-Nexus, Beligreen, Eindhoven University of Technology & Jheronimus Academy of Data Science. (2019). *Harnessing Effective Radiation Solutions with Comfortable Heated Energy Levels*. Eindhoven: O-Nexus, Beligreen, Eindhoven University of Technology & Jheronimus Academy of Data Science.
- Pan, Z., Atungulu, G., & Li, X. (2014). Infrared heating. In D. Sun, *Emerging Technologies for Food Processing* (pp. 461-471). Dublin: Academic Press.

- Peeters, L., Beausoleil-Morrison, I., & Novoselac, A. (2011). Internal convective heat transfer modeling: Critical review and discussion of experimentally derived correlations. *Energy and Buildings*, 2227-2239.
- Peeters, L., De Daer, R., Hensen, J., & D'Haeseleer, W. (2009). Thermal comfort in residential buildings: Comfort values and scales for building energy simulation. *Applied Energy*, 772-780.
- Regionaal Energieloket. (2020, September 29). *Kosten infrarood verwarming*. Retrieved from Regionaal Energieloket: <https://kennisbank.regionaalenergieloket.nl/>
- Safizadeh, R., Schweiker, M., & Wagner, A. (2018). Experimental Evaluation of Radiant Heating Ceiling Systems Based on Thermal Comfort Criteria. *Energies*, 2932.
- Samek, L., De Maeyer-Worobiec, A., Spolnik, Z., Bencs, L., Kontozova, V., Bratasz, Ł., . . . Van Grieken, R. (2007). The impact of electric overhead radiant heating on the indoor environment of historic churches. *Journal of Cultural Heritage*, 361-369.
- Spirax Sarco. (2004, August 2). *Basic control theory*. Retrieved from Spirax Sarco: <https://www.spiraxsarco.com/learn-about-steam/basic-control-theory/basic-control-theory>
- Statistics Netherlands. (2012). *WoonOnderzoek Nederland (WoON)*. Retrieved from CBS: <https://www.cbs.nl/nl-nl/onze-diensten/methoden/onderzoeksomschrijvingen/korte-onderzoeksbeschrijvingen/woononderzoek-nederland--woon-->
- Statistics Netherlands. (2016). *Vier op de tien huishoudens wonen in een rijtjeshuis*. Retrieved from Statistics Netherlands: <https://www.cbs.nl/nl-nl/nieuws/2016/14/vier-op-de-tien-huishoudens-wonen-in-een-rijtjeshuis>
- Su, X., Wang, Z., Xu, Y., & Liu, N. (2020). Thermal comfort under asymmetric cold radiant environment at different exposure distances. *Building and Environment*, Article 106961.
- Vaillant. (2017, October 12). *Wat kost een warmtepomp?* Retrieved from Vaillant: <https://www.vaillant.nl/consument/kennis-en-advies/warmtepompen/kosten/>
- Van der Knijff, J. (2018). *Praktijkvoorbeelden aardgasvrije woningen*. Utrecht: Rijksdienst voor Ondernemend Nederland.
- Van Ginkel, J., & Hasselaar, E. (2006). Indoor air quality influenced by ventilation system. *ENHR: Housing in an expanding Europe*. Ljubljana: OTB Research Institute for Housing, Urban and Mobility Studies.
- Van Hoof, J., & Hensen, J. (2006). Thermal comfort and older adults. *Gerontology*, 223-228.
- Visscher, H. (2019). Innovations for a carbon free Dutch housing stock in 2050. *IOP Conference Series: Earth and Environmental Science*.
- Wang, Z., Zhang, H., Arens, E., Lehrer, D., Huizenga, C., Yu, T., & Hoffmann, S. (2009). *Modeling thermal comfort with radiant floors and ceilings*. Berkeley: UC Berkeley: Center for the Built Environment.
- Younger, M., Morrow-Almeida, H., Vindigni, S., & Dannenberg, A. (2008). The built environment, climate change, and health: opportunities for co-benefits. *American Journal of Preventive Medicine*, 517-526.

Zhang, Y., & Zhao, R. (2007). Effect of local exposure on human responses. *Building and Environment*, 2737-2745.

Appendix I: Case buildings details

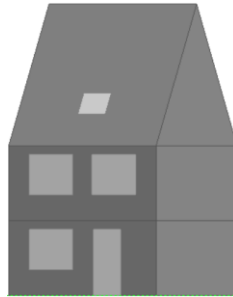


Figure 35: DesignBuilder model of the terraced house

Table 9: Details of the terraced house

Characteristic per unit	Dimension
Width	5.1 m
Depth	8.9 m
Height	2.6 m
Usable surface A_u	124.3 m ²
Heat loss area A_{loss}	165.4 m ²
Compactness ratio A_u/A_{loss}	0.8



Figure 36: DesignBuilder model of the freestanding house

Table 10: Details of the freestanding house

Characteristic per unit	Dimension
Width	6 m
Depth	10.2 m
Height	2.6 m
Usable surface	169.5 m ²
Heat loss area A_{loss}	364.4 m ²
Compactness ratio A_u/A_{loss}	0.5

Appendix II: envelope details

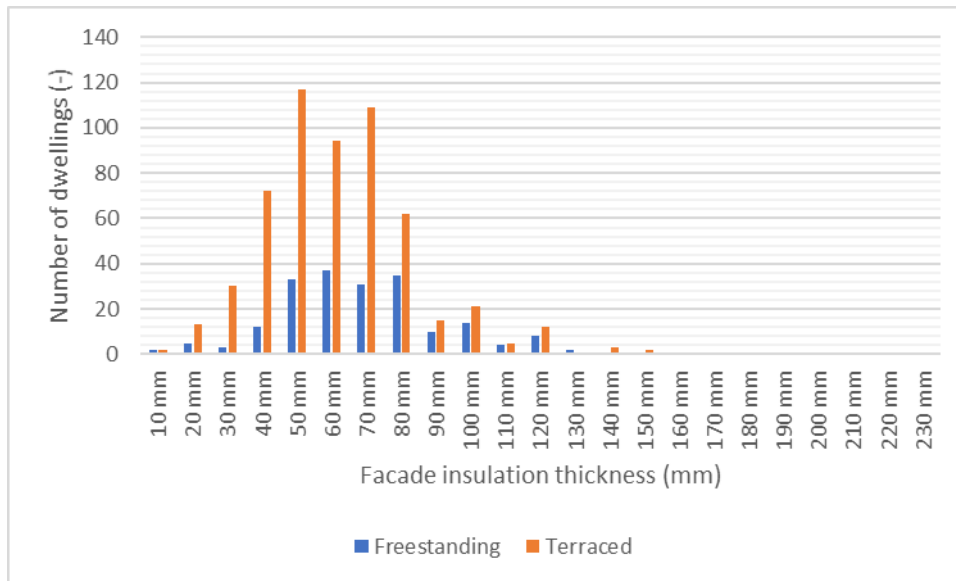


Figure 37: Distribution of different facade insulation thicknesses across the dwellings from the WoON-database (Statistics Netherlands, 2012)

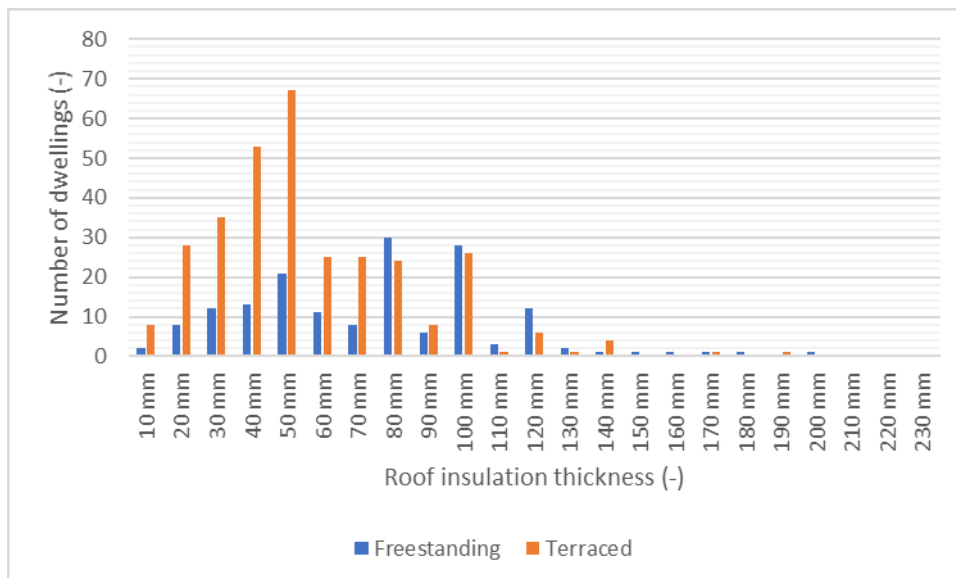


Figure 38: Distribution of different roof insulation thicknesses across the dwellings from the WoON-database (Statistics Netherlands, 2012)

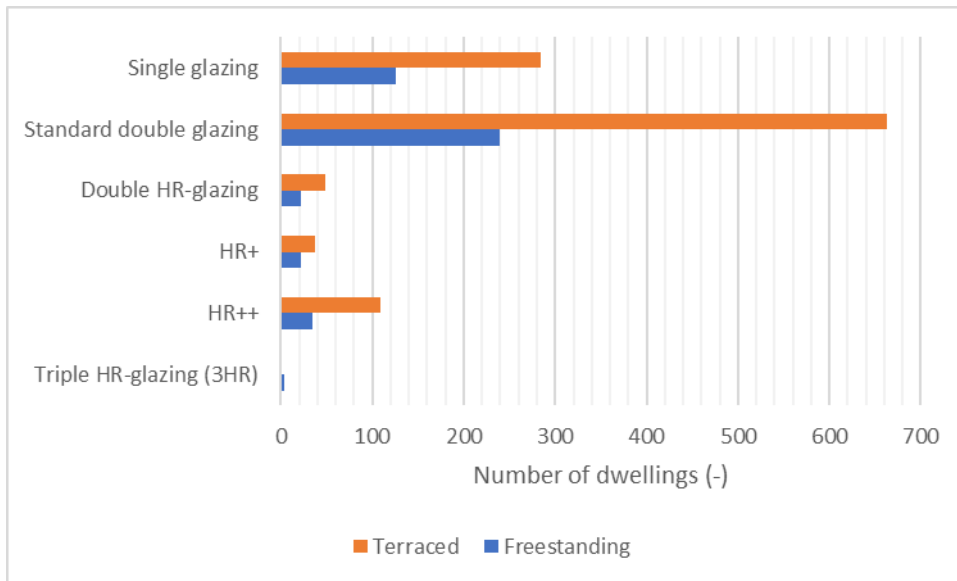


Figure 39: Distribution of different window types across the dwellings from the WoON-database (Statistics Netherlands, 2012)

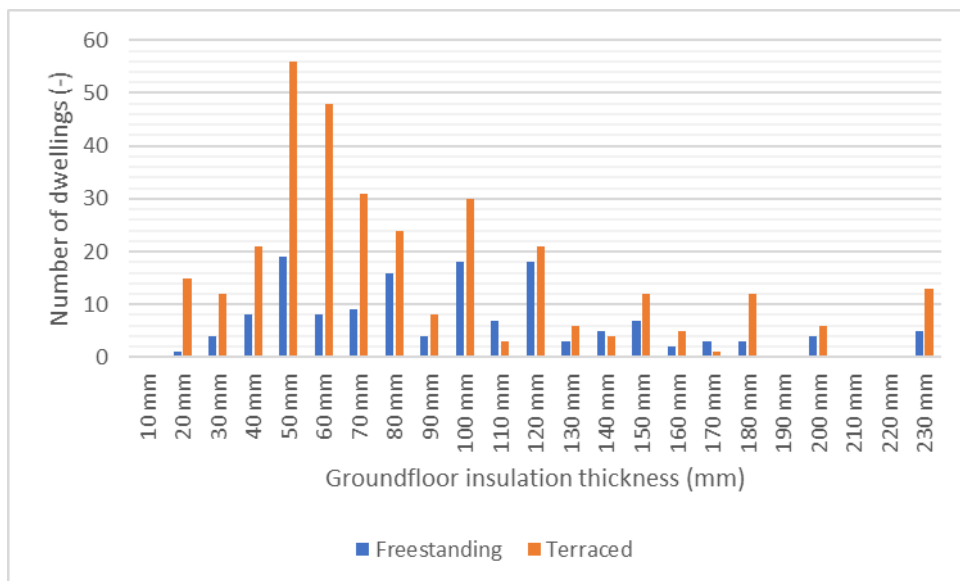


Figure 40: Distribution of different ground floor insulation thicknesses across the dwellings from the WoON-database (Statistics Netherlands, 2012)

Low insulation terraced house details

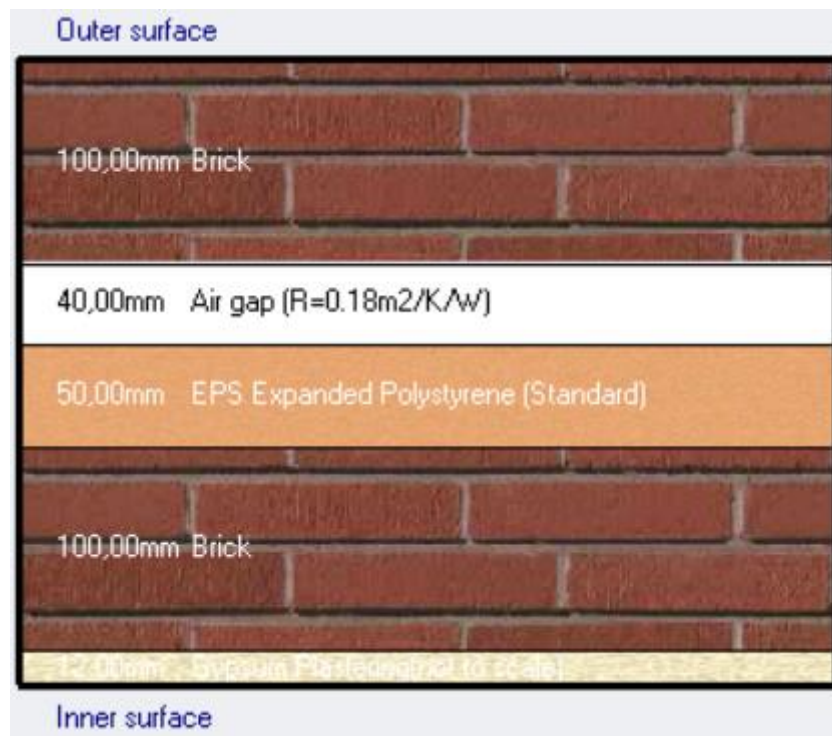


Figure 41: Detail of the exterior wall of the terraced house in DesignBuilder (low insulation)

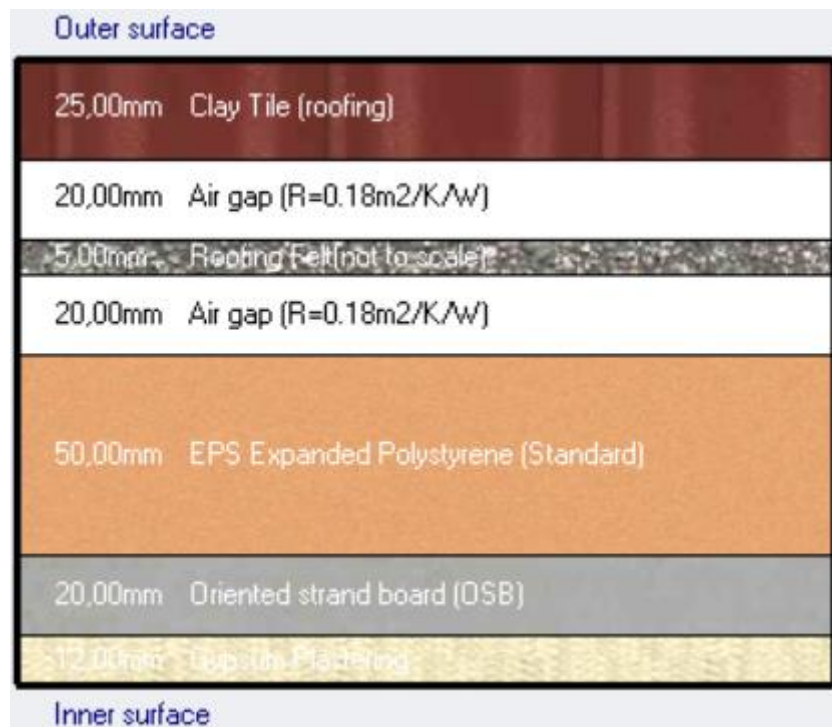


Figure 42: Detail of the roof of the terraced house in DesignBuilder (low insulation)



Figure 43: Detail of the ground floor of the terraced house in DesignBuilder (low insulation)

Low insulation freestanding house details

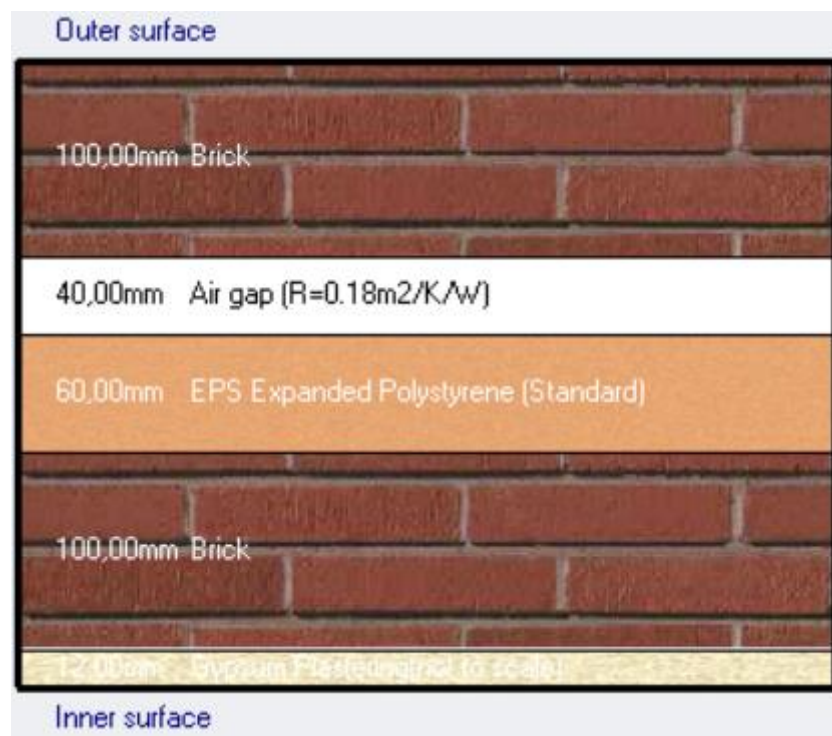


Figure 44: Detail of the exterior wall of the freestanding house in DesignBuilder (low insulation)

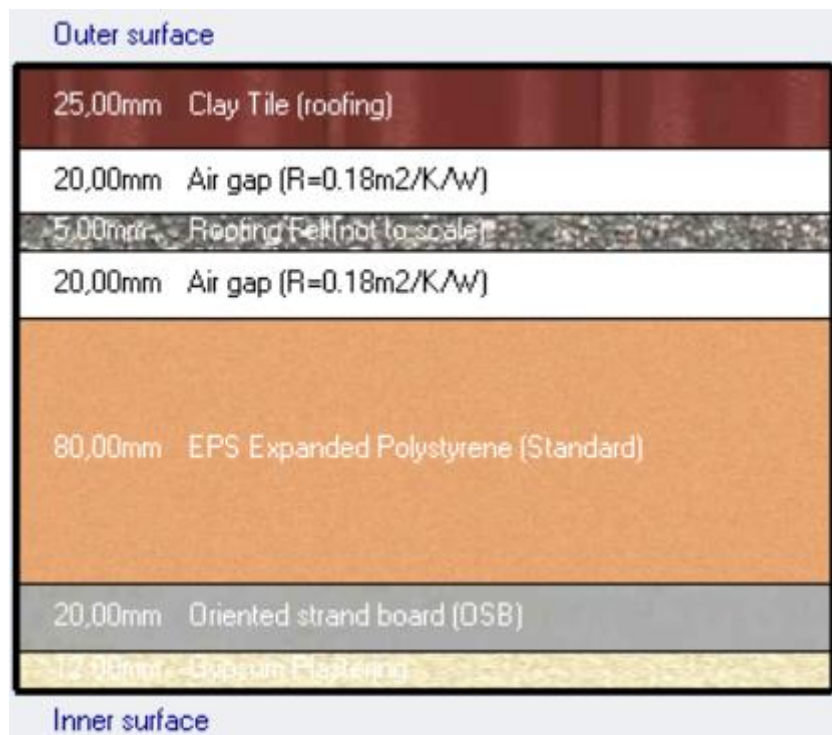


Figure 45: Detail of the roof of the freestanding house in DesignBuilder (low insulation)



Figure 46: Detail of the ground floor of the freestanding house in DesignBuilder (low insulation)

High insulation details

The constructions of the high insulation variants are identical for the terraced house and freestanding house, therefore the following figures can be considered representative for both houses.

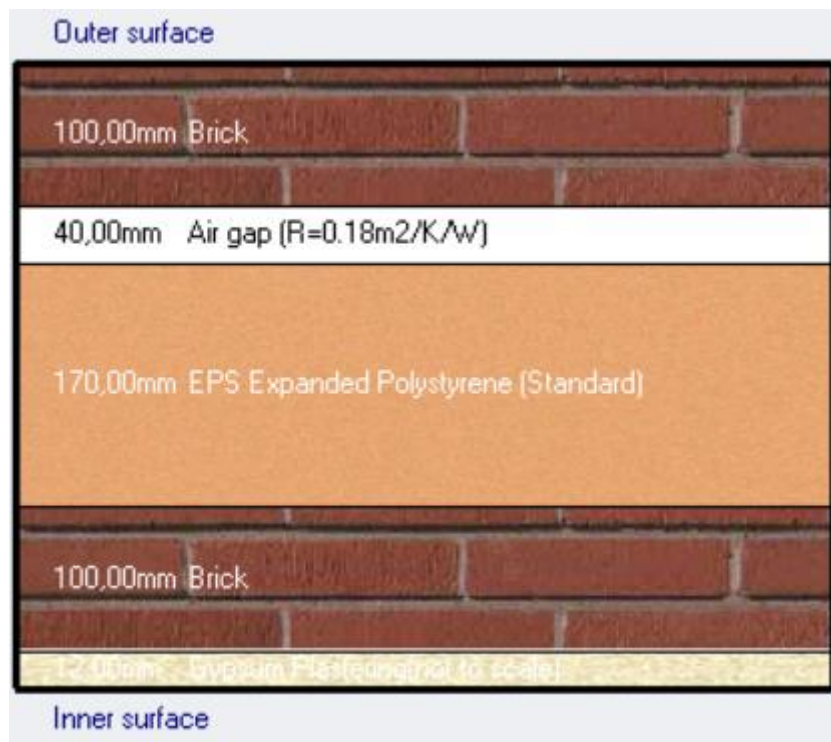


Figure 47: Detail of the exterior wall of both houses in DesignBuilder (high insulation)

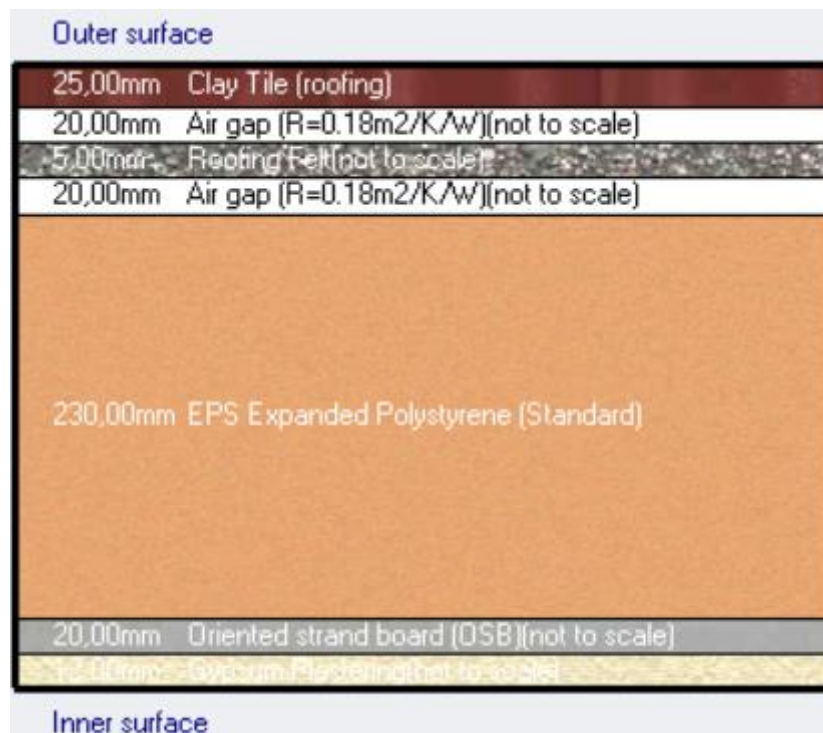


Figure 48: Detail of the roof of the both houses in DesignBuilder (high insulation)



Figure 49: Detail of the ground floor of both houses in DesignBuilder (high insulation)

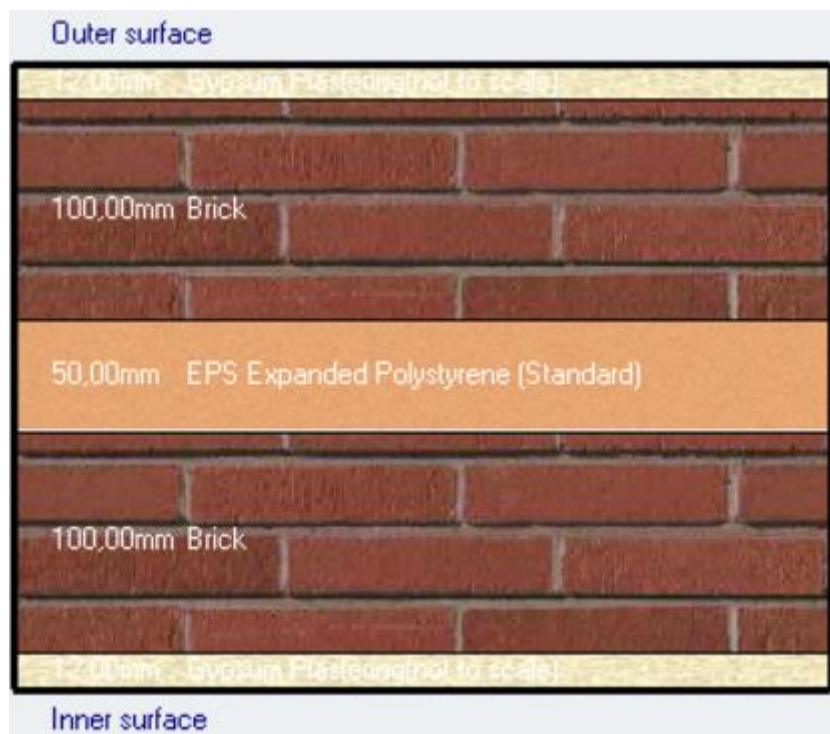


Figure 50: Detail of the separation wall between two dwellings of the terraced house in DesignBuilder. This detail applies to both the low and high insulation variants.

Appendix III: Occupancy schedules

Single senior

Table 11: Presence schedule of the single senior household. A 0 indicates that the occupant is not at home. A 1 indicates that the occupant is at home and the room where the occupant is, is shown in the upper row.

	23:00 - 06:00	06:00 - 06:30	06:30 - 09:00	09:00 - 12:00	12:00 - 12:30	12:00 - 15:00	15:00 - 17:30	17:30 - 19:00	18:00 - 23:00
Days	Bed-room	Kitchen	Living room	Living room	Kitchen	Living room	Living room	Kitchen	Living room
Mon-Wed	1	1	1	1	1	1	1	1	1
Thu	1	1	1	1	1	0	1	1	1
Fri	1	1	1	0	0	0	0	0	1
Sat-Sun	1	1	0	0	0	0	0	0	0

Table 12: Heating setpoint schedule of the single senior household. T1 is the living room, T2 the bedroom and T3 is for the kitchen, bathroom and hallway. The black cells represent the nighttime setback temperature and the grey cells the daytime setback temperature.

	23:00 - 06:00		06:00 - 09:00		09:00 - 12:00		12:00 - 15:00		15:00 - 18:00		18:00 - 23:00	
Days	T1	T2/T3	T1	T2/T3	T1	T2/T3	T1	T2/T3	T1	T2/T3	T1	T2/T3
Mon - Wed	20	20	22	22	23	22	23	22	23	22	24	22
Thu	20	20	22	22	23	22	21	21	23	22	24	22
Fri	20	20	22	22	21	21	21	21	21	21	24	22
Sat-Sun	20	20	21	21	21	21	21	21	21	21	21	21

Table 13: Lighting and appliances schedule for the single senior household. The black cells mean that the lights are on and the appliances are off

	24:00 - 05:00	05:00 - 06:00	06:00 - 09:00	09:00 - 18:00	18:00 - 23:00	23:00 - 24:00
Days	All	Bedrooms	Common areas	All	Common areas	Bedrooms
Mon-Wed	0	1	1	0	1	1
Thu	0	1	1	0	1	1
Fri	0	1	1	0	1	1
Sat-Sun	0	1	0	0	0	1

Nuclear family

Table 14: Presence schedule of the nuclear family household. *2 persons in the main bedroom and 1 in each remaining bedroom. **3 persons in the living room, 1 person in the kitchen for cooking. ***3 persons in the living room, 1 person in the bathroom (assumed 15 minutes of showering per person, so 1 hour in total)

	23:00 - 06:00	06:00 - 06:30	06:30 - 08:00	08:00 - 19:00	19:00 - 19:30	19:30 - 20:30	20:30 - 21:30	21:00 - 23:00
Days	Bedroom	Kitchen	Living room	Living room	Living room	Kitchen	Living room	Living room
Weekdays	2/1*	4	4	0	3**	4	3***	4
Weekend	2/1*	4	4	0	3**	4	3***	4

Table 15: Heating setpoint schedule of the nuclear family household. The black cells refer to the nighttime setback temperature and the grey cells to the daytime setback temperature

	T1/T2/T3	T1/T2/T3	T1/T2/T3	T1/T2/T3
Days	23:00 - 06:00	06:00 - 08:00	08:00 - 19:00	19:00 - 23:00
Weekdays	18	20	16	20
Days	23:00 - 08:00	08:00 - 13:00	13:00 - 18:00	18:00 - 23:00
Weekend	18	20	16	20

Table 16: Lighting and appliances schedule of the nuclear family household. The black cells indicate that the lights are on and appliances are off

Days	All	Bedrooms	Common areas	All	Common areas	Bedrooms
	24:00 - 05:00	05:00 - 06:00	06:00 - 08:00	08:00 - 19:00	19:00 - 23:00	23:00 - 24:00
Weekdays	0	1	1	0	1	1
	24:00 - 05:00	07:00 - 08:00	08:00 - 12:30	12:30 - 18:30	18:30 - 23:00	23:00 - 24:00
Weekend	0	1	1	0	0	1

Table 17: Internal gains for the simulations (Big Ladder, 2018) (Damaskou, 2016)

Internal heat source	Internal heat gain (W)
Occupant – sitting (relaxed)	108
Occupant – sitting (eating)	126
Occupant - sleeping	72
Showering	180
Cooking	189
Lights (per light)	14
TV	25
Radio	20
Laptop	25
Fridge	10
Freezer	30
Dishwasher	50
Coffee machine	32

Appendix IV: Heating systems

Infrared panels

Table 18: Number of infrared panels and total capacity for each building, for low and high insulation variants

Dwelling type	Insulation level	Number of panels	Total capacity
Terraced house	Low	32	7680
	High	19	4560
Freestanding house	Low	46	11040
	High	26	6240

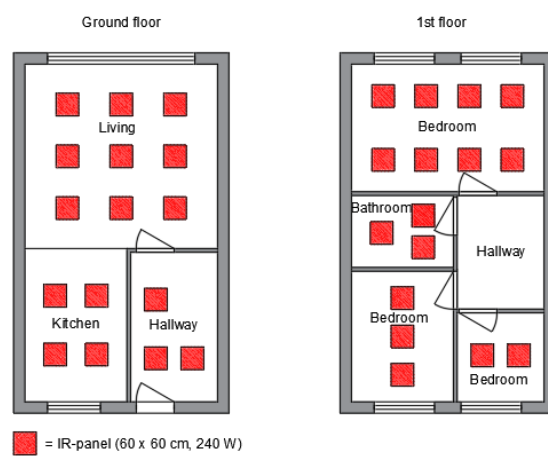


Figure 51: Overview of the placement of the infrared panels in each room of the low insulation terraced house

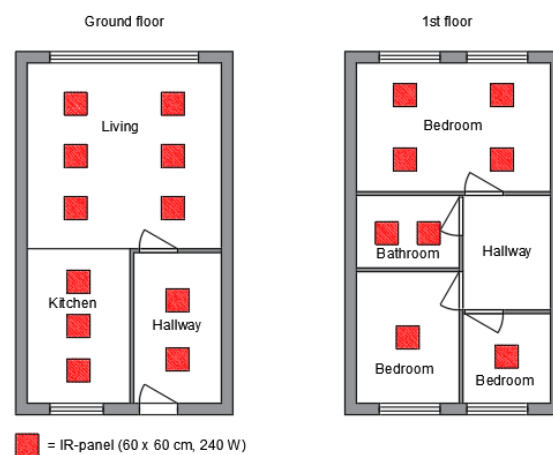


Figure 52: Overview of the placement of the infrared panels in each room of the high insulation terraced house

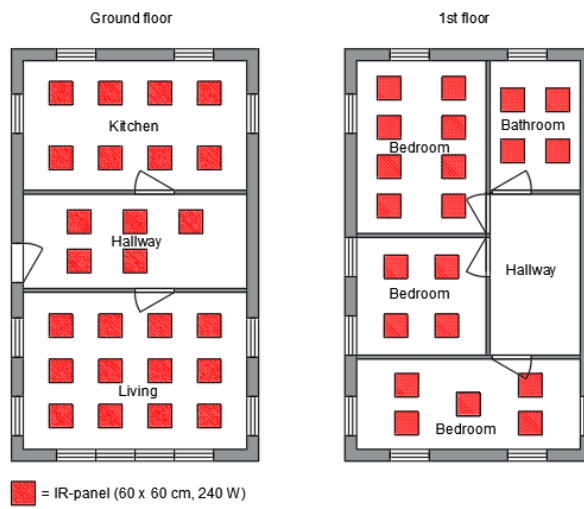


Figure 53: Overview of the placement of the infrared panels in the low insulation freestanding house

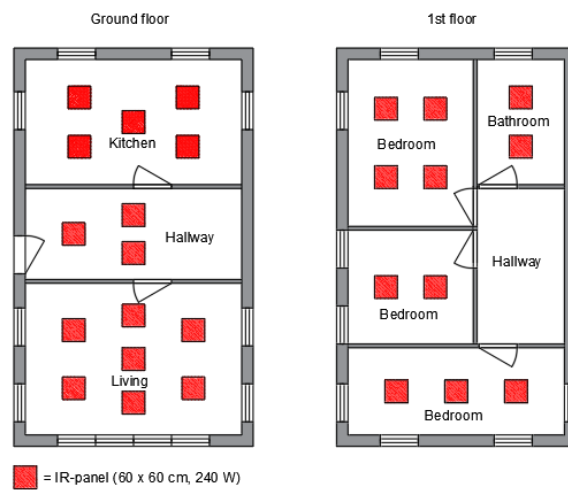


Figure 54: Overview of the placement of the infrared panels in the high insulation freestanding house

Heat pump

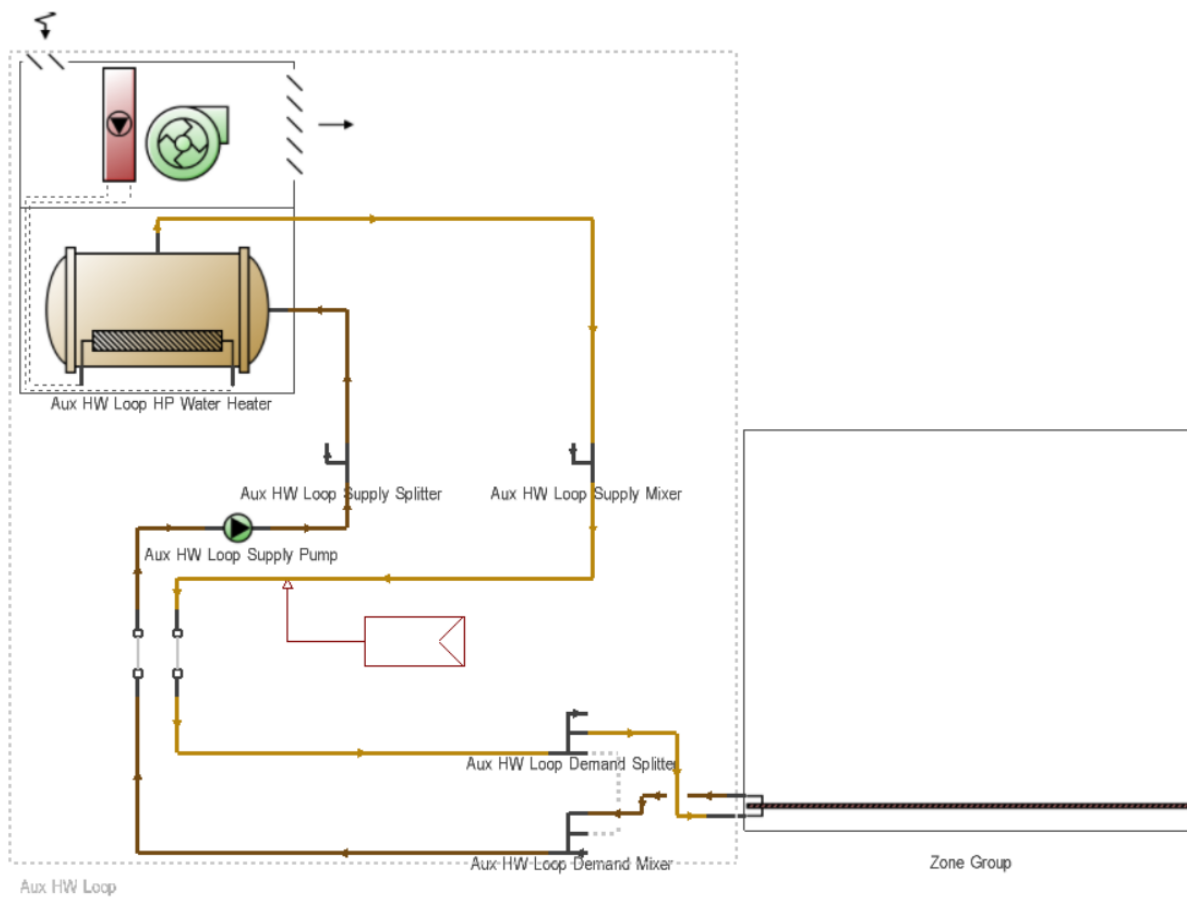


Figure 55: Overview of the heat pump model and floor heating in DesignBuilder

Table 19: Capacities and COPs of the heat pumps in both buildings, for low and high insulation variants

Dwelling type	Insulation level	Heating capacity (kW)	Floor heating COP
Terraced house	Low	7	4.76
	High	3	5.33
Freestanding house	Low	9	4.48
	High	5	5.08

Gas boiler

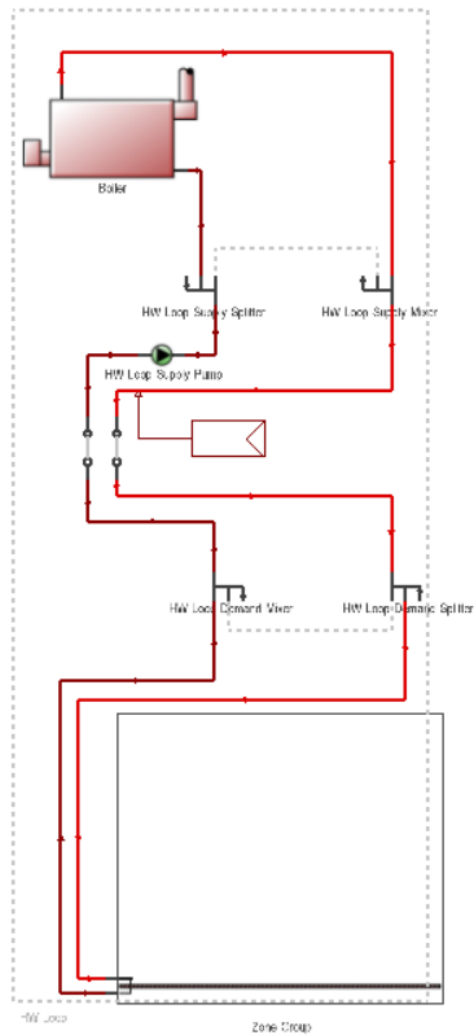


Figure 56: Overview of the gas boiler model and floor heating in DesignBuilder

Table 20: Capacities of the gas boiler in the different buildings

Dwelling type	Insulation level	Heating capacity (kW)
Terraced house	Low	17
	High	5
Freestanding house	Low	23
	High	11

Appendix V: Radiant temperature asymmetry analysis

This appendix contains visualizations of the positions for the radiant temperature asymmetry analysis. In order to determine the angle factors, the surfaces were divided into four quadrants, which are visualized by means of green lines here.

Terraced house position 1

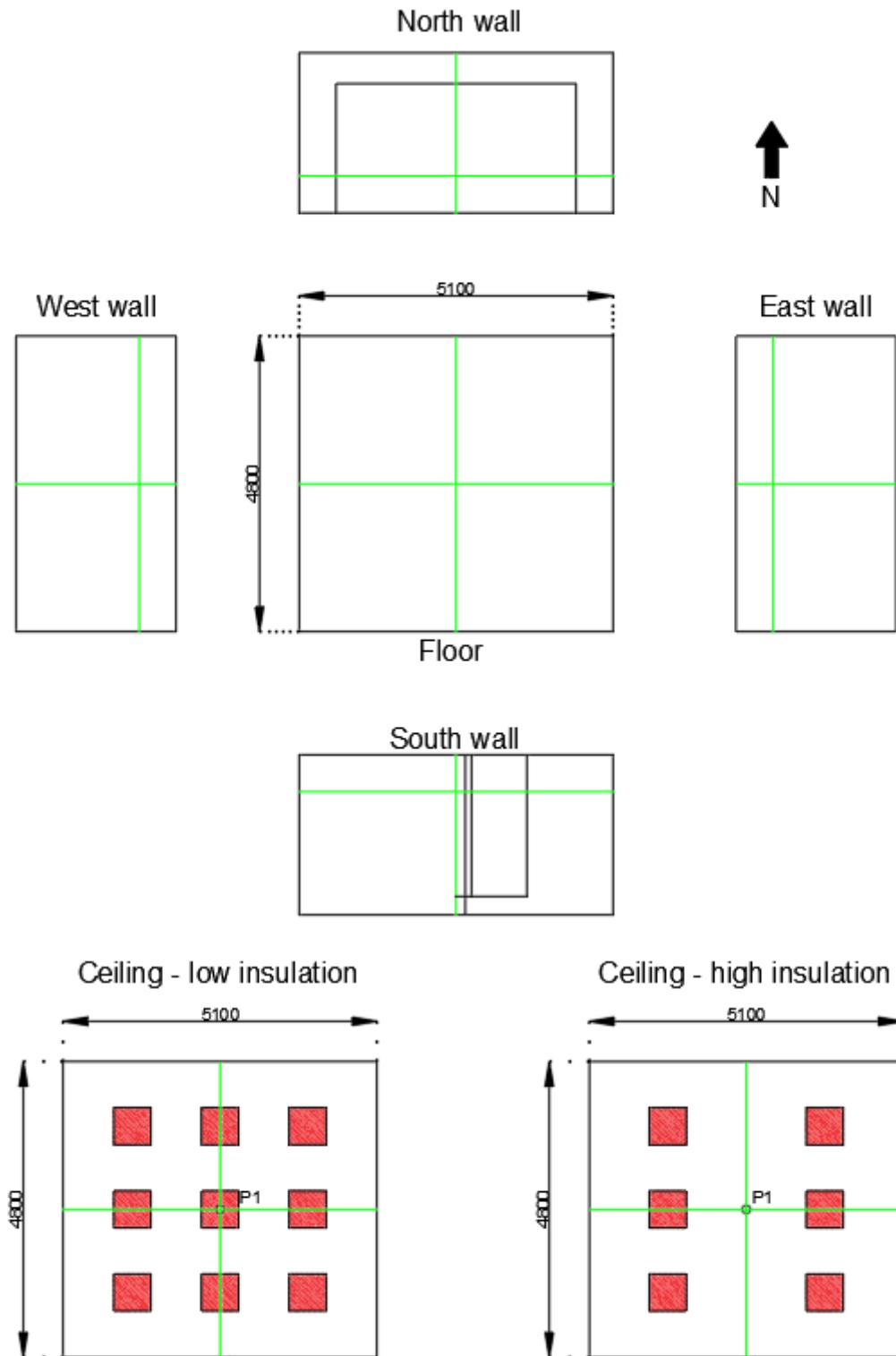


Table 21: angle factors for each of the surfaces in the vertical direction (infrared panels, ceiling and floor) for position 1 in the terraced house.

Surface (low insulation)	Angle factor (-)	Surface (high insulation)	Angle factor (-)
IR-panel 1	0.001923365	IR-panel 1	0.002050874
IR-panel 2	0.003375741	IR-panel 2	0.002050874
IR-panel 3	0.001923365	IR-panel 3	0.00386873
IR-panel 4	0.003602316	IR-panel 4	0.00386873
IR-panel 5	0.006676472	IR-panel 5	0.002050874
IR-panel 6	0.003602316	IR-panel 6	0.002050874
IR-panel 7	0.001923365	Ceiling (excl. panels)	0.172514816
IR-panel 8	0.003375741	Floor	0.382767965
IR-panel 9	0.001923365		
Ceiling (excl. panels)	0.160129725		
Floor	0.382767965		

Terraced house position 2

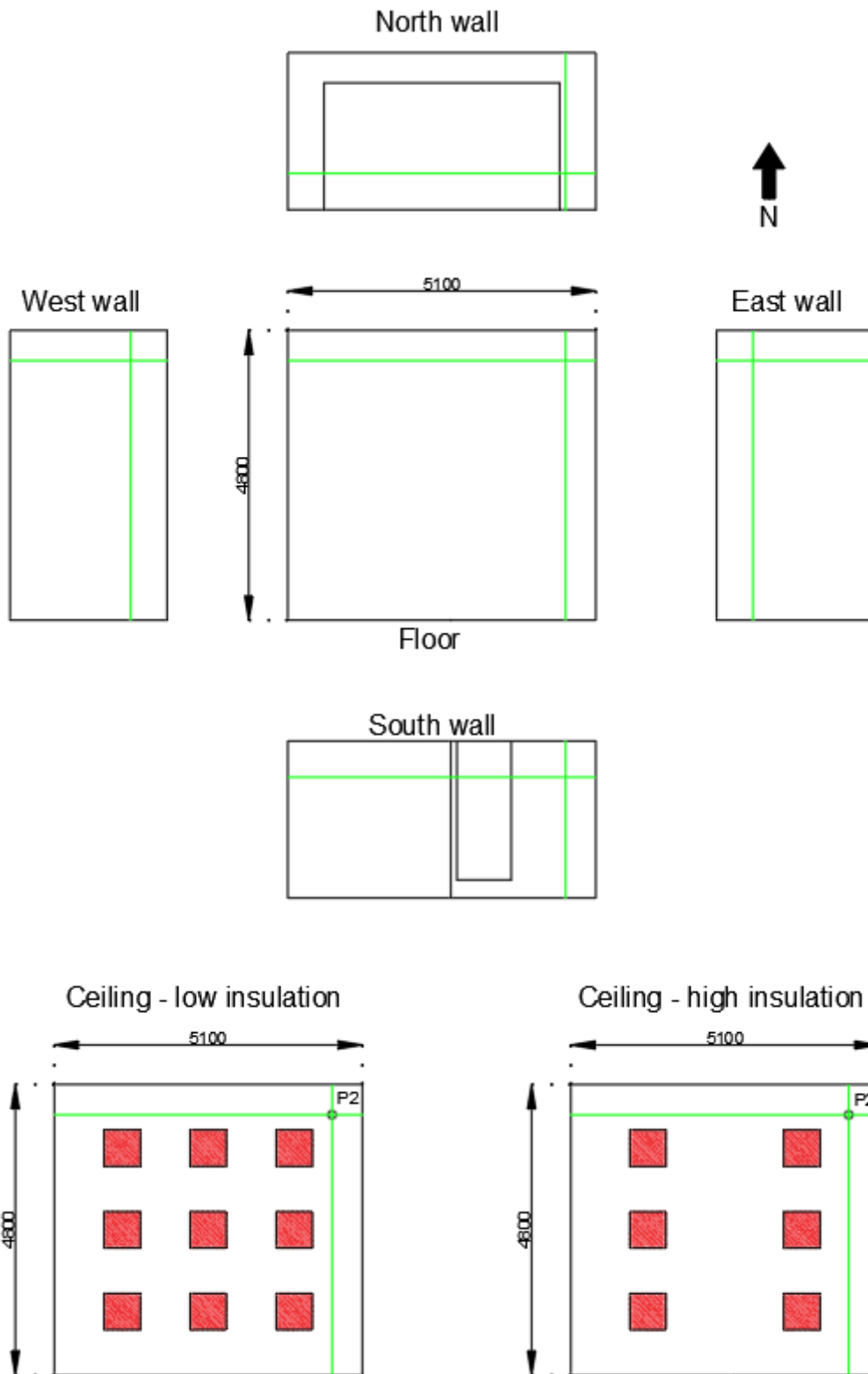


Table 22: angle factors for each of the surfaces in the vertical direction (infrared panels, ceiling and floor) for position 2 in the terraced house.

Surface (low insulation)	Angle factor (-)	Surface (high insulation)	Angle factor (-)
IR-panel 1	0.001170858	IR-panel 1	0.001250381
IR-panel 2	0.002195704	IR-panel 2	0.003938953
IR-panel 3	0.004228578	IR-panel 3	0.000707025
IR-panel 4	0.000669788	IR-panel 4	0.001918897
IR-panel 5	0.001141292	IR-panel 5	0.000411504
IR-panel 6	0.002046285	IR-panel 6	0.000996522
IR-panel 7	0.000393052	Ceiling (excl. panels)	0.117053002
IR-panel 8	0.000623911	Floor	0.233033657
IR-panel 9	0.001056955		
Ceiling (excl. panels)	0.112749861		
Floor	0.233033657		

Freestanding house position 1

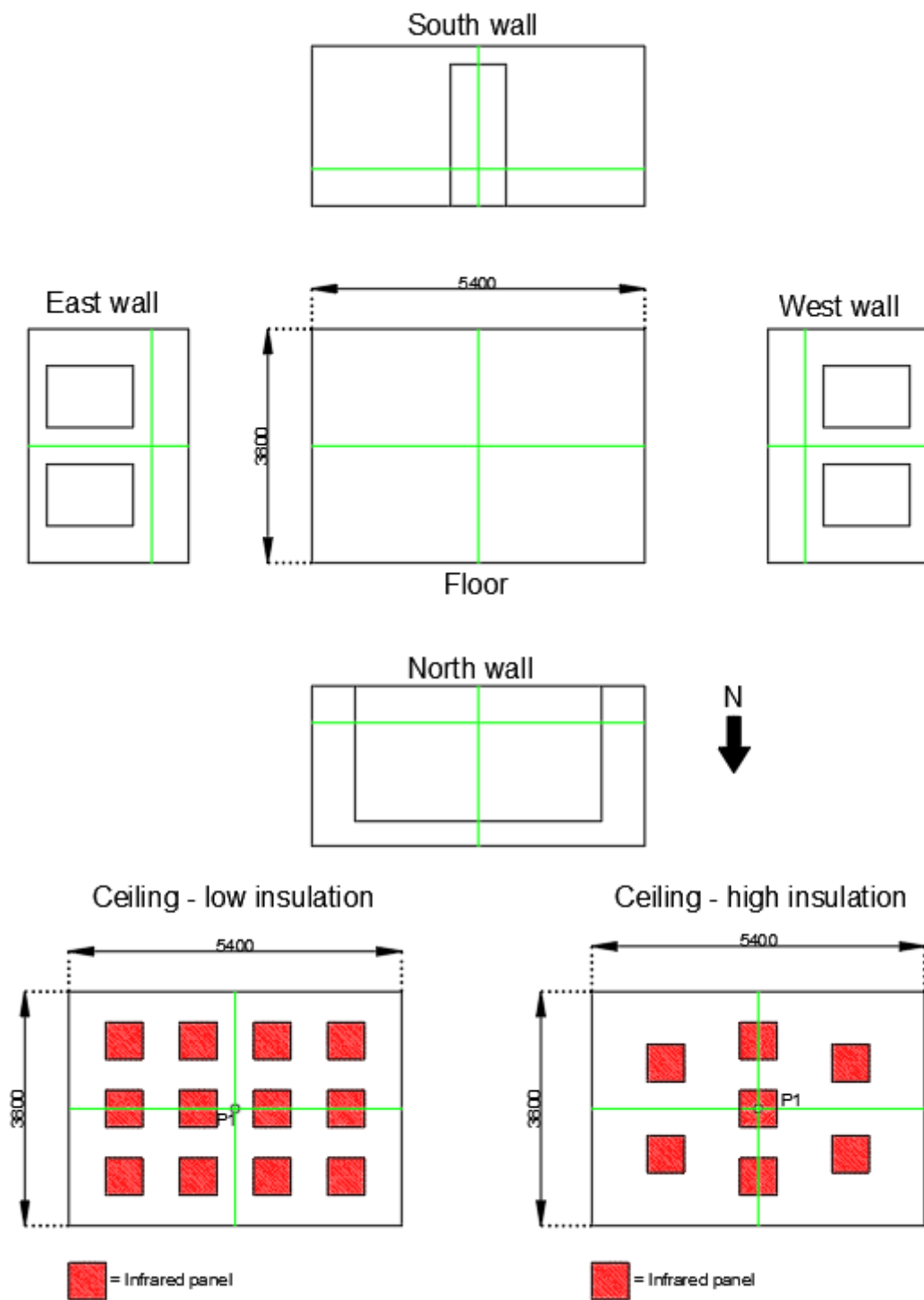


Table 23: angle factors for each of the surfaces in the vertical direction (infrared panels, ceiling and floor) for position 1 in the freestanding house.

Surface (low insulation)	Angle factor (-)	Surface (high insulation)	Angle factor (-)
IR-panel 1	0.001858373	IR-panel 1	0.002547049
IR-panel 2	0.003155191	IR-panel 2	0.003875178
IR-panel 3	0.003155191	IR-panel 3	0.002547049
IR-panel 4	0.001858373	IR-panel 4	0.006676472
IR-panel 5	0.003017957	IR-panel 5	0.002547049
IR-panel 6	0.005359793	IR-panel 6	0.003875178
IR-panel 7	0.005359793	IR-panel 7	0.002547049
IR-panel 8	0.003017957	Ceiling (excl. panels)	0.143659891
IR-panel 9	0.001858373	Floor	0.369151938
IR-panel 10	0.003155191		
IR-panel 11	0.003155191		
IR-panel 12	0.001858373		
Ceiling (excl. panels)	0.131465153		
Floor	0.369151938		

Freestanding house position 2

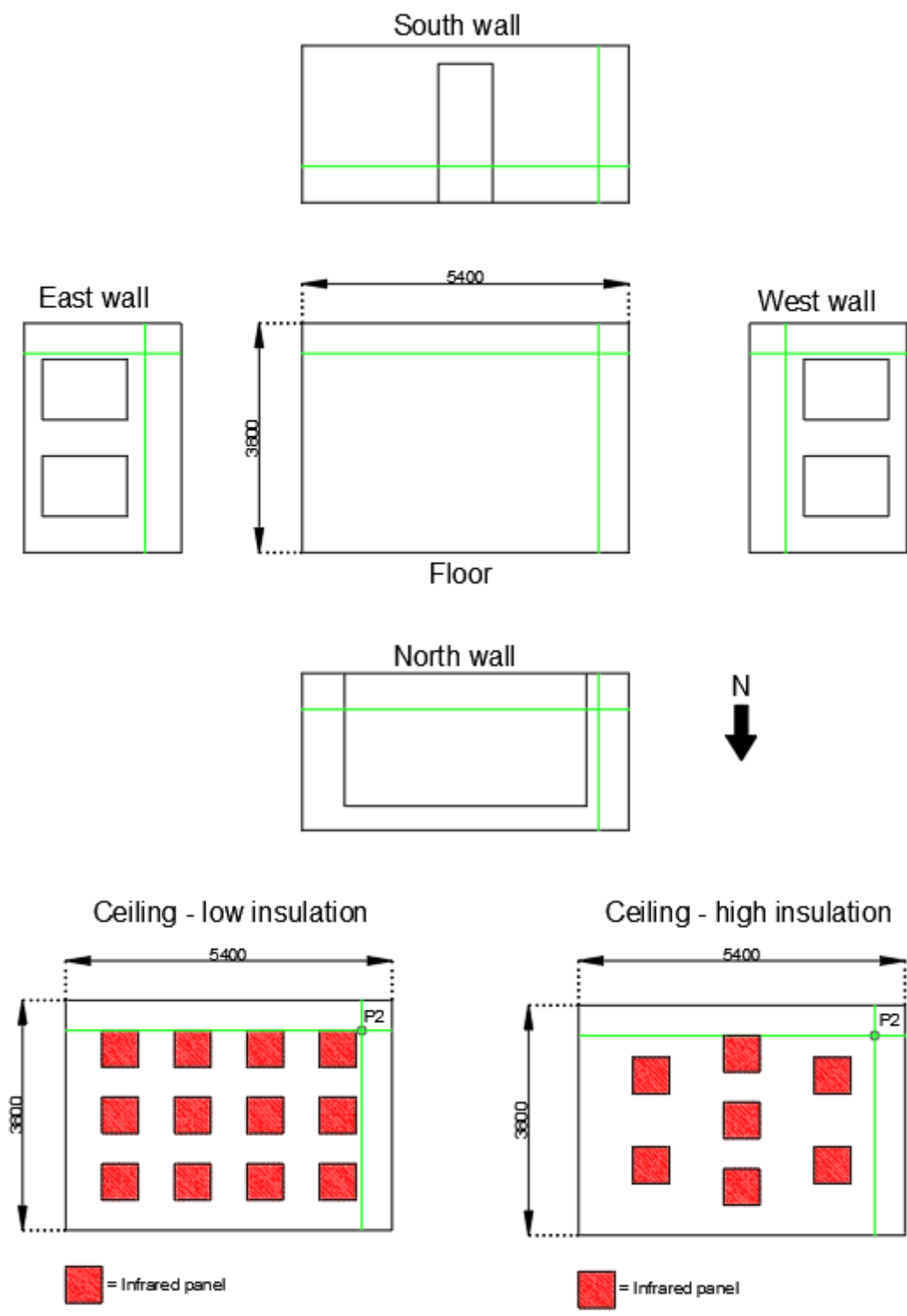


Table 24: angle factors for each of the surfaces in the vertical direction (infrared panels, ceiling and floor) for position 2 in the freestanding house.

Surface (low insulation)	Angle factor (-)	Surface (high insulation)	Angle factor (-)
IR-panel 1	0.001022661	IR-panel 1	0.000384044
IR-panel 2	0.001769502	IR-panel 2	0.002080806
IR-panel 3	0.003070638	IR-panel 3	0.010534802
IR-panel 4	0.00543992	IR-panel 4	0.001168381
IR-panel 5	0.000672315	IR-panel 5	0.000416754
IR-panel 6	0.001068932	IR-panel 6	0.000457208
IR-panel 7	0.001741927	IR-panel 7	0.00149111
IR-panel 8	0.002938383	Ceiling (excl. panels)	0.10120597
IR-panel 9	0.000443715	Floor	0.229718743
IR-panel 10	0.00066279		
IR-panel 11	0.001027286		
IR-panel 12	0.001663626		
Ceiling (excl. panels)	0.096217378		
Floor	0.229718743		

Appendix VI: Indoor operative temperature

Single senior

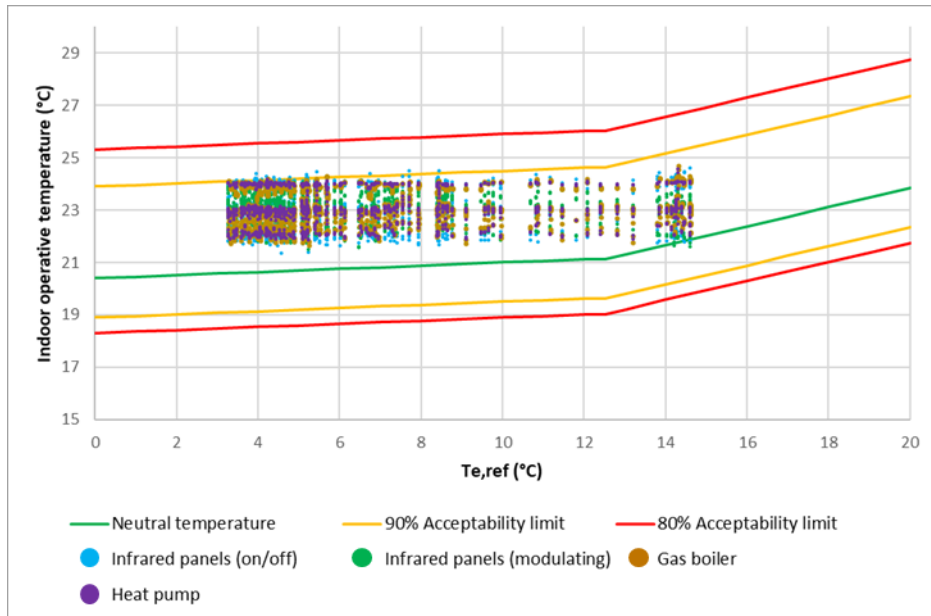


Figure 57: Operative temperatures in the living room throughout the heating season during the occupied hours for all heating systems in the low insulation terraced house for a single senior profile

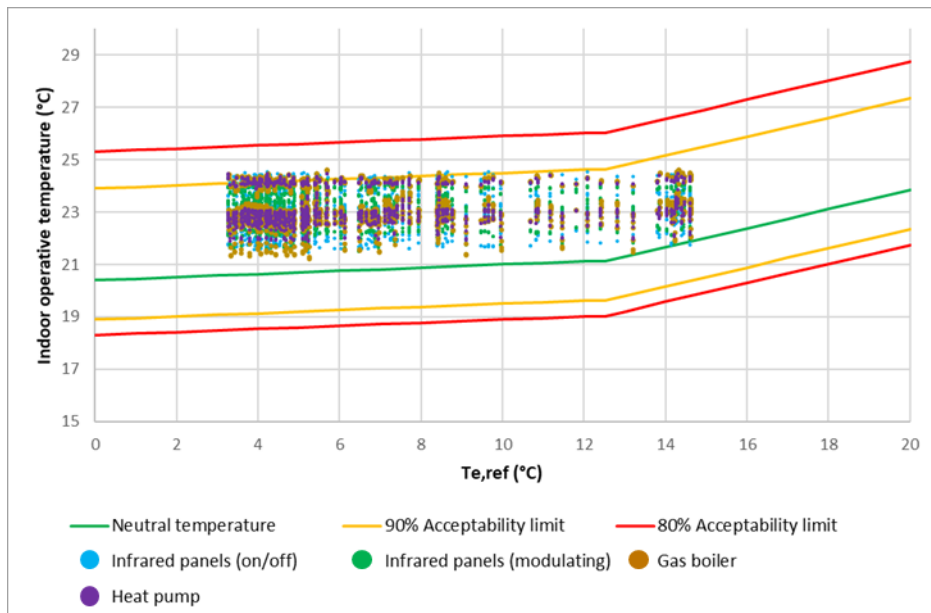


Figure 58: Operative temperatures in the living room throughout the heating season during the occupied hours for all heating systems in the high insulation terraced house for a single senior profile

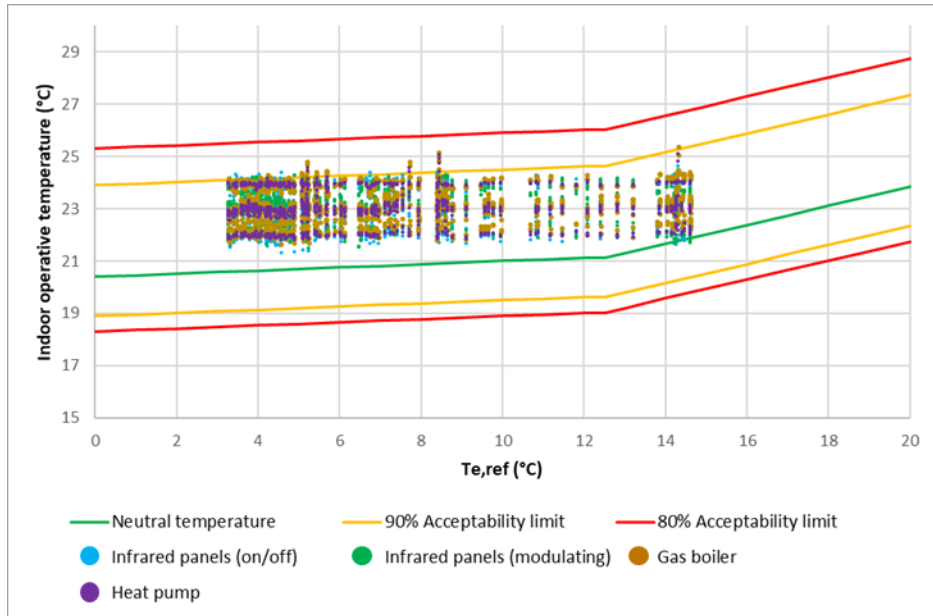


Figure 59: Operative temperatures in the living room throughout the heating season during the occupied hours for all heating systems in the low insulation freestanding house for a single senior profile

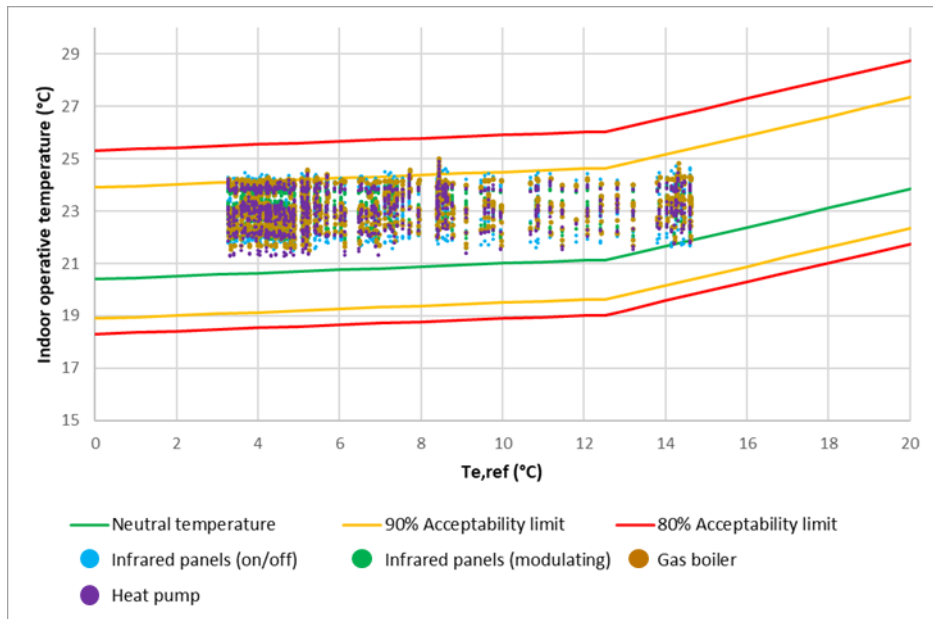


Figure 60: Operative temperatures in the living room throughout the heating season during the occupied hours for all heating systems in the high insulation freestanding house for a single senior profile

Nuclear family

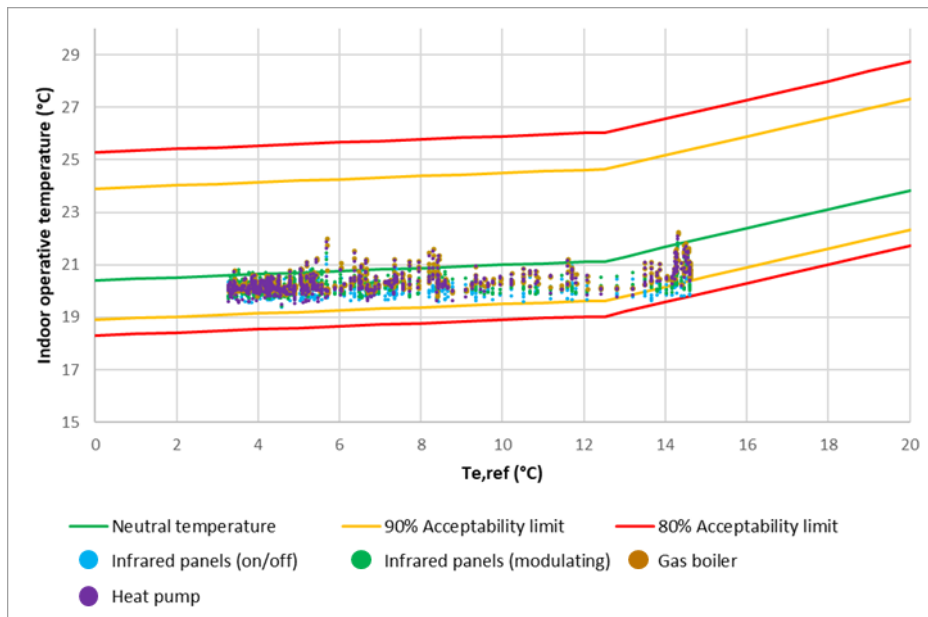


Figure 61: Operative temperatures in the living room throughout the heating season during the occupied hours for all heating systems in the low insulation terraced house for a nuclear family profile

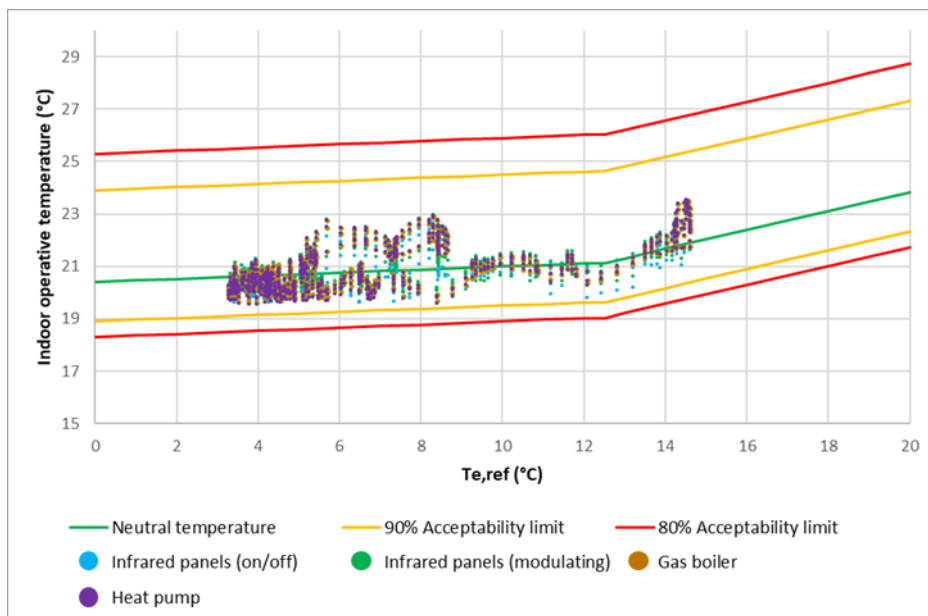


Figure 62: Operative temperatures in the living room throughout the heating season during the occupied hours for all heating systems in the high insulation terraced house for a nuclear family profile

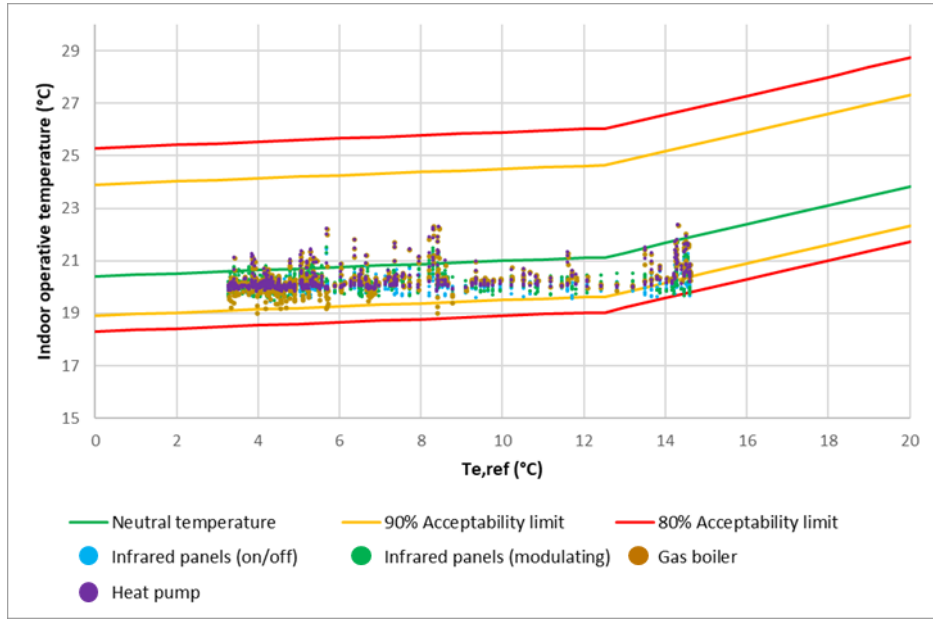


Figure 63: Operative temperatures in the living room throughout the heating season during the occupied hours for all heating systems in the low insulation freestanding house for a nuclear family profile

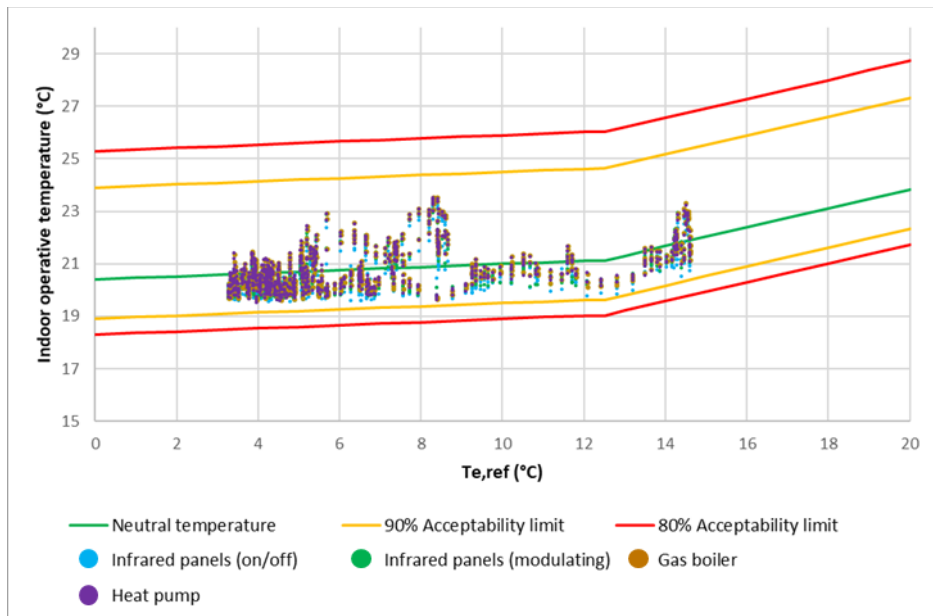


Figure 64: Operative temperatures in the living room throughout the heating season during the occupied hours for all heating systems in the high insulation freestanding house for a nuclear family profile

Appendix VII: Radiant temperature asymmetry

The figures presented in this appendix are meant to provide insight into the exceedance over the comfort limits in terms of temperature regarding the radiant temperature asymmetry. The figures show the lines representing a PPD of 5% and 10%, which correspond to ΔT_{pr} -values of 4.0 °C and 6.6 °C respectively.

Single senior

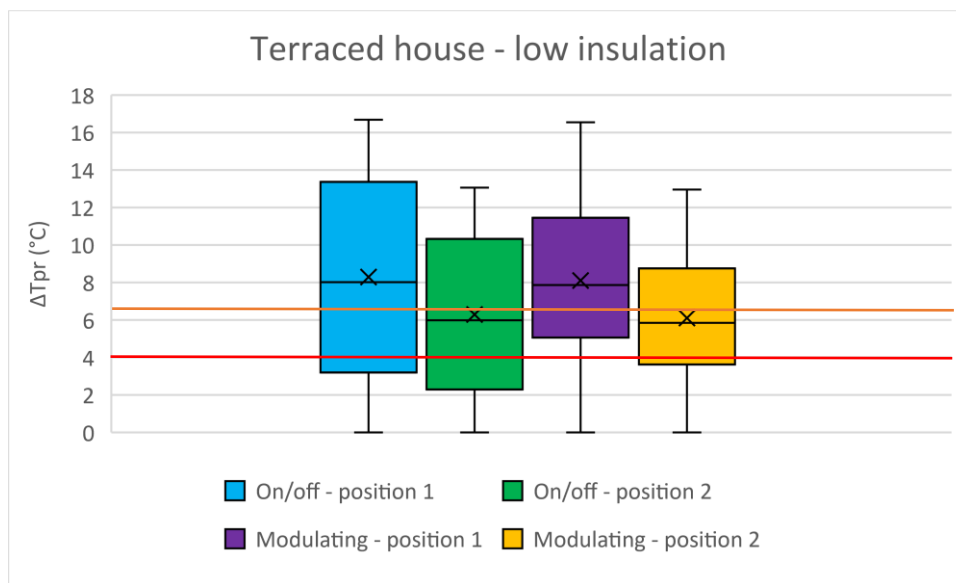


Figure 65: Difference in plane radiant temperature between the ceiling and the floor throughout the heating season for the infrared panels at different positions, taking into account both control types. The dark orange line represents a PPD of 10% and the red line a PPD of 5%

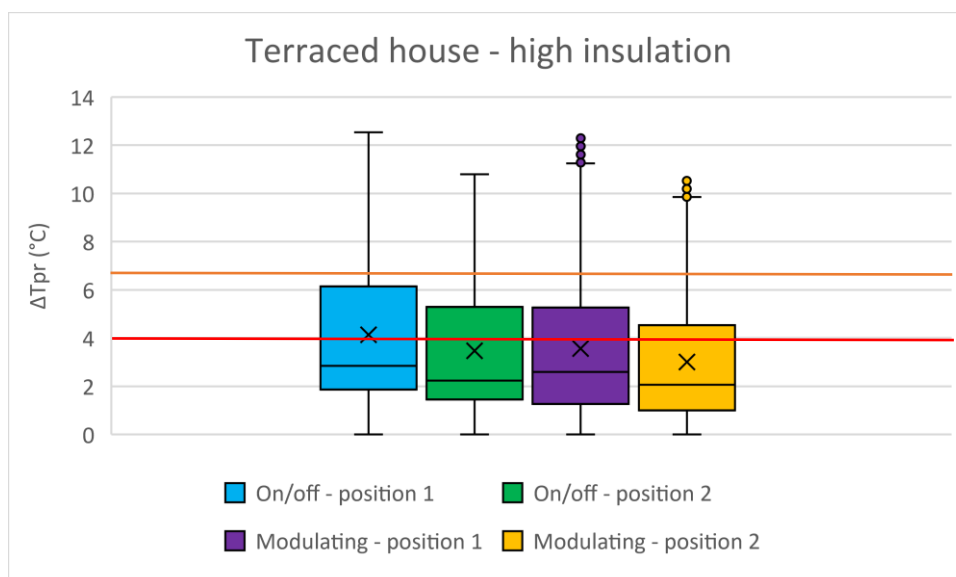


Figure 66: Difference in plane radiant temperature between the ceiling and the floor throughout the heating season for the infrared panels at different positions, taking into account both control types. The dark orange line represents a PPD of 10% and the red line a PPD of 5%

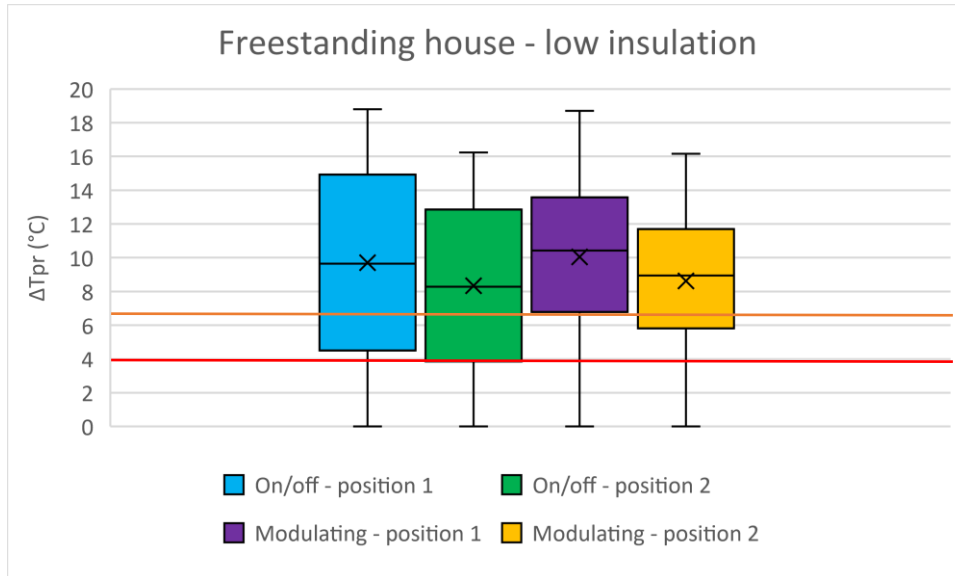


Figure 67: Difference in plane radiant temperature between the ceiling and the floor throughout the heating season for the infrared panels at different positions, taking into account both control types. The dark orange line represents a PPD of 10% and the red line a PPD of 5%

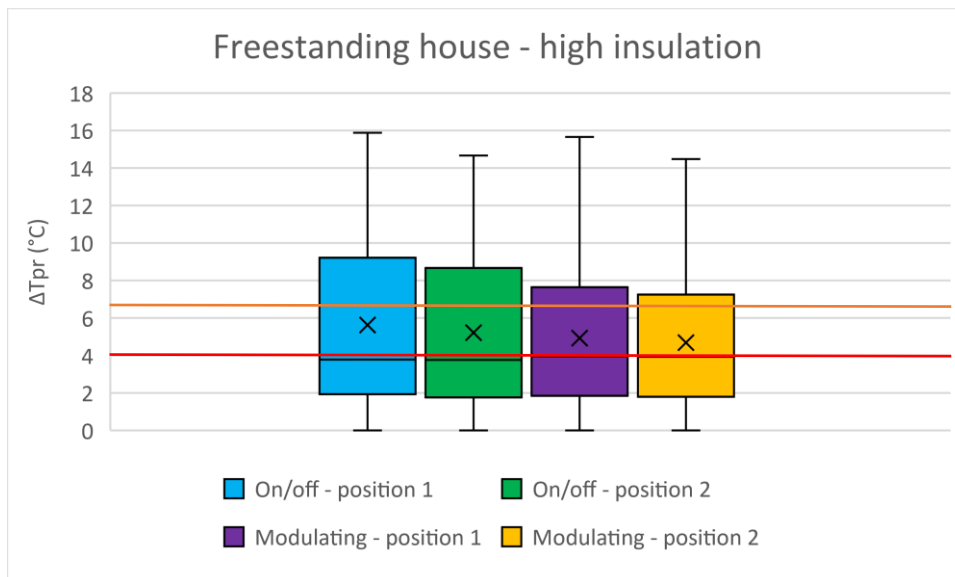


Figure 68: Difference in plane radiant temperature between the ceiling and the floor throughout the heating season for the infrared panels at different positions, taking into account both control types. The dark orange line represents a PPD of 10% and the red line a PPD of 5%

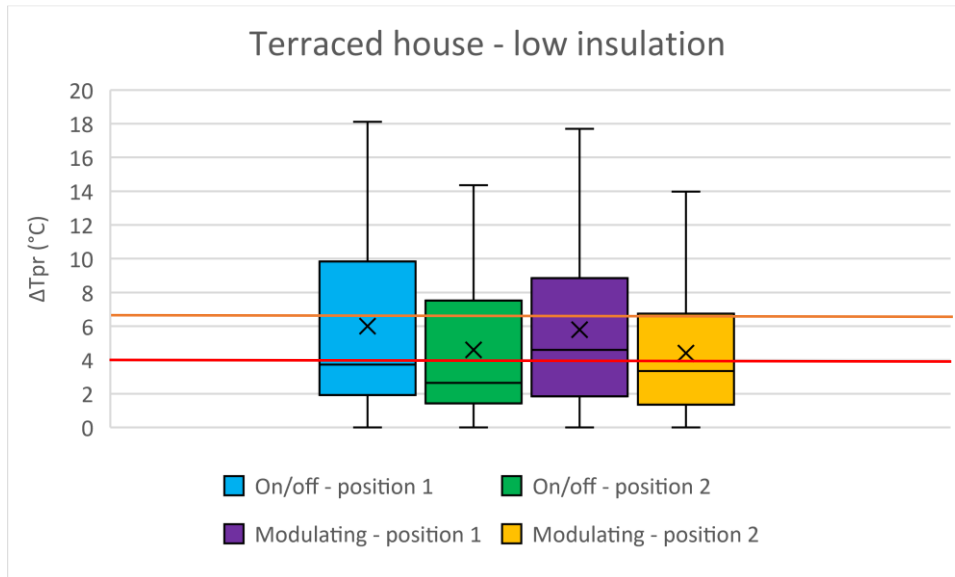


Figure 69: Difference in plane radiant temperature between the ceiling and the floor throughout the heating season for the infrared panels at different positions, taking into account both control types. The dark orange line represents a PPD of 10% and the red line a PPD of 5%

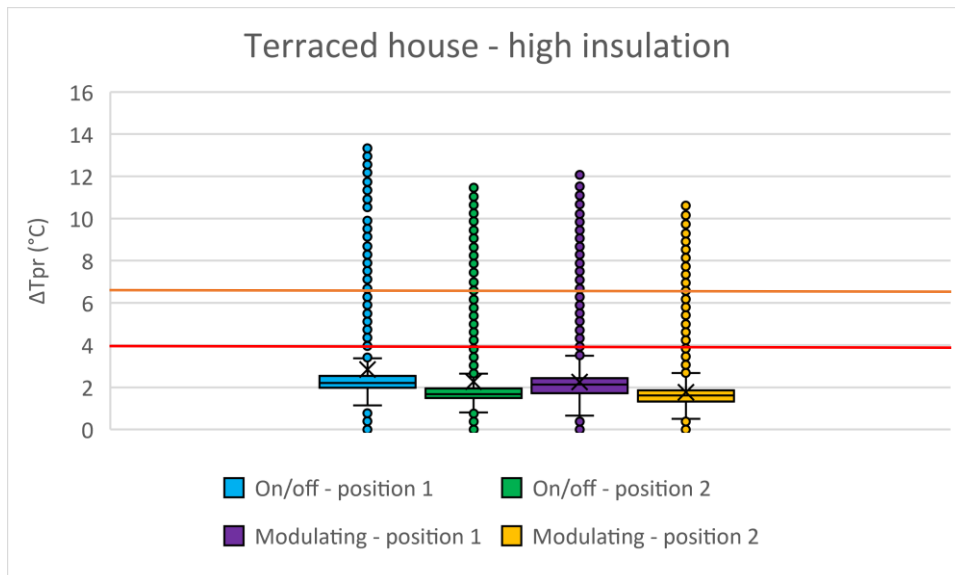


Figure 70: Difference in plane radiant temperature between the ceiling and the floor throughout the heating season for the infrared panels at different positions, taking into account both control types. The dark orange line represents a PPD of 10% and the red line a PPD of 5%

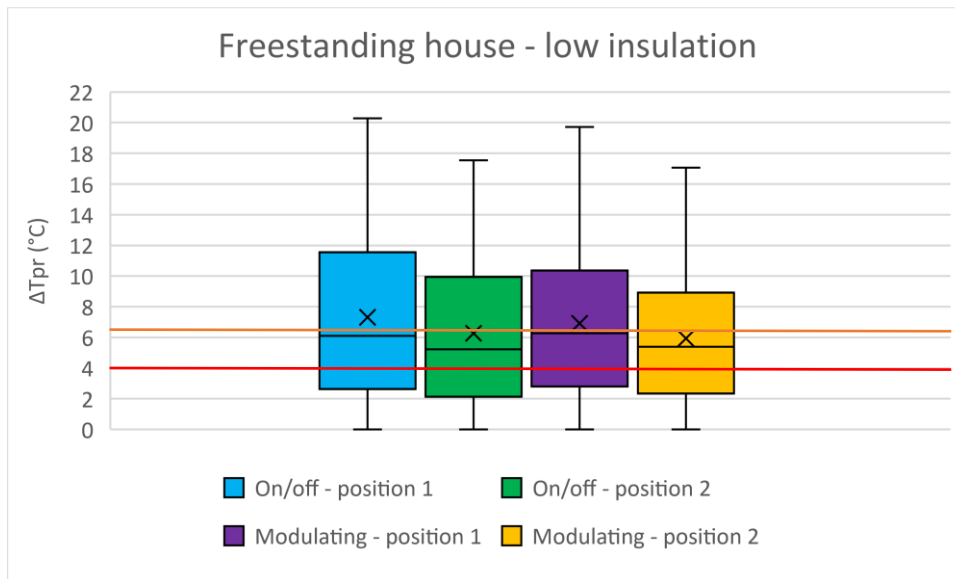


Figure 71: Difference in plane radiant temperature between the ceiling and the floor throughout the heating season for the infrared panels at different positions, taking into account both control types. The dark orange line represents a PPD of 10% and the red line a PPD of 5%

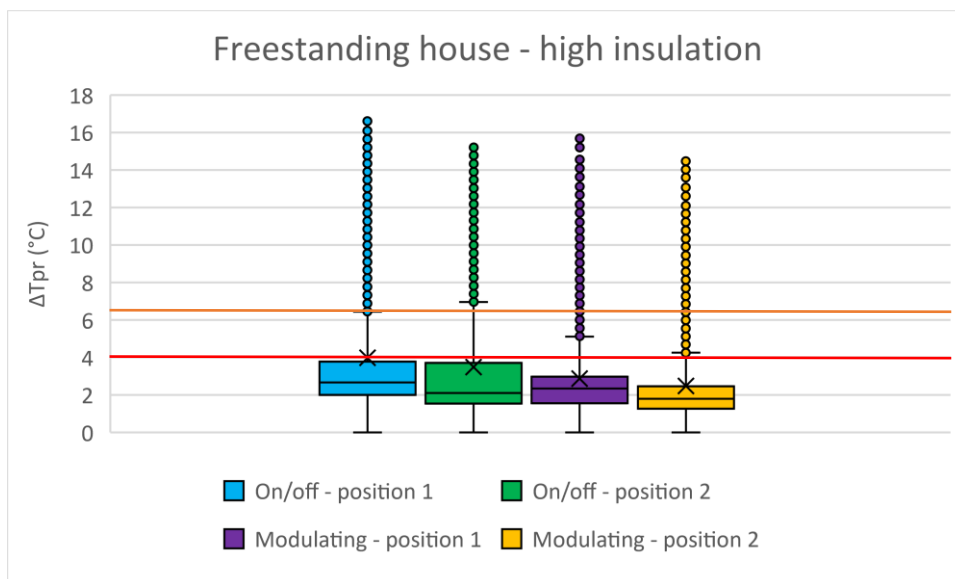


Figure 72: Difference in plane radiant temperature between the ceiling and the floor throughout the heating season for the infrared panels at different positions, taking into account both control types. The dark orange line represents a PPD of 10% and the red line a PPD of 5%

Appendix VIII: Infrared panel load duration curves

Single senior

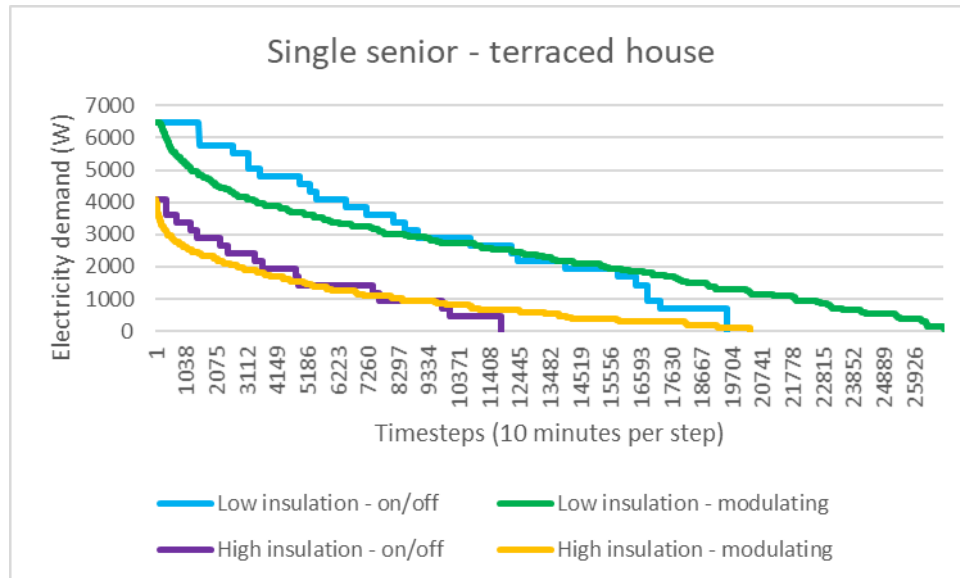


Figure 73: Load duration curves of the infrared panels for both control types for the terraced house with a single senior occupancy profile. Both the low and high insulation variants are shown here

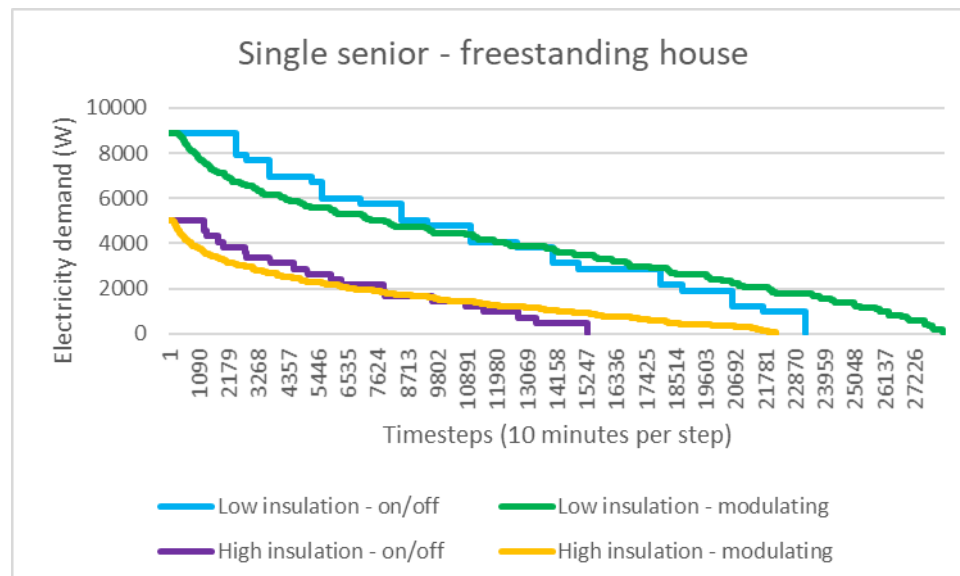


Figure 74: Load duration curves of the infrared panels for both control types for the freestanding house with a single senior occupancy profile. Both the low and high insulation variants are shown here

Nuclear family

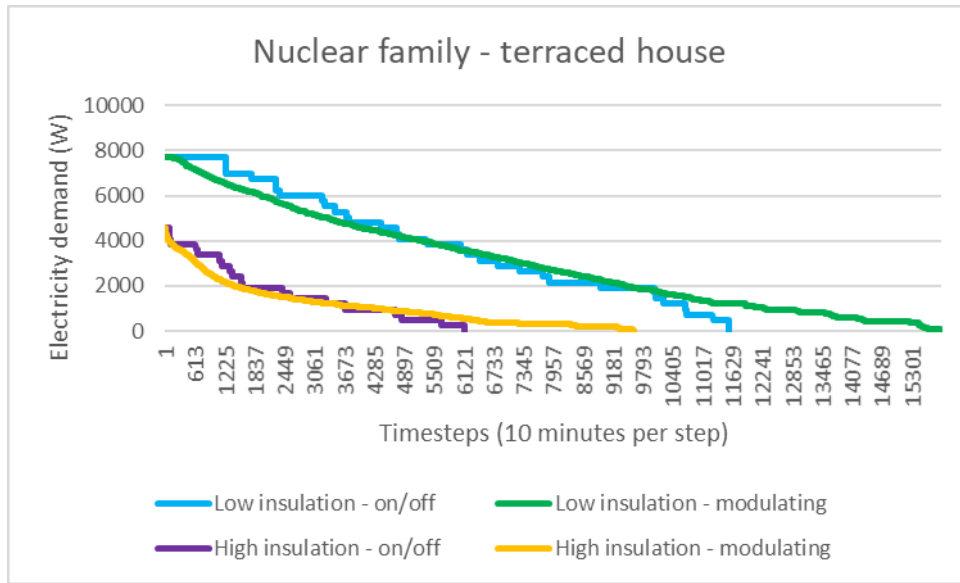


Figure 75: Load duration curves of the infrared panels for both control types for the terraced house with a nuclear family occupancy profile. Both the low and high insulation variants are shown here

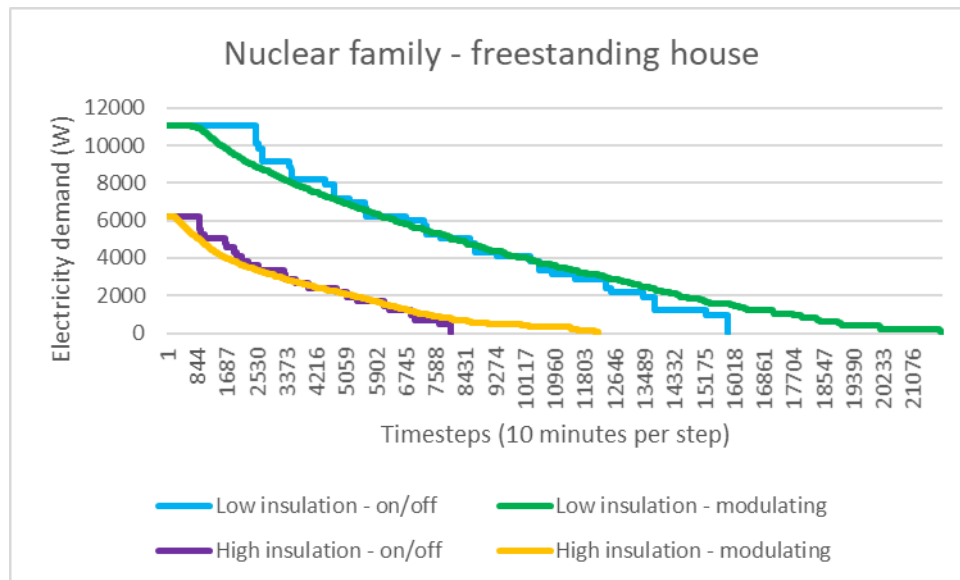


Figure 76: Load duration curves of the infrared panels for both control types for the freestanding house with a nuclear family occupancy profile. Both the low and high insulation variants are shown here

Appendix IX: Total cost of ownership

This appendix contains information on the investment costs of each heating system. The investment cost per heating unit is shown in Table 25. However, the number of infrared panels changes depending on the type of house and envelope quality, so the adjusted investment cost for the infrared panels is shown in Table 26.

Table 25: overview of prices for total investment costs (purchase and installation) for all three heating systems, including the floor heating for the heat pump and gas boiler (Regionaal Energieloket, 2020) (Vaillant, 2017) (Cvketel-Weetjes, 2015) (Meijer & Loonen, 2020)

Heating system	Heat source cost (€)	Heating terminal unit cost terraced house (€)
Infrared panel	250	-
Air-to-water heat pump	7000 - 10000	7000
High efficiency gas boiler	1500 - 3500	7000

Table 26: number of infrared panels and corresponding investment costs per house

Dwelling type	Insulation level	Number of infrared panels	Total investment costs
Terraced house	Low	32	8000
	High	19	4750
Freestanding house	Low	46	11500
	High	26	6500